การประเมินสมรรถนะของกระบวนการรวมของแก๊สซิฟิเคชั่นของถ่านไม้และรีฟอร์มเมอร์
ที่ดำเนินการด้วยคาร์บอนไดออกไซด์ที่วนกลับมาใช้ใหม่

นายปริพัตร์ ไกรศรขจิต

วิทยานิพนธ์นี้เป็นส่วนหนึ่งของการศึกษาตามหลักสูตรปริญญาวิศวกรรมศาสตรมหาบัณฑิต
สาขาวิชาวิศวกรรมเคมี ภาควิชาวิศวกรรมเคมี
คณะวิศวกรรมศาสตร์ จุฬาลงกรณ์มหาวิทยาลัย
ปีการศึกษา 2557

PERFORMANCE EVALUATION OF COMBINED PROCESS OF CHARCOAL GASIFICATION AND REFORMER OPERATED WITH RECYCLED CO_2

Mr. Paripat Kraisornkachit

A Thesis Submitted in Partial Fulfillment of the Requirements
for the Degree of Master of Engineering Program in Chemical Engineering
Department of Chemical Engineering
Faculty of Engineering
Chulalongkorn University
Academic Year 2014

Thesis Title	PERFORMANCE EVALUATION OF COMBINED PROCESS OF CHARCOAL GASIFICATION AND REFORMER OPERATED WITH RECYCLED CO_2
By	Mr. Paripat Kraisornkachit
Field of Study	Chemical Engineering
Thesis Advisor	Professor Suttichai Assabumrungrat, Ph.D.
Thesis Co-Advisor	Supawat Vivanpatarakij, D.Eng.

Accepted by the Faculty of Engineering, Chulalongkorn University in Partial Fulfillment of the Requirements for the Master's Degree

.....Dean of the Faculty of Engineering
(Professor Bundhit Eua-arporn, Ph.D.)

THESIS COMMITTEE

.....Chairman
(Associate Professor Anongnat Somwangthanaroj, Ph.D.)

.....Thesis Advisor
(Professor Suttichai Assabumrungrat, Ph.D.)

.....Thesis Co-Advisor
(Supawat Vivanpatarakij, D.Eng.)

.....Examiner
(Palang Bumroongsakulsawat, Ph.D.)

.....External Examiner
(Peangpit Glinrun, D.Eng.)

ปริพัตร์ ไกรศรขจิต : การประเมินสมรรถนะของกระบวนการรวมของแก๊สซิฟิเคชั่นของถ่านไม้และรีฟอร์มเมอร์ที่ดำเนินการด้วยคาร์บอนไดออกไซด์ที่วนกลับมาใช้ใหม่ (PERFORMANCE EVALUATION OF COMBINED PROCESS OF CHARCOAL GASIFICATION AND REFORMER OPERATED WITH RECYCLED CO_2) อ.ที่ปรึกษาวิทยานิพนธ์หลัก: ศ. ดร. สุทธิชัย อัสสะบำรุงรัตน์, อ.ที่ปรึกษาวิทยานิพนธ์ร่วม: ดร. สุภวัฒน์ วิวรรธ์ภัทรกิจ, 112 หน้า.

การใช้งานแก๊สสังเคราะห์สามารถช่วยลดการใช้งานเชื้อเพลิงจากปิโตรเลียม โดยแก๊สสังเคราะห์สามารถผลิตได้จากกระบวนการแก๊สซิฟิเคชันและเปลี่ยนรูป ในงานวิจัยนี้ศึกษาการประเมินผลของการรวมระบบแก๊สซิฟิเคชั่นและเปลี่ยนรูป ของถ่านไม้ด้วยการนำ CO_2 กลับมาใช้ใหม่ โดยทำการศึกษาทั้งการใช้แบบจำลองและการทดสอบในห้องปฏิบัติการ จากการจำลองกระบวนการผลที่ได้พบว่า เมื่อเพิ่มอุณหภูมิทำให้ค่าร้อยละการเปลี่ยนแปลงของถ่านไม้สูงขึ้น การเพิ่มอัตราส่วนเชิงโมลของออกซิเจนต่อถ่านไม้ในสายป้อนที่เหมาะสมคือ 0.2 ทำให้ได้พลังงานจากระบบสูงที่สุด การเพิ่มอัตราส่วนเชิงโมลของไอน้ำต่อถ่านไม้จะช่วยทำให้ได้ H_2 เป็นผลิตภัณฑ์มากขึ้น และการปรับอัตราส่วนเชิงโมลของ CO_2 ต่อถ่านไม้ สามารถช่วยปรับอัตราส่วนการปลดปล่อย CO_2 และอัตราส่วนของ แก๊สสังเคราะห์ได้ด้วย สำหรับเงื่อนไขที่ใช้อัตราส่วน O_2/ไอน้ำ/CO_2/ถ่าน ไม้ เป็น 0.2/1/1/1 จะให้ค่าประสิทธิภาพของแก๊สผลิตภัณฑ์สูงที่สุดที่ 0.742 ในส่วนของการทำการทดลองศึกษาผลการใช้ตัวเร่งปฏิกิริยา พบว่าที่อุณหภูมิการทำปฏิกิริยา 800 องศาเซลเซียส จะทำให้ค่าร้อยละการเปลี่ยนแปลงของถ่านไม้สูงที่สุด ผลของการใช้ตัวเร่งปฏิกิริยาเป็น Ni/SiO_2 พบว่าเมื่อเพิ่มปริมาณของ Ni ในตัวเร่งปฏิกิริยาจะได้แก๊สผลิตภัณฑ์มากขึ้นเนื่องจากการเกิดปฏิกิริยา เปลี่ยนรูปของก๊าซขาออกมากขึ้น ส่วนผลการศึกษาอัตราส่วนการป้อนของ O_2/ไอน้ำ/CO_2/ถ่านไม้ ให้ผลเป็นไปตามแนวโน้มเดียวกันกับผลจากการจำลองกระบวนการ ที่อัตราส่วนการป้อน CO_2 ต่อถ่านไม้เป็นศูนย์ ส่งผลให้ค่าผลได้ของแก๊สผลิตภัณฑ์สูงที่สุด อย่างไรก็ตามการป้อนคาร์บอนไดออกไซด์เป็นการ ช่วยในการลดการปลดปล่อยก๊าซเรือนกระจกและสามารถปรับอัตราส่วนของแก๊สสังเคราะห์ได้

ภาควิชา	วิศวกรรมเคมี	ลายมือชื่อนิสิต .....
สาขาวิชา	วิศวกรรมเคมี	ลายมือชื่อ อ.ที่ปรึกษาหลัก .....
ปีการศึกษา	2557	ลายมือชื่อ อ.ที่ปรึกษาร่วม .....

5670274021 : MAJOR CHEMICAL ENGINEERING

KEYWORDS: GASIFICATION / REFORMING / CARBON DIOXIDE USAGE

PARIPAT KRAISORNKACHIT: PERFORMANCE EVALUATION OF COMBINED PROCESS OF CHARCOAL GASIFICATION AND REFORMER OPERATED WITH RECYCLED CO_2. ADVISOR: PROF. SUTTICHAI ASSABUMRUNGRAT, Ph.D., CO-ADVISOR: SUPAWAT VIVANPATARAKIJ, D.Eng., 112 pp.

Using syngas as fossil fuel offers the benefit in term of suppress consumption of petroleum fuel. Gasification and reforming process can be used for syngas production. This work investigated the combined of gasifier and reformer process of charcoal with recycled CO_2. The investigation was carried on both simulation and experimental. The simulation results show that carbon conversion depended on operating temperature. The effect of O_2 in feed stream offered more heat obtained from process which optimum at O_2/B = 0.2. At higher S/B in feed stream led to more H_2 in syngas product. And the effect of CO_2/B feed ratio affect on both of CO_2 emr and syngas ratio. For feed ratio $O_2/S/CO_2/B$ = 0.2/1/1/1 offered the highest Cold Gas Efficiency (CGE) of 0.742. From experimental study, the operating temperature of 800 ºC was observed for the highest carbon conversion. For the effect of Ni/SiO_2 catalysts, increasing Ni% loading offered more product gas due to the reforming reaction of gas product. Varying of $O_2/S/CO_2/B$ feed ratio showed in similar trend of product gas mole fraction to the simulation result. For condition of CO_2/B ratio = 0, provided the highest for syngas yield. However, using CO_2 was beneficial in reducing GHG emissions and adjusting syngas ratio.

Department:	Chemical Engineering	Student's Signature .....
Field of Study:	Chemical Engineering	Advisor's Signature .....
Academic Year:	2014	Co-Advisor's Signature .....

ACKNOWLEDGEMENTS

This thesis consumed huge amount of inner and outer strength. Implementation would not have been possible if the author did not have a support from this people. Therefore the author would like to sincere gratitude to all of them.

First, the author would like to thank to his advisor, Professor Suttichai Assabumrungrat, Ph.D., for his suggestions and motivations. His suggestions ehchanced the author knowlegde and his motivations improved the author to be hardworking person.

Secondly, the author would like to sincere grateful to his co-advisor, Supawat Vivanpatarakij, D.Eng., for providing necessary guidance concerning thesis implementation.

Moreover, the author would like to thank to Thailand Research Fund for support this thesis.

Finally, sincere gratitude to the author family for their encouragement, adoration and inspiration. The author dedicate this thesis to his family.

CONTENTS

Page

Page

Page

LIST OF TABLES

Page

Page

LIST OF FIGURES

Page

Page

Page

Page

CHAPTER 1
INTRODUCTION

1.1 Rationale

Global warming and energy crisis are among important issues. Biomass is well-known as renewable energy with high energy yield and to suppress consumption of petroleum [1]. Synthesis gas (syngas) consists of carbon monoxide and hydrogen. Controllable syngas ratio can be used in different applications such as electrical energy source [2, 3], fuel cell [4, 5] and other downstream processes [6, 7].

Gasification process can utilize many types of gasifying agent. Air is the cheapest gasifying agent but provides the low heating value of syngas due to impurity of nitrogen. Therefore, enriched oxygen in air leads to increase in heating value of syngas product [8]. Steam has been used as gasifying agent. The higher steam content and reaction temperature produce syngas product with more hydrogen yield [9, 10]. However, increasing steam and reaction temperature are required more energy to process. Carbon dioxide as a gasifying agent was recently presented the most benefit before emission to the atmosphere. Furthermore, using CO_2 as gasifying agent offers several advantages such as producing more reactive char for better efficiency of gasification process, and adding CO_2 involved in adjusting syngas ratio with more flexible for syngas application [11, 12].

Gasifier effluents are fed to reforming process for upgrading products. There are many types of reforming reactions. Steam reforming is a well-known technology that reforms light-hydrocarbons into syngas product. Higher steam as reforming agent offers higher H_2 yield of syngas product due to steam reforming and water gas shift reaction [13]. Additionally, the advantage of steam reforming, fed excessive steam, is reducing coke formation. Although steam reforming is the most feasible and provides high hydrogen yield, but it is highly endothermic reaction and required heat for generating steam which causes high fuel consumption [14]. Dry reforming uses CO_2 to reform light-hydrocarbon into syngas product. This reaction not only reduces

greenhouse gas emission, but also it can produce alternative energy. Propane dry reforming was studied [15]. Increasing molar CO_2/Propane feed ratio lead to decrease intermediate methane [15]. Furthermore, increasing CO_2 can also increase carbon conversion to reach 100% and offer higher cold gas efficiency (CGE) of syngas product [12]. Syngas ratio (H_2/CO) can be adjusted by varying CO_2 as well as temperature and pressure [11], and also reduce methane emission [16-19]. Several catalysts were used for upgrading gas products. Fe/CaO was reported to provide a high percentage of carbon conversion but it showed medium cold gas efficiency [20], Rh/CeO_2/SiO_2 provides a higher carbon conversion and cold gas efficiency but also higher cost And dolomite provide a low carbon conversion and cold gas efficiency [14]. Nickel catalyst is the most widely used in the industry and it gives an appropriate in performance and cost price, Ni/γ Al_2O_3 gives the moderate conversion but syngas ratio over 2 [21]. Activated carbon gives lower conversion and syngas ratio over 3 [20]. Catalytic activity of Ni on various supporters can be rearranged, Ni/Y-zeolite(CBV500)<Ni/H-ZSM-5(CBV2030E)<Ni/CeO_2/SiO_2 [19] [22].

Many researchers studied the combined process of gasification and catalytic reformer using steam and air as reaction agents. The experiments revealed that addition of catalytic bed unit offers product gases yield higher than using a single gasification unit [14, 23-25], but only a few studies observe the combined gasifier and reformer process using a set of O_2-steam-CO_2 as reaction agents [12]. Using the charcoal as biomass is beneficial in term of lower volatile matters and more fixed carbon than fresh biomass which offers reduction in tar and heavy molecular-weight hydrocarbons [26, 27]. In this work, combined biomass gasifier with reformer using steam-oxygen as agent and recycled CO_2 was studied to determine its product gas compositions, cold gas efficiency and CO_2 emission. The simulations were carried out using Aspen Plus software. The effects of various operating parameters such as temperatures of gasifier and reformer, molar feed ratio of steam-oxygen-CO_2, were considered in terms of product gas composition, syngas ratio, cold gas efficiency (CGE), net heat required and CO_2 emission. Reaction experiments were also studied;

using combined fixed bed of charcoal and Ni/SiO_2 catalyst in a quartz tube reactor representing gasification and dry reforming processes under reaction agents O_2, steam and CO_2. Several values of reaction temperature, molar feed ratio of steam-oxygen-CO_2 and percentage of Nickel metal catalyst loading were studied to determine their influence on product gases composition, carbon conversion, hydrogen yield, syngas ratio and cold gas efficiency (CGE).

1.2 Objective

To investigate the performance of combined process of gasifer and reformer using recycled CO_2 for syngas production.

1.3 Scopes of work

1) Simulation of combined gasifier and reformer using Aspen Plus to specify suitable operating condition for the laboratory studies.
2) Literature survey of the information of various catalysts suitable for reforming reaction.
3) Characterization of catalysts by using X-ray diffraction (XRD), Scaning Electron Microscope (SEM), BET surface area measurement and H_2 temperature programmed reduction (H_2-TPR) to observe the physical and chemical properties.
4) Characterization of charcoal, represented biomass, by using proximate and ultimate analysis to investigate the physical properties.
5) Investigation of several operating conditions including %Ni loading, reaction temperature and feed ratio for combined biomass gasification and reforming reaction.

CHAPTER 2
THEORY

2.1 Gasification process

Gasification is a commonly process that converts organic compounds or fossil fuel materials based carbonaceous into various gas products, such as hydrogen (H_2), carbon monoxide (CO), methane (CH_4), char, tar (higher hydrocarbon compound) and etc.. Figure 2.1 shows block diagram of gasification process. The process occurs at high reaction temperature with air or steam using as gasifiying agents without completely combustion. Main desirable products are H_2 and CO, called "syngas". The advantage of gasification process is the more potential efficiency of using syngas than original fuel direct combustion. Syngas has been used in various processes for example as raw material of methanol synthesis, Fischer-Tropsch process or burn directly in gas engine as renewable energy.

Figure 2.1 Block diagram of gasification process.

2.1.1 Types of gasifiers

There are several common types of gasifiers that provide different usage. Some of them are shown in Figure 2.2. Summary of gasifiers in term of features, advantages and disadvantages are shown in Table 2.1.

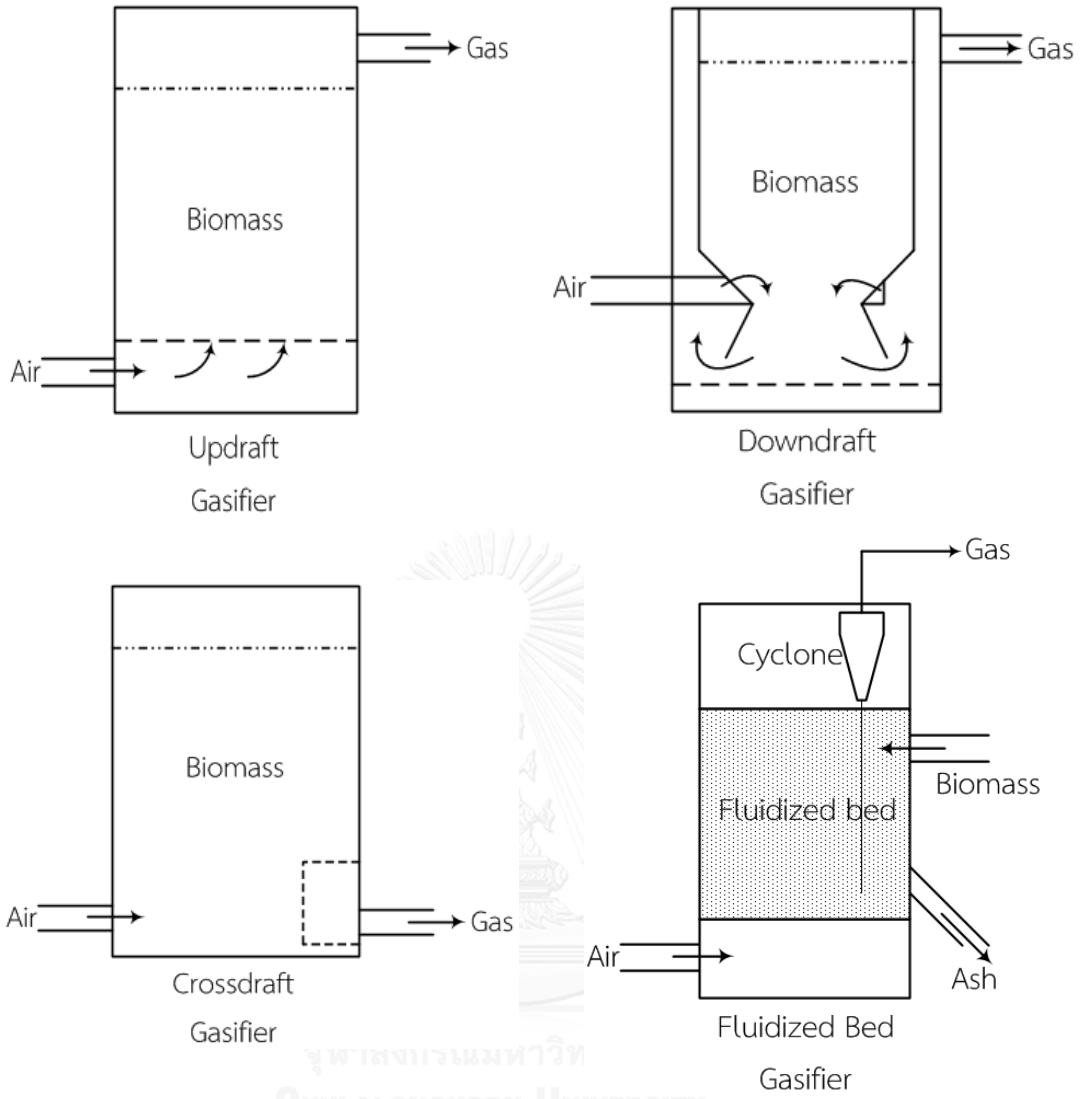

Figure 2.2 Schematic of gasifiers [28]

Updraft gasifier operates by flowing air at the bottom through biomass bed for gasification then produce gases flow out at the top of gasifier. For downdraft gasifier, air is introduced above the oxidation zone at the middle of gasifier then the gasified gases are discharged at top of reactor. Crossdraft gasifier is adapted for using charcoal as biomass. Introduced air and discharged gas products occur at the bottom of column. Fluidized bed gasifier is a widely-used type because it gives a high efficiency in view of controlling a temperature and yield of products. Air is blown with solid particles for a minimum limitation velocity through a bed to make the

suspension state then reacts with biomass. Product gases are fed through an internal cyclone to separate a solid phase recycle back to column at the top.

Table 2.1 Qualification of each gasifier [28]

Gasifier type	Advantages	Disadvantages
Updraft gasifier	- High thermal efficiency - Slight slag formation	- Sensitive with tar and moisture content of fuel - Time lagging in start up step - High pressure drop
Downdraft gasifier	- Practical to charcoal dust and tar content fuel - Adjustable to gas production to load	- Scale limitation - Inappropriate for small particle size of fuel - High pressure drop
Crossdraft gasifier	- Be able to operate in small scale - Flexible gas production - Fast response time to load	- High slag formation - High pressure drop
Fluidized bed gasifier	- Low pressure drop - Slight slag formation - Easy control of temperature	- High tar content of product gases - Instability bed

2.1.2 Process zones

Four mechanisms of gasifier process are determined in:

I. Drying
II. Pyrolysis
III. Combustion
IV. Reduction

The assumption is supposed for gasification process zones separation occurs in fundamentally different thermal and chemical reactions. Figure 2.3 illustrated the updraft gasifier in different zones and temperatures.

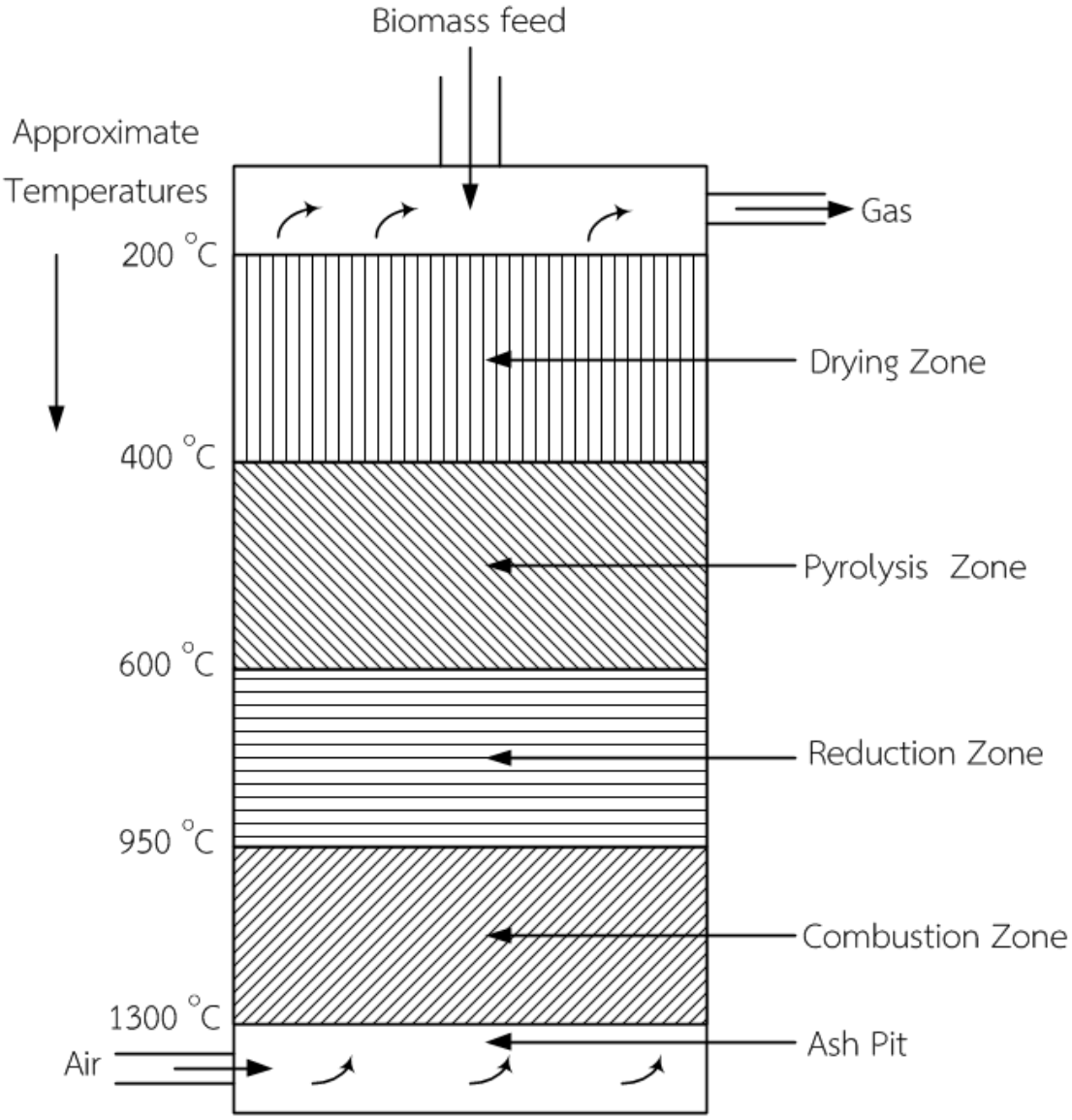

Figure 2.3 Various zones of updraft gasifier [28]

2.1.3 Gasification reaction

The main reaction for gasification is generally occurred in combustion and reduction zone.

I. Combustion or oxidation zone

Biomass, normally consists of carbon, hydrogen and oxygen elements, is completely oxidized by O_2 in air to produce carbon dioxide and water. For complete combustion carbon dioxide is generated from carbon element and water is generated from hydrogen, usually in form of steam. Combustion is an exothermic reaction and theoretical reaction temperature is above 1300 ℃ [29]. The main reactions are:

$$C + O_2 \longrightarrow CO_2 \qquad \Delta H_r = -393 \text{ MJ/kmol} \qquad (2.1)$$

$$2H_2 + O_2 \longrightarrow 2H_2O \qquad \Delta H_r = -242 \text{ MJ/kmol} \qquad (2.2)$$

II. Reaction zone

Partial oxidation products; water, carbon dioxide and partially combusted product; is flowed into next zone of reduction. Temperature in a reduction zone is usually 600 – 900 ℃ and the main reactions are listed below (Eqs. 2.3-2.7).

$$C + CO_2 \leftrightarrow 2CO \qquad \Delta H_r = 164.9 \text{ MJ/kmol} \qquad (2.3)$$

$$C + H_2O \leftrightarrow CO + H_2 \qquad \Delta H_r = 122.6 \text{ MJ/kmol} \qquad (2.4)$$

$$CO + H_2O \leftrightarrow CO_2 + H_2 \qquad \Delta H_r = -42 \text{ MJ/kmol} \qquad (2.5)$$

$$C + 2H_2 \leftrightarrow CH_4 \qquad \Delta H_r = -75 \text{ MJ/kmol} \qquad (2.6)$$

$$CO_2 + H_2 \leftrightarrow CO + H_2O \qquad \Delta H_r = 42.3 \text{ MJ/kmol} \qquad (2.7)$$

III. Pyrolysis and drying zone

Biomass entering gasifier is dried in drying zone which temperature about 200 – 400 ℃. Moisture content, carbon dioxide and acetic acid are discharged from biomass in drying zone. Temperature range of 400 – 600 ℃ causes the pyrolysis zone

take place. In this zone many quantities of tar, hydrogen, carbon dioxide and some methyl alcohol are produced.

2.2 Reforming process

Reforming process is a method for producing hydrogen, carbon monoxide or useful products from reforming the hydrocarbon fuels commonly with steam (steam reforming), oxygen (partial oxidation) or carbon dioxide (dry reforming).

2.2.1 Steam reforming

The general reaction is hydrocarbon reacted with steam to produce syngas (Eq. 2.8). The reaction between steam and methane (Eq 2.9) is a highly endothermic reaction, for thermodynamically, higher temperature and steam to methane ratio, nevertheless, lower pressure offers methane conversion increased [30]. The main steam reforming reactions are listed below:

$$C_nH_m + nH_2O \leftrightarrow nCO + (n + 0.5m)H_2 \quad (2.8)$$

$$CH_4 + H_2O \leftrightarrow CO + 3H_2 \qquad \Delta H_r = 206\ MJ/kmol \quad (2.9)$$

Operating at excess steam, more than theoretical requirement, assist in improvement of H_2 yield and reduction of coke formation on catalyst [30]. There are many metal catalysts used in reforming reaction such as nickel, ceria, molybdenum carbide and tungsten carbide [30].

2.2.2 Partial oxidation

Alternatively process, catalytic partial oxidation used for H_2 and CO production from hydrocarbon fuel using in fuel cell applications such as solid oxide fuel cells and polymer electrolyte membrane fuel cells. Water gas shift reaction is followed by the catalytic partial oxidation in order to improve H_2 content of gas products. There are several metal catalysts used in this reaction such as Nickel, Iron and Cobalt. The main reaction is informed by Eq. 2.10 and the side reactions such as combustion (2.11), Water gas shift (2.12), methane steam reforming (2.13), CO_2

reforming (2.14), Methane decomposition (2.16) and reverse Boudouard reaction (2.17) are listed below [31]:

$$C_nH_mO_p + q(O_2 + 3.76N_2) \longrightarrow wCO + xCO_2 + yH_2 + zH_2O + (3.76q)N_2 \quad (2.10)$$

$CH_4 + 2O_2 \longrightarrow CO_2 + 2H_2O$	Combustion	(2.11)
$CO + H_2O \leftrightarrow CO_2 + H_2$	Water gas shift	(2.12)
$CH_4 + H_2O \leftrightarrow CO + 3H_2$	Methane steam reforming	(2.13)
$CH_4 + CO_2 \leftrightarrow 2CO + 2H_2$	CO_2 reforming	(2.14)
$CO + H_2 \leftrightarrow C + H_2O$	Carbon steam reforming	(2.15)
$CH_4 \leftrightarrow C + 2H_2$	Methane decomposition	(2.16)
$2CO \leftrightarrow CO_2 + C$	Boudouard	(2.17)
$CO + 0.5O_2 \longrightarrow CO_2$	CO_2 formation	(2.18)
$H_2 + 0.5O_2 \longrightarrow H_2O$	H_2O formation	(2.19)

2.2.3 CO_2 reforming

Dry reforming, alternatively name of CO_2 reforming, is an environmentally reaction due to use the greenhouse gases, CO_2 and CH_4, in the reaction. H_2 and CO are the main products. The water gas shift reaction is also a side reaction that support in improving the H_2 content of product gases. Because of the highly endothermic reaction, catalysts such as nickel, cobalt, rhodium and platinum are necessary for the reaction. The main reactions are listed below [32]:

$CH_4 + CO_2 \leftrightarrow 2CO + 2H_2$	ΔH_r = 247.2 MJ/kmol	(2.14)
$CO + H_2O \leftrightarrow CO_2 + H_2$	ΔH_r = -42.1 MJ/kmol	(2.12)

2.3 CO_2 recycled process

CO_2 is captured and recycled back for reducing the emission of CO_2 to atmosphere. CO_2 recycled process is regularly conducted by amine absorption. Simplified flow sheet is shown in Figure 2.4.

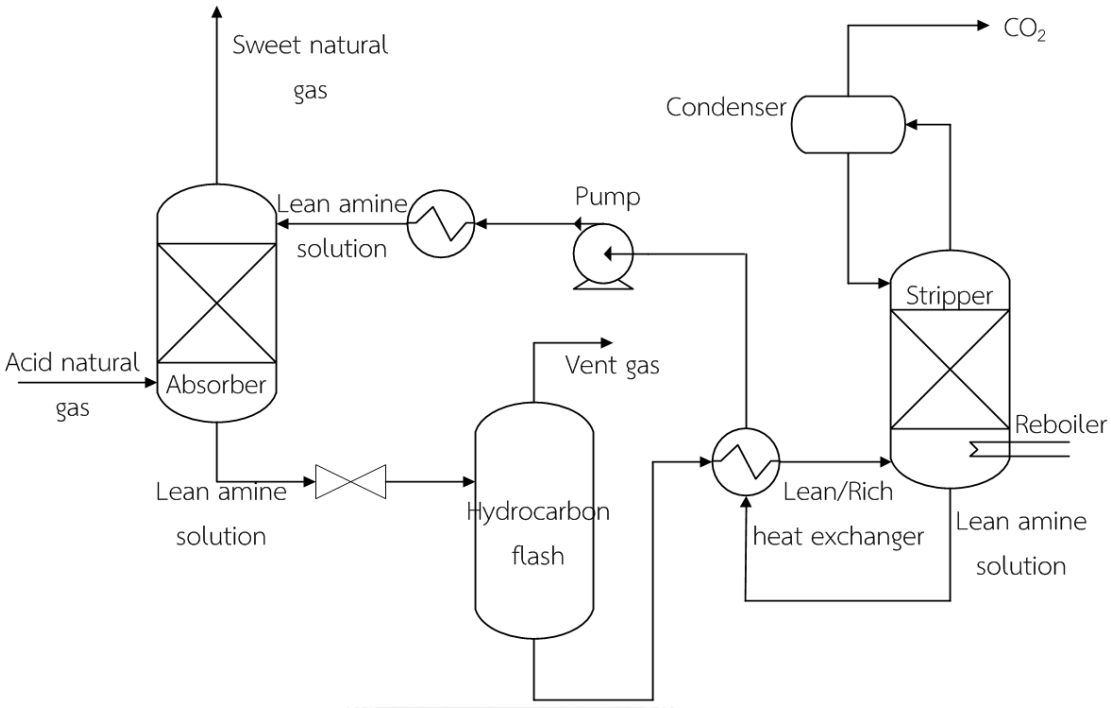

Figure 2.4 Simplified flow sheet of CO_2 removal by amine absorption process [33]

CO_2 enrich gas enters absorber at the bottom of column to remove CO_2 by counter current flow with lean amine solution which enters the column at the top. CO_2 reacts with amine and dissolves into liquid phase. Sweet gas, slightly CO_2 contained gas, flows out at the top of column. Rich amine solution leaves absorber column at the bottom subsequently reduces pressure to an almost atmospheric and separates gases in the flash column. The liquid stream is fed to heat exchanger for pre-heat before enters the stripper in order to regenerate. Stripper temperature is up to 125 ℃ for purges acid gases, including CO_2, from the rich amine solution and flow out at the top of column. Regenerated amine solution leaves column at the bottom and flow to heat exchanger for cool down. Then the regenerated amine solution is

adjusted to the suitable pressure and temperature conditions for recycled to the absorber. Energy required for CO_2 capture by amine process is 3 MJ/kg CO_2 captured [33].

Amine absorption process efficiency is approximately 90% and used the energy required of CO_2 captured process for calculation including recycled process as in the present work.

CHAPTER 3
LITERATURE REVIEWS

3.1 Gasification process

Gasification is the thermo-chemical conversion of biomass to syngas and other products, consist of H_2, CO, CO_2, CH_4, H_2O, char, tar (high molecular hydrocarbon) and etc. Gasification oxidizing agents were air, O_2, steam and CO_2. Air is the cheapest and easy to use due to availability. However, the produced gases have a low calorific value (Udomsirichakorn and Salam [34]). Xiong *et al*. [35] investigated the effect of air quantity by experimental study on biomass gasification using fluidized bed. Pine sawdust was used as biomass feed at rate of 0.512 kg/h for gasification at temperature 800 °C with steam at rate 0.8 kg/h and air in various feed rate. Results showed that the large amount of air fed degraded the product gases because of oxidation reaction. Increasing of air lead to increase in O_2, therefore rising of CO_2 via oxidation reaction cause to low quality of product gases. Brown *et al*. [36] conducted the experiment study of air-blown gasifier, results are shown that only air-blown gasifier produce gas products at low H_2 concentrations. While tar steam reformer unit was introduced, tars and hydrocarbon were reformed to increase H_2 content in product gases. At high tar steam reforming temperature and low space velocity, the results offered the higher of H_2 content. And steam is required for improving the quality of syngas product and water- gas shift reaction (Eq 3.1), steam shows an important role in producing the H_2 content in syngas product.

$$CO + H_2O \leftrightarrow CO_2 + H_2 \qquad \Delta H_r = -41.1 \text{ MJ/kmol} \qquad (3.1)$$

Steam gasification of legume straw and pine sawdust in a free-fall reactor was investigated [10]. The effects of *S/B* feed ratio, reactor temperature on product gases yield and compositions were considered. The results showed that increasing reactor temperature from 750 °C to 850 °C and *S/B* feed ratio offer not only beneficial in the higher of H_2 content in the product gases but also lower of generated tar. Furthermore, water-gas shift reaction is reversed at the higher temperature range

from 730 °C to 930 °C due to endothermic behavior [37]. The experiment was conducted using interconnected fluidized bed investigated a steam gasification of pine wood. The results also showed that CO is increasing with reaction temperature. At *steam/biomass* of 1.4, H_2 yield is reached the maximum value at reaction temperature of 820 °C because the excess of steam fed to reactor. Because of the behavior of water-gas shift reaction, which acting in forward or reverse reaction, is depending on *steam/biomass* ratio and reaction temperature. Figure 3.1 indicated that at the temperature above 800 °C water-gas shift acting to be a reverse reaction.

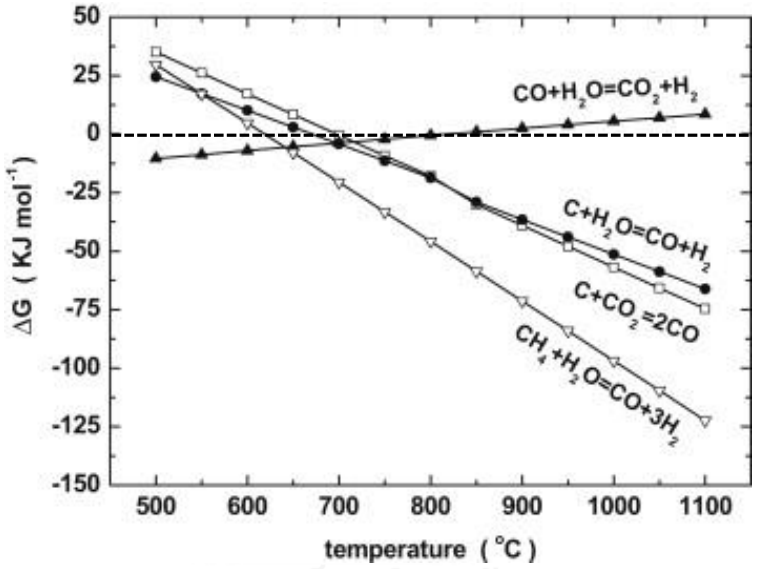

Figure 3.1 Standard Gibbs free energy changes of gasification reactions [37]

CO_2 gasification is recently attractive because using the recycled CO_2 offers reducing in CO_2 emission. Effect of temperature on characteristic of cardboard and paper gasification with CO_2 was investigated by Ahmed and Gupta [38]. The results showed that increasing reactor temperature offers higher of CO in product due to reverse Boudouard's reaction (Eq. 3.2), increased in fraction of H_2 at the initial of time on stream and required more CO_2 because of endothermic of reverse Boudouard's reaction (Eq. 3.2).

$$C + CO_2 \leftrightarrow 2CO \qquad \Delta H_r = 172 \text{ MJ/kmol} \qquad (3.2)$$

Enhancing syngas via catalyst occurred by used catalysts to decompose the residue tar and hydrocarbon. Biomass gasification with Fe/CaO catalyst in a fluidized bed reactor was studied by Wey *et al.* [20]. The experiments were conducted using saw dust as biomass and air as gasifying agent. Effect of Fe percentage loading on CaO supporter was studied on 0%, 10%, 15% and 20% Fe loading. Results showed loading Fe on CaO made $Ca_2Fe_2O_5$ form on catalyst particles that improved the decomposition of tar cause to increase in H_2 yield. At 15% of Fe loading and reaction temperature 660 ℃, the reaction offer the highest carbon conversion of 97% and cold gas efficiency (CGE) of 57.8%. Bilbao *et al.* [39] were investigated the fluidized bed gasification of pine sawdust by used CO_2 as gasifying agent on Ni/Al catalyst. Catalyst weight/biomass flow rate (*W/mb*) was studied by fixed reaction temperature at 700 ℃ and atmospheric pressure. At operating condition of *CO_2/biomass* feed ratio around 1, the results showed increasing in *W/mb* ratio offers higher both conversion of CO_2 and syngas yield. Consequently, it offers lower of CH_4 and long-chained hydrocarbon. The problem of Ni/Al catalyst is stability. For reaction time above 40 min the activity of catalyst was dropped due to coke formation. Tomishige *et al.* [14] have studied cedar wood as biomass gasification with fluidized bed reactor. Effect of various metal catalysts with CeO_2/SiO_2 support were investigated on product gases formation rate and coke yield. The results showed in case of syngas formation rate the highest is Pt>PD>Ru=Ni and coke yield is Ru>Pt=Pd>Ni. Furthermore, the commercial catalysts G-91 (14% Ni, 65-70% Al_2O_3, 10-14% CaO and 1.4-1.8% K_2O) and dolomite (21% MgO, 30% CaO, 0.7% SiO_2, 0.1% Fe_2O_3 and 0.5% Al_2O_3) were also investigated. The results showed higher formation rate of syngas and cold gas efficiency followed by Rh>G-91>Dolomite. Summarize of gasification catalysts list in Table 3.1.

Renganathan *et al.* [12] have studied a thermodynamic analysis of carbonaceous feedstock gasification using CO_2 utilization. Performances of gasification using CO_2, CO_2+steam and CO_2+O_2 are thermodynamically simulated carried on Aspen Plus software. These results were reported in term of product gases composition, cold gas efficiency (CGE) and carbon conversion. At first condition using

only CO_2 as gasifying agent, increasing in reaction temperature for CO_2/carbon of feedstock (CO_2/C) feed ratio of 0.5 the carbon conversion was reached 100% at around 800 °C. CO mole fraction (y_{CO}) rise with reaction temperature increased. On the other hand, H_2 mole fraction (y_{H2}) almost constant due to the endothermic reaction of reverse Boudouard's reaction (BD) (Eq. 3.2) and reverse of water-gas shift reaction (rWGS) (Eq. 3.1), and CGE increase reaching maximum value then constant at 1.2. Effect of CO_2 flow rate was investigated, for rising of CO_2/C, carbon conversion take to 100% at CO_2/C ratio of 0.3, CGE and y_{CO} increased but y_{H2} decreased. The reason is the more CO_2 lead the reaction BD and rWGS shift to product. Second condition using CO_2 and steam as gasifying agents at reaction temperature of 850 °C, introducing more steam lead carbon conversion reaching 100% and also CGE achieve the maximum boundary value at the lower of CO_2/C ratio. In any of CO_2/C value increase in percentage of steam cause rising of y_{H2} but dropping in y_{CO} due to forward shift reaction of WGS and the steam reforming reaction in Eq. 3.3.

$$C + H_2O \leftrightarrow CO + H_2 \qquad \Delta H_r = 131 \text{ MJ/kmol} \qquad (3.3)$$

For third condition using gasifying agents as CO_2 and O_2 at temperature of 850 °C, inlet more of O_2/C is leaded carbon conversion reaching 100%, however, CGE increased to maximum value at the initial of CO_2/C ratio then decrease rapidly by rising of CO_2/C. Correspond to y_{CO} in any of O_2/C, y_{CO} reach maximum at initial of CO_2/C ratio follow by decreasing of y_{CO} in higher CO_2/C. This is the effect of oxidation reaction which O_2 is reacted with carbon easier than CO_2. And y_{H2} decreased by increasing either of CO_2/C and O_2/C.

Combined of biomass gasification with porous ceramic reformer was investigated by Gao *et al*. [23]. This work is using steam and oxygen as reaction agents in updraft fixed-bed gasifier then connected with porous ceramic (mainly consist of SiO_2, Al_2O_3 and MgO) reformer for H_2 production. The results reveal that H_2 composition increased with reaction temperature, but slightly decrease in CO composition because the endothermic behavior of reforming reaction. Increased of O_2 feed ratio from 0 to 0.3 causes the H_2 composition drop for 47% and CO increased at first phase then decreased with O_2 feed ratio. The presence of O_2 in

feed stream affect to the product gases was inferred that the higher of O_2 ratio favor the combustion reaction (Eq. 3.4) more than the reforming (Eq. 3.3) and water gas shift reaction (Eq. 3.1). The effect of steam/biomass ratio was also studied; the product gases were increasing with steam/biomass ratio from 1 to 3.5 that because reforming reaction (Eq. 3.3) and water gas shift reaction (Eq. 3.1) takes an important role in the process.

$$C + O_2 \leftrightarrow CO_2 \qquad \Delta H_r = -393.5 \text{ MJ/kmol} \qquad (3.4)$$

Finally, effect of porous ceramic reforming was studied. As the result, the tar of installed ceramic porous case was less than the case of without ceramic porous. So, installed the ceramic porous unit was improved the H_2 content in product gases by catalytic cracking of tar and heavy hydrocarbon. According to Wu and Williams [24] experiment the combined of steam gasification of polypropylene with fixed-bed catalytic reformer. Using the various nickel catalysts compared to sand bed, representing to non-catalyst, and the results reveal that more gases yield was produced by using nickel bed catalysts. And effect of steam feed was also observed. Feeding steam into system was not only upgraded the gas yield but also both reduced the coke and solid residue of reaction.

Table 3.1 Summarized of gasification catalysts

Metal	Support	Operating Temperature (℃)	Conditions	Carbon Conversion (%)	CGE (%)
Fe[20]	CaO	660	-15 % Fe/CaO ratio -Biomass is Sawdust	97	57.8
-	CaO[20]	660	-Biomass is Sawdust	74.2	45.5
Rh[14]	CeO_2/SiO_2	550	-60 % mass of CeO_2 -Biomass is Cedar Wood	88	55
		600		97	71
		650		99	77
		700		99	82
Pt[14]		550	-Using dual-bed reactor -Biomass is Cedar Wood	48	-
		600		66	-
		650		76	-
Pd[14]		550		55	-
		600		69	-
		650		73	-
Ru[14]		550		45	-
		600		61	-
		650		57	-
Ni[14]		550	-1.2x10-4 mol/gcat of Ni	50	-
		600		64	-
		650		73	-

Table 3.1 Summarized of gasification catalysts (cont'd)

Metal	Support	Operating Temperature (°C)	Conditions	Carbon Conversion (%)	CGE (%)
Dolomite[14]	-	550	-Biomass is Cedar Wood	43	12
		600		48	17
		650		75	32
		700		89	50
G-91[14]	-	550	-Biomass is Cedar Wood	54	22
		600		73	41
		650		79	52
		700		89	69

3.2 Reforming process

There are mainly two types of reforming process to convert higher hydrocarbons to light hydrocarbon and/or hydrogen, including steam reforming and dry reforming. The widely used reactions of hydrocarbon such as CH_4, tar, and etc. with steam called steam reforming or CO_2 called dry reforming for produce syngas.

Non-catalytic steam reforming of natural gas for H_2 production was conducted by Karim and Metwally [40]. They conclude that the non-catalytic reaction is favored for high temperature above 1500 °C. The reaction is rarely sensitive with pressure but sensitive with steam/methane ratio. Furthermore, addition the small amount of O_2 to reaction was improved in reduces the energy input to complete the reaction.

For reducing steam reforming temperature, catalyst was used for improve this disadvantage. Nickel was a widely-used due to performance and price. Park *et al.* [41] studied the various types of support with Ni metal catalyst using in steam reforming

of tar. Benzene was used as tar from biomass gasification process for this study. The effects of temperature (550 °C, 600 °C and 700 °C), Ni loading (5%, 10% and 15%), reaction time (1 to 5 hour) and support including γ-Al_2O_3, ZrO_2, CeO_2, and bi-support CeO_2(75%)-ZrO_2(25%) were examined. Results indicated that all of catalysts at low temperature (<700 °C) give low level of benzene conversion and the suitable reaction temperature is over 700 °C due to endothermic reaction of steam reforming. Condition of supports, the activity orders follow by Ni/CeO_2-ZrO_2 > Ni/γ-Al_2O_3 > Ni/CeO_2 > Ni/ZrO_2 which the reason explained by the redox characteristic of bi-functional support. Ni metal loading of 15% gives the highest activity. Time on stream was studied for evaluate the stability, Ni/γ-Al_2O_3 showed the lowest stability due to conversion decreased rapidly after 5 h and Ni/CeO_2-ZrO_2 gives the highest stability. Mirodatos *et al.* [42] have investigated the reforming of biomass for H_2 production in fuel cell applications using Ni-Cu/SiO_2 catalyst. Ethanol was used as biomass for studied the effect of several operating parameters including reaction temperature, Steam/Ethanol feed ratio and O_2/Ethanol feed ratio. Ni-Cu/SiO_2 catalyst was prepared by impregnation method using $Ni(NO_3)_2{\cdot}6H_2O$ and $Cu(NO_3)_2{\cdot}3H_2O$ as precursor on commercial Silica support. The results revealed that in O_2 absence and Steam/Ethanol ratio of 3.7 conditions, increasing reaction temperature give selectivity of, H_2 and CO higher but CO_2, CH_4 and coke lower. At reaction of 600 °C is presented to be the suitable for reforming reaction. Then rising of Steam/Ethanol feed ratio is focused cause to increase in H_2 selectivity but decrease in CH_4 selectivity, coke formation and lower of CO in product, the appropriate Steam/Ethanol ratio is 3.6. Presence of O_2 was also examined; the highest of H_2 selectivity and the lowest of coke formation is occurred at O_2/Ethanol ratio of 0.4, therefore adding small amount of O_2 improved both of activity and stability. Vicente *et al*. [43] investigated the performance and coke formation of ethanol steam reforming with Ni/SiO_2 catalyst, using fluidize bed reactor with vary the operating condition of reaction temperature, catalyst weight and steam/biomass ratio. Results shown that increasing the reaction temperature, catalyst weight and steam/biomass ratio offer to produce more ethanol conversion and H_2 yield. Coke formation on catalyst was also reduced by using higher of steam/biomass feed ratio.

Dry reforming, used CO_2 as reaction agent, was an interesting process for reduced the global warming issued. Bermudez *et al.* [21] studies parameters of Ni/γ Al_2O_3 as catalyst for CO_2 reforming by using coke oven gas (COG). Presence of H_2 in feed, temperature, volumetric hourly space velocity (VHSV) and catalyst deactivation were investigated. The results shown feed stream that have only CH_4 gave methane and carbon dioxide conversion higher than feed stream that have H_2 because 2 reasons (i) equilibrium shifted to reactants side of the CO_2 reforming reaction and (ii) reverse water gas shift reaction had more effect than CO_2 reforming reaction. Temperature unaffected the H_2/CO ratio however increasing the reaction temperature gave methane and carbon dioxide conversion increased and the highest conversion reach 100% at temperature 1000 ^{o}C. Effect of VHSV indicated that increasing VHSV caused reverse water gas shift increased. In term of R parameter increasing of temperature caused R parameter increased but increasing the VHSV caused R parameter decreased. Catalyst deactivation was effected when reaction processed over 50 hour. Bermudez *et al.* [44] studies dry reforming of coke over gases (COG) for produce syngas which use in methanol synthesis. Activated carbon was used as catalysts, the CO_2 reforming reaction carried out in a fixed-bed quartz reactor under atmospheric pressure. Controlled reaction temperature, 800 ^{o}C, 900 ^{o}C and 1000 ^{o}C respectively, and volumetric hourly space velocity (VHSV) was studies. The results showed that as increasing temperature caused the conversion increased become greater, 80% for methane and 95% for carbon dioxide. Thus water was decreased and completely disappears at 1000 ^{o}C H_2/CO ratio fall but R parameter rose that appropriate for methanol synthesis. At low volumetric hourly space velocity (VHSV), the ratio of H_2/CO was decreased and R parameter was increased, it possible to produce a syngas which appropriate for methanol production. So at high temperature and VHSV not greater than 1.5 $Lg^{-1}h^{-1}$, the activated carbon was a good catalyst for dry reforming of COG to produce a syngas for methanol synthesis. Taufiq-Yap *et al.* studies supporter for nickel catalyst that using in methane dry reforming process to produce syngas. CeO_2/SiO_2 is support that was investigated by varied percent weight of CeO_2 loading; 0 (pure SiO_2), 3, 9, 18, 30, and 100 (pure CeO_2) wt.% respectively. Gas mixture feed has CH_4/CO_2 ratio equivalent and operated at

temperature vary from 100 to 800 °C. Results shown that 9 and 18 wt.% loading of CeO_2 were the best condition by they gave approximately same number that is the highest CH_4 and CO_2 conversion, and the highest stability which reaction time at 600 min. CH_4 has a higher conversion than CO_2 because reverse Boudouard reaction and methane decomposition which are side reaction were take place and it cause H_2/CO ratio close to unity. Fakeeha *et al.* [22] compared zeolite-supported of Ni metal catalysts for dry reforming of methane in term of stabilities. Using Ni/γ-Al_2O_3 (SA-6175), Ni/Y-zeolite (CBV500), and Ni/H-ZSM-5 (CBV2030E) as competitor for analyze. Dry reforming perform in reactor, at 101.3 kPa, various temperature, 500, 600, and 700 °C, equivalent feed ratio of CH_4 and CO_2. It found that using Ni/γ-Al_2O_3 as catalyst gave CO_2 conversion higher than CH_4 conversion at all calcination and reaction temperature because reverse water gas shift reaction is resulting the syngas ratio lower than one, confirming Bermudez *et al.* [21] studies Ni/H-ZSM-5 is the optimum catalyst in term of high stability, low carbon deposition, and syngas ratio close to unity. Zhang and Li [45] studied the coke resistant of core-shell Ni@SiO_2 catalyst in dry reforming of methane reaction. The catalyst exhibits the higher coke resistant for CH_4/CO_2 feed ratio = 1:1, operating temperature above 850 °C and 39 hours reaction, the carbon deposition on catalyst was 0.5 %wt. Ni/SiO_2 was also interested by other experiment. Li *et al.* [46] studied the syngas production by methane dry reforming combined with partial oxidation with Ce-promoted Ni/SiO_2 catalyst. Reaction experiment using fix-bed reactor with CH_4/CO_2/O_2 feed ratio = 40/20/10. Adding Ce to Ni/SiO_2 was able to improve the conversion, H_2 selectivity and syngas ratio for reaction time 360 min, but at reaction time of 180 min, for non Ce doping Ni/SiO_2 offer the low different of results value compared to doping Ce catalysts. Summarized of dry reforming catalysts is list in Table 3.2.

Table 3.2 Summarized of dry reforming catalysts

Metal	Support	Operating Temperature (°C)	Conditions	CH_4 conversion (%)	CO_2 conversion (%)	H_2/CO ratio
Ni[21]	γAl_2O_3	800	-VHSV 0.75 $Lg^{-1}h^{-1}$ -CH_4/CO_2 =1	87	95	2.25
Activated carbon[44]	-	800	-VHSV 0.75 $Lg^{-1}h^{-1}$ -CH_4/CO_2 =1	30	68	3.09
Ni[45]	SiO_2	850	-Core-shell catalyst -CH_4/CO_2 =1	55	70	0.7
Ni[46]	SiO_2	850	-CH_4/CO_2 =2	70	40	1.05
Ni[19]	SiO_2	800	-CH_4/CO_2 =1 -5wt.% of Ni	96	92	1.22
Ni[19]	CeO_2/SiO_2	800	-CH_4/CO_2 =1 -18wt.% of CeO_2 -5wt.% of Ni	97	97	1.14

Table 3.2 Summarized of dry reforming catalysts (cont'd)

Metal	Support	Operating Temperature (°C)	Conditions	CH_4 conversion (%)	CO_2 conversion (%)	H_2/CO ratio
Ni[22]	Y-zeolite (CBV500)	700	-CH_4/CO_2 =1 -Calcine temp 700 °C	65	64	0.97
Ni[22]	H-ZSM-5 (CBV2030E)	700	-CH_4/CO_2 =1 -Calcine temp 700 °C	77	83	0.98

According to gasification and reforming catalysts, Ni/SiO_2 was selected for representing of both processes catalyst. The main reasons are inexpensive, commercial available, the satisfied performance, widely-used in industrial and suitable for used in combined gasification and reforming processes. The catalyst preparation procedure is explained in the next chapter.

CHAPTER 4
EXPERIMENTAL AND MODELING

Experimental and simulation methods were described in this chapter by divided into 3 sections. Section 4.1 explains feedstock preparation and characterization. Simulation of combined gasifier with reformer is described in section 4.2. Finally, details of reaction study are provided in section 4.3.

4.1 Materials preparation and characterization

4.1.1 Biomass

A charcoal was used for representing biomass, because it shows lower volatile matter than fresh sawdust [27]. Mangrove charcoal was chosen to represent as biomass in Thailand. The samples were sieved to get samples with mesh sizes between 16-20 mesh. Consequently, characterizations of charcoal were carried out to determine weight percentage of components (including carbon, hydrogen, nitrogen and oxygen) and percentage of physical properties (including moisture, volatile matter, fixed carbon and ash) by using ultimate and proximate analysis methods, respectively.

4.2 Simulation of combined gasifier and reformer

The simulation used Aspen Plus software. The main purpose was to find out the possible boundary of operating condition for experimental study.

4.2.1 Process description

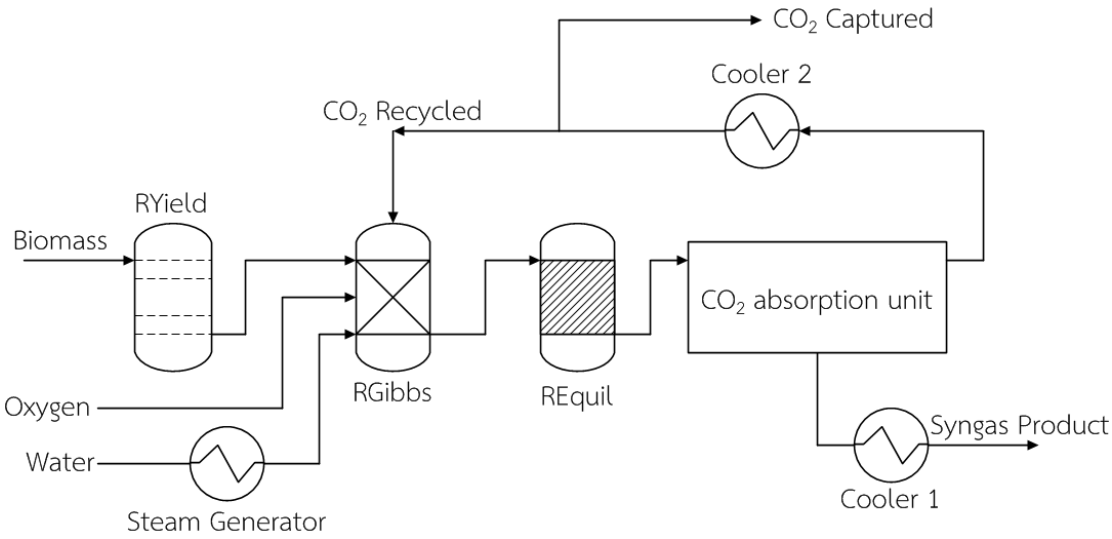

Figure 4.1 Process flow diagram of combined gasifier and reformer

Combined gasification with reforming system composes of gasifier, reformer and CO_2 separation unit. Biomass represented by charcoal is used as feedstock for utilization with inlet reaction agents of steam and oxygen. Produced carbon dioxide is later recycled back to the process for use as reaction agent. Process flow diagram is illustrated in Figure 4.1 and conditions of feedstock and reaction agents are summarized in Table 4.1.

Table 4.1 Inlet conditions of feedstock and reaction agents

Feedstock	Charcoal
Inlet temperature of biomass and O_2	25 °C
Inlet temperature of CO_2	150 °C
Inlet temperature of steam	327 °C
Pressure	1 atm

Charcoal was fed to the gasifer, separated into two reactors (RGibbs and RYield). RYield reactor is used for breaking charcoal down to elements containing carbon, hydrogen, oxygen and nitrogen. Consequently, the elements are fed to RGibbs reactor for gasification process with other reaction agents. Subsequently, gasifier effluent is directly fed to reformer modeled by using a REquil reactor in order to upgrade syngas product. The product is treated in the CO_2 absorption unit for eliminating CO_2 out of the product stream, for this step heat required is 3 MJ/kg CO_2 captured. Finally, the CO_2 is recycled to RGibbs for use as reaction agents again. CO_2 capturing stream is installed in order to adjust the CO_2/Biomass feed ratio.

4.2.2 System modeling

Modeling of gasification process can be done by using each stoichiometric or non-stoichiometric approach, called Gibbs minimization approach. Set of reactions and extent of reaction are known parameters for the case of stoichiometric approach. For non-stoichiometric approach, only the expected product gas components are defined. Many researches confirm that the Gibbs minimization method give good agreement of results as the experimental results [47-49].

Charcoal used as unconventional component in Aspen Plus is fed to RYield reactor for breaking down to elements has input data as listed in Table 4.2. The high heating value of charcoal using the correlation provided by Channiwala and Parikh [49] is shown in Eq. 4.1.

$$HHV\ (MJ/kg) = 0.3491x_C + 1178.3x_H - 0.1034x_O \quad (4.1)$$

Carbon conversion of simulation process is calculated by Eq. 4.2.

$$\text{Carbon conversion} = \frac{(C_{in} - C_{out})}{C_{in}} \times 100 \quad (4.2)$$

Table 4.2 Input data of charcoal

Variable	Data
Feed rate	100 kg/h
Stream class	MIXCINC
Properties	PENG-ROB
Valid phases	Vapor-Liquid
Enthalpy	HCOALGEN (6 1 1 1)
Density	DCOALIGT

Table 4.3 Range of studied parameters

Gasifier temperature	200-800 °C
Reformer temperature	500-1,000 °C
O_2/Biomass ratio (*O_2/B*)	0-0.5
Steam/Biomass ratio (*S/B*)	0-1
CO_2/Biomass ratio (*CO_2/B*)	0-1

Table 4.3 shows the range of studied parameters including gasification temperature, reforming temperature, *O_2/B* feed ratio, *S/B* feed ratio and *CO_2/B* feed ratio. This work was simulated under isothermal condition. *O_2/B* was set in the range of 0 to 0.5 for assuring the partial oxidation occurred. Figure 4.1, cooler 1 was installed to reduce temperature of syngas product to 30 °C and cooler 2 set for removing heat from CO_2 stream in order to obtain the temperature at value of 150 °C. Long-chained hydrocarbon compounds are neglected for this work.

Performances were evaluated in terms of efficiency and CO_2 emission. Efficiency ordinarily reported as cold gas efficiency (CGE) parameter, total net heat of process, and also product gases composition. CGE was defined by Ghassemi and Shahsavan-Markadeh [50] as the following equation (4.3):

$$CGE = \frac{M_{syngas} LHV_{syngas}}{M_{biomass} LHV_{biomass}} \tag{4.3}$$

$$LHV_{biomass} = \frac{M_{biomass} HHV_{biomass} - 0.5 M_H L_{298}}{M_{biomass}} \tag{4.4}$$

$$LHV_{syngas} = \frac{n_{CO} H^0_{CO,298} + n_{H_2} H^0_{H_2,298} + n_{CH_4} H^0_{CH_4,298}}{M_{syngas}} \tag{4.5}$$

Where M_{syngas} = Mass flow rate of syngas (kg/h)

$M_{biomass}$ = Mass flow rate of biomass (kg/h)

LHV_{syngas} = Lower heating value of syngas (MJ/kg)

$LHV_{biomass}$ = Lower heating value of biomass (MJ/kg)

$HHV_{biomass}$ = Higher heating value of biomass (MJ/kg)

M_H = Mass flow rate of atomic hydrogen in biomass (kg/h)

L_{298} = Latent heat of water at standard condition 298 K (MJ/kg)

n_i = Molar flow rate of i component in syngas product (kmol/h)

$H^0_{i,298}$ = Heat of combustion of i component in syngas product (MJ/kmol)

CO_2 emission is evaluated in the proposed parameter. CO_2 emission ratio (CO_2emr) is a fraction of CO_2 emission to total CO_2 produced by process, shown in Eq. 4.6. CO_2 emission ratio value is varied between nearly 0 to 1, lower value indicated less emission, nevertheless, higher value indicated the more CO_2 emission to atmosphere.

$$CO_2 \text{ emission ratio} (CO_2 emr) = \frac{CO_2 \text{emission}}{CO_2 \text{total}} \tag{4.6}$$

4.3 Reaction study

All of reaction agents (O_2, steam and CO_2) were fed simultaneously to the reactor for investigating the effect of feed ratio. This section describes the apparatus, procedure and studied parameters of reaction study. Schematic of reaction study set was illustrated in Figure 4.2.

4.3.1 Procedure

CO_2 (purity 99.8%) was fed at 0.12 ml/s directly from a cylinder instead of recycled process gas due to limitation of equipment. Argon (purity 99.99%) was fed at 2 ml/s as carrier gas in the system added with O_2 (purity 99.99%) with a feed rate of 0.06 ml/s as reaction agent. Steam was generated using water pumped through the syringe pump of 0.3 ml/h and heated up by heating tape to 180 °C. Quartz tube (ID. 8 mm) was used as reactor filled with 2 stages of packed bed, the first stage was a 1 g of charcoal used as biomass with 0.05 g of packed quartz wool and the second was 0.2 g of Ni/SiO_2 catalyst with 0.05 g of packed quartz wool. Gasification and reforming process occurred simultaneous in the same quartz tube reactor for production of syngas. Developed combine gasification with reforming in the same reactor offered the advantage in term of reducing the energy requirement. Furnace was heated up temperature to reach 400 °C, 600 °C and 800 °C for studying the effect of temperature on charcoal gasification. Then the optimum temperature was fixed to study the percentage of Ni loading on catalysts following 5%, 10% and 15%. Finally the effect of $O_2/H_2O/CO_2$ feed ratio was also investigated. Product gases are later introduced to steam trap for removing water and residue tar before being fed into gas chromatography that was used for analyzing the product gases composition. Table 4.4 summarizes the operating condition of reaction study. All of conditions in reaction study were fixed for 3 hours to achieve the feed ratio conditions.

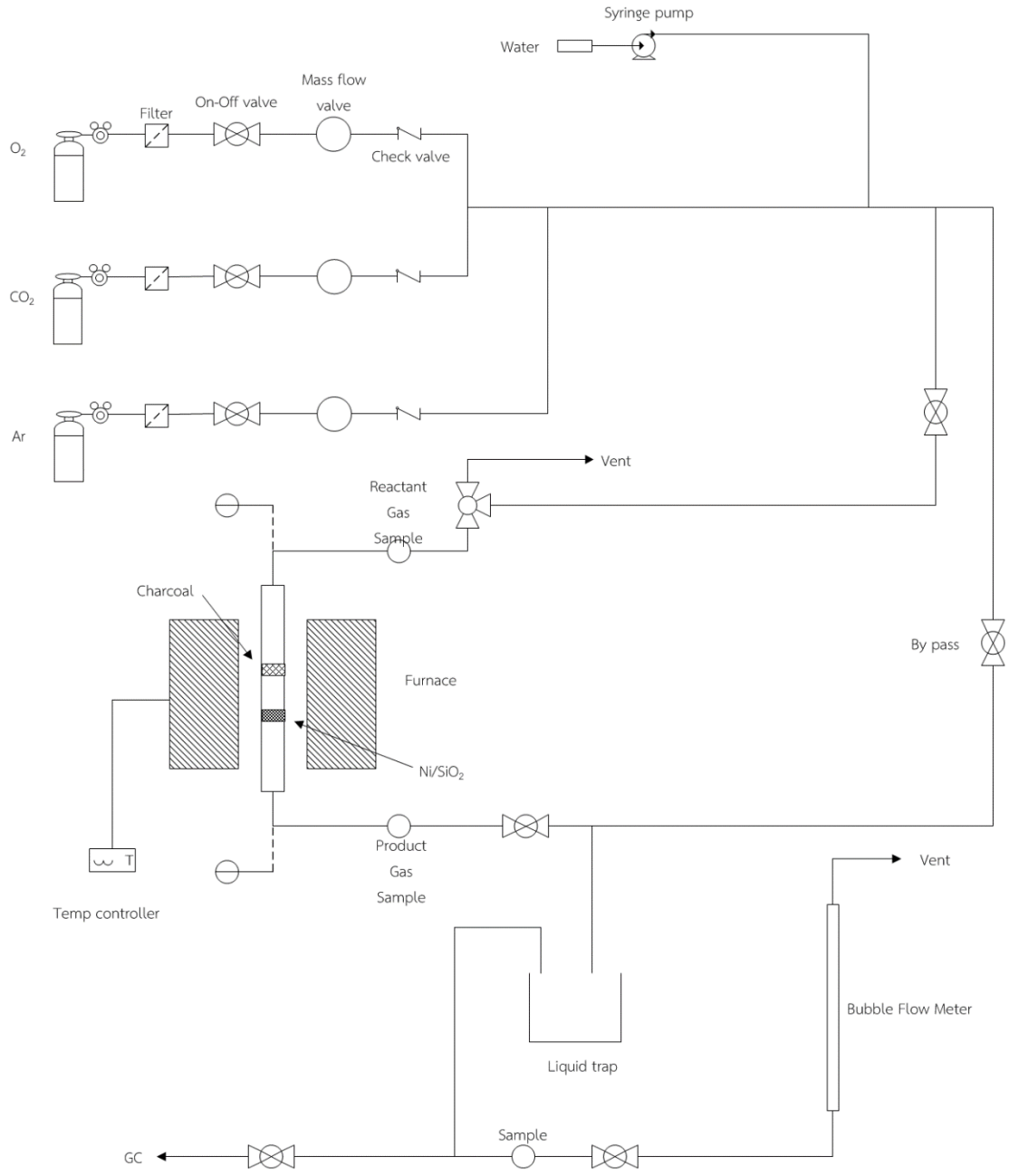

Figure 4.2 Schematic of reaction study

Table 4.4 Operating conditions

% Ni loading	5 – 15 %
Temperature	400 – 800 °C
Pressure	Atmosphere

Table 4.4 Operating conditions (cont'd)

O_2/Biomass ratio (*O_2/B*)	0-0.5
Steam/Biomass ratio (*S/B*)	0-2
CO_2/Biomass ratio (*CO_2/B*)	0-1.5

Table 4.5 Operating conditions of Gas Chromatography

Gas chromatography	Shimadzu GC
Detector	TCD
Carrier gas	Ar (purity 99.99%)
Column temperature	70 °C
Injector temperature	100 °C
Detector temperature	70 °C
Current	70 mA

4.3.2 Catalysts and characterization

Ni/SiO_2 catalysts were used in this experiment with various percentages of nickel loading by 5%, 10% and 15%. Nickel(II) nitrate hexahydrate (Sigma-Aldrich) solution, dissolved with distillate water, is used as precursor for impregnation on the commercially available silica sand (SiO_2) (Sigma-Aldrich) as supporter. Consequently, the catalysts were dried at 105 °C overnight in order to evaporate water. Subsequently, calcination was able to remove the volatile compound under condition of air with temperature of 500 °C for 4 hours.

Prepared catalysts were characterized by X-ray diffraction (XRD) techniques to observe the XRD peak pattern which indicated the presence of metal catalyst and support element using X-ray diffractometer SIEMENS D 5000. The results were shown in a range of 2θ of 20° and 80°.

BET surface area measurement (BET) technique was conducted by BET Micromeritrics ASAP 2020 using 0.1 g of sample to obtain surface area and pore volume of prepared catalysts.

Scanning Electron Microscope (SEM) is used for investigating the morphology and also measuring the particle size of prepared catalysts analyzed by Hitachi S-3400N with accelerating voltage of 15kV.

H_2 temperature-programmed reduction (H_2-TPR) was used for investigating the optimum reduction temperature of catalysts before using in the reaction study by Micrometrics Chemisorb 2750. Catalyst sample of 0.1 g was packed with quartz wool of 0.03 g in U-tube quartz reactor, then removed the moisture content from catalyst particle by using N_2 gas with heating to 200 °C and held for 1 hour. Subsequent, the catalyst was cooled down to ambient temperature and heated up to 800 °C under 25 ml/min of 10% H_2/Ar for temperature programmed reduction. Hydrogen gas used in this step was observed by thermal conductivity detector (TCD) and plot versus temperature.

Thermal gravimetric analysis (TGA) is used for analyzing the coke formation of spent catalysts. Using Mettler-Toledo TGA/SDTA for investigated the percentage of weight loss by carbon on catalysts combustion versus temperature.

4.3.3 Product analysis

Effect of reaction temperature was studied by controlling furnace temperature at 400 °C, 600 °C and 800 °C. Percentages of nickel loading on catalyst were varied at 5%, 10% and 15% in order to obtain the optimum condition for the following parameter. Finally, out of optimum %Ni loading and reaction temperature then the several of reaction agents to biomass feed ratio, O_2/B, S/B and CO_2/B, were studied.

Product gases were investigated using gas chromatography (TCD) equipment (detailed in Table 4.5). Carbon conversion is calculated using carbon balance of CO_2, CO, CH_4 and charcoal method by Eq. 4.5 [14].

$$\text{Carbon conversion (\%)} = \frac{\text{formation of } (CO + CO_2 + CH_4)}{\text{feeding of } (\text{Carbon} + CO_2)} \times 100 \quad (4.5)$$

H_2 and CO yields from experimental were reported by proportion of total mole of H_2 and CO to gram of biomass used by Eq. 4.6 [9].

$$\text{Yield (mol/gram-biomass)} = \frac{\text{mole of product gas(mole)}}{\text{biomass feed(gram)}} \quad (4.6)$$

CHAPTER 5
RESULTS AND DISCUSSION

5.1 Charcoal characterization

In order to study the combined gasifier with reformer process, characterization of raw material charcoal was tested by proximate and ultimate analysis and the results are presented in Table 5.1. Data from proximate and ultimate analysis were used for this study in both of simulation and experiment.

Table 5.1 Proximate and ultimate analysis of charcoal

Proximate (wt%)	
Moisture	5.30
Volatile matters	36.26
Fixed carbon	56.40
Ash	2.05
Ultimate (wt%)	
C	66.46
H	4.37
O (balance)	29.14
N	0.03
High heating value (MJ/kg)[a]	50.581

[a] calculated using correlation proposed by Channiwala and Parikh [49]

5.2 Characterization of fresh catalysts

Before reaction test, characterization of catalysts were conducted by X-Ray Diffraction (XRD), BET surface area measurement, hydrogen temperature programmed reduction (H_2-TRP) and Scanning Electron Microscopy (SEM).

5.4.1 X-Ray Diffraction (XRD)

The XRD peaks of Ni/SiO_2 catalysts with varying loading percentage of Ni from 5%, 10% and 15% were illustrated in Figure 5.1. The diffraction peaks of NiO on catalysts were observed at degree of 37.2°, 43.3 ° and 62.9 ° for 3 types of catalysts as reported by Taufiq-Yap *et al*. [19] and Wang *et al*. [51]. NiO degree shows higher peaks with increasing of %Ni loading.

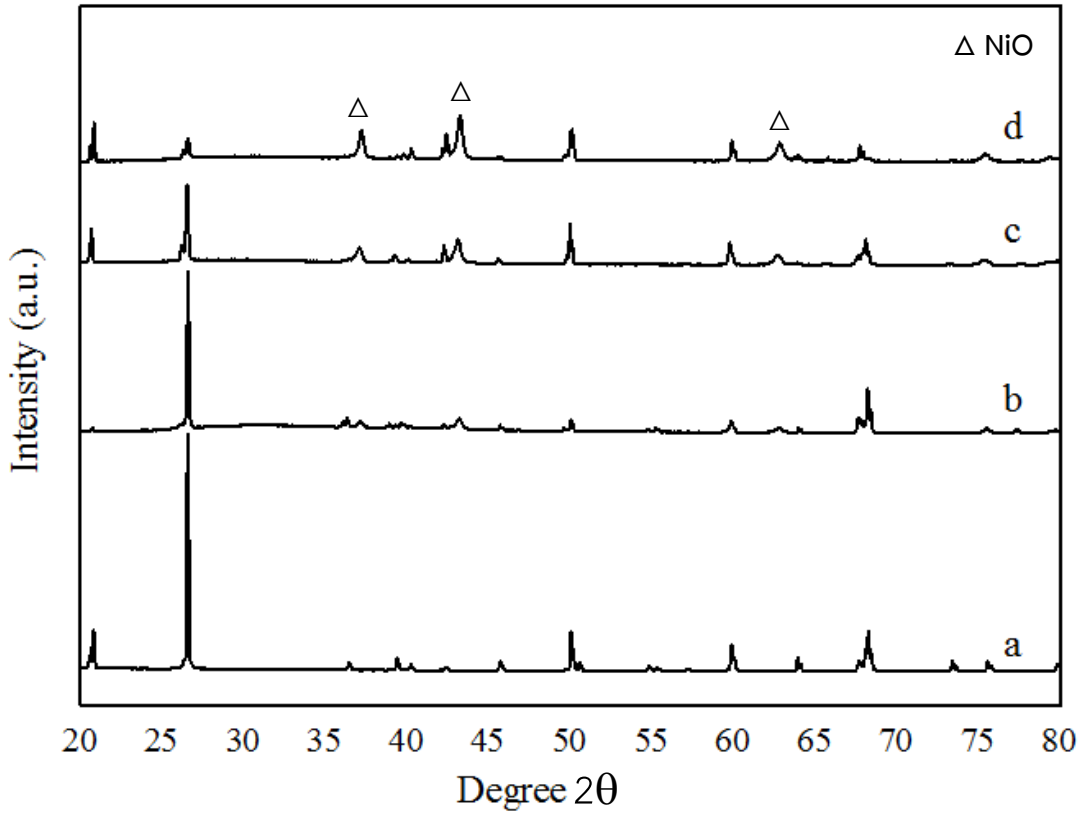

Figure 5.1 XRD patterns of SiO_2 and Ni/SiO_2 with various percentages loading (a) SiO_2, (b) 5%Ni/SiO_2, (c) 10%Ni/SiO_2 and (d) 15%Ni/SiO_2

5.4.2 BET surface area measurement

Surface area results of catalysts are shown in Table 5.2. Increasing in %Ni loading on support results in reduction of surface area (SiO_2 > 5%Ni/SiO_2 > 10%Ni/SiO_2 > 15%Ni/SiO_2, respectively).

Table 5.2 Physical properties of catalysts

Catalysts	Surface area (m^2/g)
SiO_2	5.47
5%Ni/SiO_2	3.82
10%Ni/SiO_2	3.28
15%Ni/SiO_2	2.22

5.4.3 Hydrogen temperature programmed reduction (H_2-TRP)

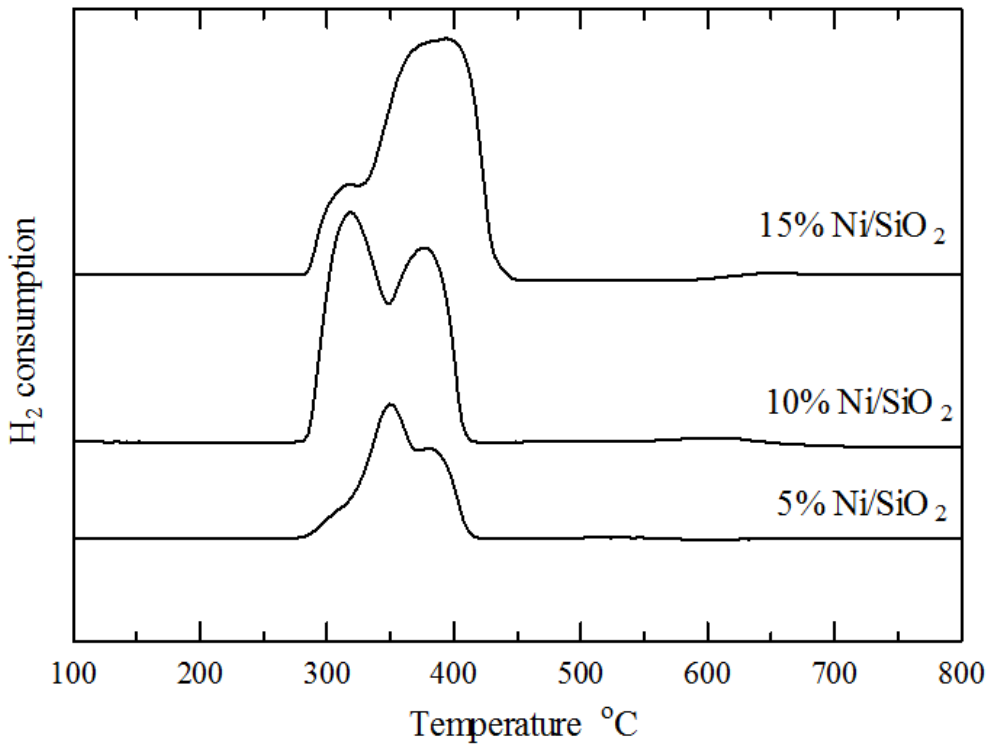

Figure 5.2 H_2-TPR profiles of catalysts

H_2-TPR analysis was conducted for the catalysts. Reducibility of NiO on support was presented as TPR profile as shown in Figure 5.2. The main reduction peaks of catalysts were observed clearly for temperature around 350 ºC to 400 ºC. The results are in agreement with Taufiq-Yap *et al*. [19] and Wang *et al*. [51].

5.4.4 Scanning Electron Microscopy (SEM)

To understand the influence of %Ni loading on SiO_2 support, catalysts were characterized using SEM as shown in Figure 5.3. The morphology of Ni/SiO_2 with various %Ni loading was observed and compared to SiO_2. Higher %Ni loading shows higher of NiO sites as seen in Figure 5.3(d). $5\%Ni/SiO_2$ displayed the slightly difference with SiO_2 support as in Figures 5.3(a) and (b).

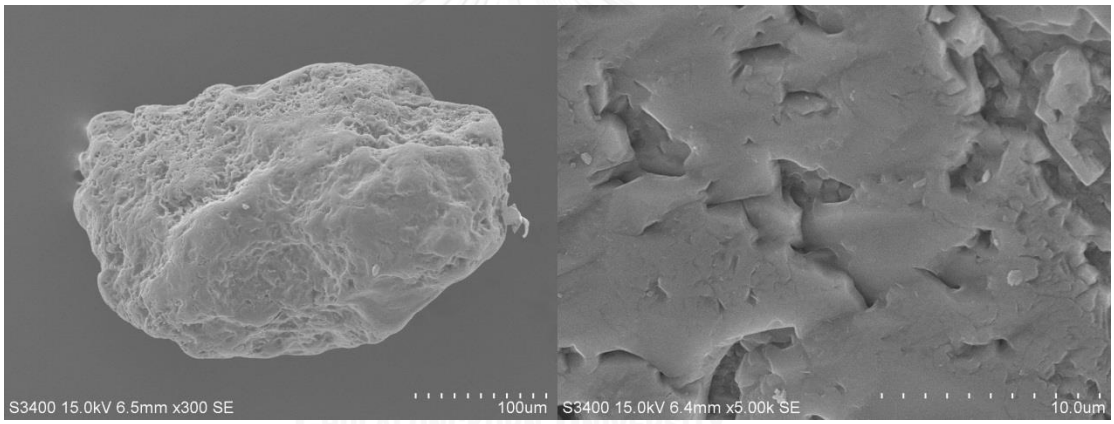

(a) SiO_2

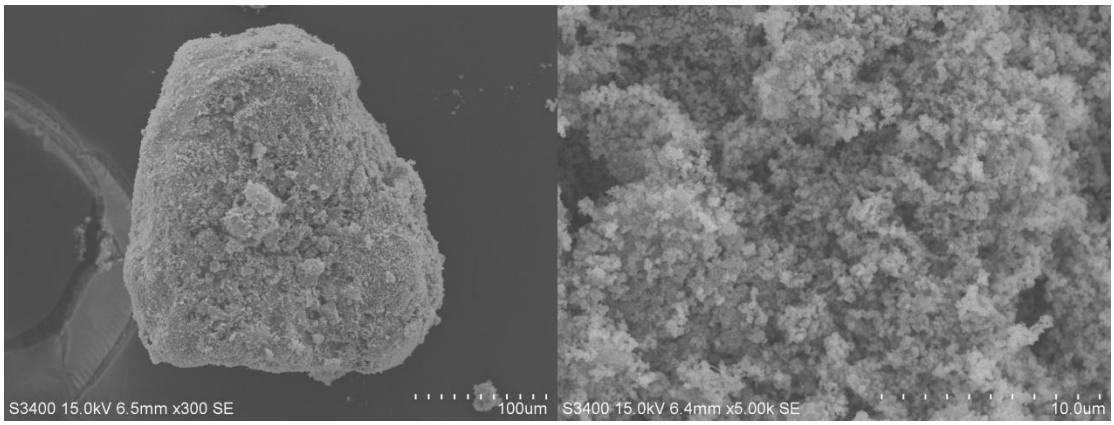

(b) $5\%Ni/SiO_2$

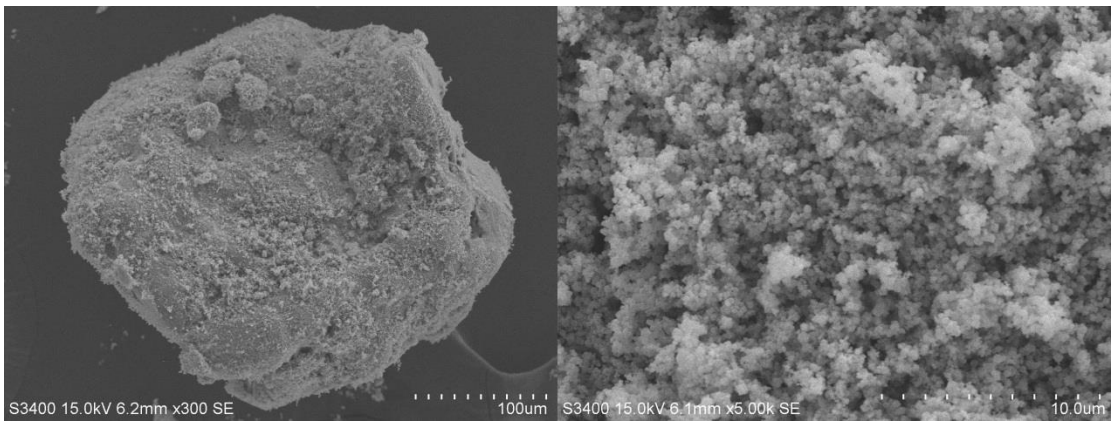

(c) 10%Ni/SiO_2

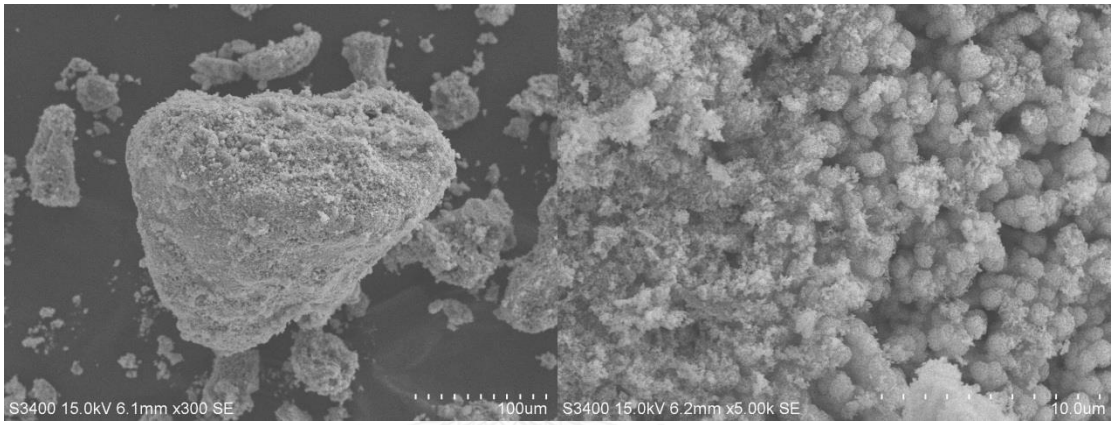

(d) 15%Ni/SiO_2

Figure 5.3 SEM images of fresh catalysts

5.3 Model validation

Before studying the simulation, the model was verified by comparing the gasifier model with Renganathan [12] and Chaiwatanodom [11]. The differences were less than 10%, revealing the good agreement of this model as shown in Table 5.3.

Table 5.3 Model validation of gasifier (biomass $CH_{1.4}O_{0.6}$, CO_2/C = 0.5, P = 1 atm)

	[12]	[11]	This work	%error [12]	%error [11]
T = 800 °C					
yH_2	0.3070	0.3098	0.3108	1.23	0.32
yCO	0.6000	0.5978	0.5977	0.39	0.02
yCO_2	0.0980	0.0901	0.0892	8.99	1.01
yCH_4	0.0000	0.0430	0.0023	n/a	94.54[a]
T = 1000 °C					
yH_2	0.2900	0.3025	0.3036	4.68	0.35
yCO	0.6250	0.6241	0.6238	0.19	0.05
yCO_2	0.0810	0.0733	0.0726	10.38	0.97
yCH_4	0.0000	0.0587	0.0000	n/a	n/a
T = 1200 °C					
yH_2	0.2900	0.2943	0.2957	1.95	0.46
yCO	0.6500	0.6429	0.6424	1.18	0.08
yCO_2	0.0670	0.0628	0.0620	7.49	1.31
yCH_4	0.0000	0.0710	0.0000	n/a	n/a

[a] Neglect due to insignificant value

Model validation of reformer was also verified. Comparison of the model with Gopaul and Dutta [52] also showed a good agreement, confirmed by the difference less than 10% as shown in Table 5.4.

Table 5.4 Model validation of reformer (CH_4/CO_2 = 1.43, P = 1 atm)

	[52]	This work	%error [52]
T = 800 °C			
H_2 (kmol/kmol biogas)	0.900	0.830	7.77
CO (kmol/kmol biogas)	0.630	0.690	9.52
CO_2 (kmol/kmol biogas)	0.036	0.039	8.33
CH_4 (kmol/kmol biogas)	0.020	0.018	10.00
T = 900 °C			
H_2 (kmol/kmol biogas)	0.970	0.907	6.49
CO (kmol/kmol biogas)	0.705	0.770	9.22
CO_2 (kmol/kmol biogas)	0.010	0.011	10.00
CH_4 (kmol/kmol biogas)	0.008	0.007	8.75
T = 1000 °C			
H_2 (kmol/kmol biogas)	0.990	0.903	8.78
CO (kmol/kmol biogas)	0.741	0.776	4.95
CO_2 (kmol/kmol biogas)	0.000	0.002	n/a
CH_4 (kmol/kmol biogas)	0.000	0.000	n/a

5.4 Thermodynamic analysis of combined gasifier and reformer process

The simulation results of combined gasifier and reformer process using various reaction agents are reported below.

5.3.1 Effect of gasifier temperature

The simulations were proceeded to study the conversion of carbon at different gasifier temperatures. Figure 5.4 illustrates that the gasifier temperature (T_g) of 600 °C offers the maximum conversion of charcoal to reach 100%. Due to endothermic reaction of reverse boudouard and steam reforming, increasing reaction temperature leaded to higher conversion accordingly to standard Gibbs free energy changes of gasification reactions [37]. The calculation was showed in appendix A.

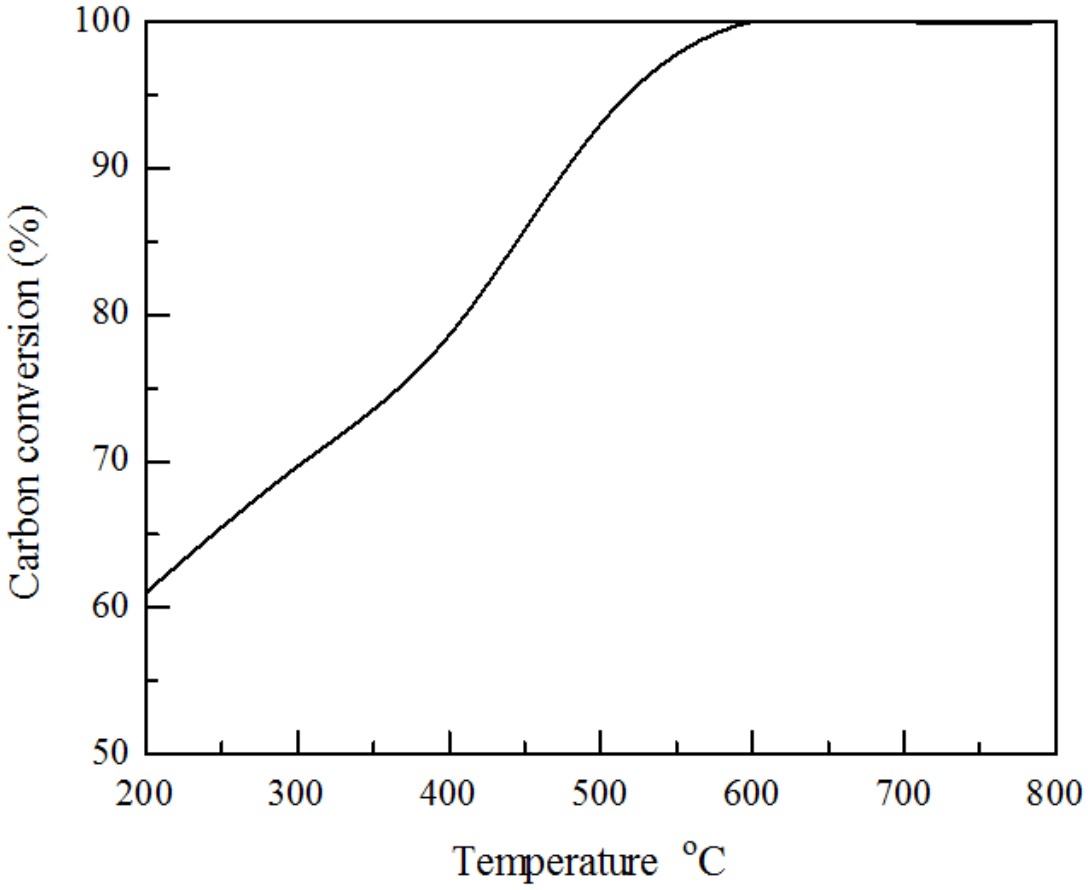

Figure 5.4 Effect of gasification temperature on carbon conversion (O_2/B = 0.5, CO_2/B and S/B = 1)

5.3.2 Effect of reformer temperature

Previously, the gasifier temperature (T_g) of 600 °C offers the carbon conversion reaching maximum, this condition is used for studying the reforming temperature (T_r) parameter. Figure 5.5(a) shows the effect of reformer temperature on product gases composition, cold gas efficiency (CGE) and syngas ratio (H_2/CO). Higher reformer temperature offers the lower trend of H_2 and CH_4 composition, but rising of CO. They are mainly explained by endothermic reverse water gas shift and methane reforming reaction. So, syngas ratio is presented in downtrend. CGE is reached the maximum value of 0.51 at 700 °C of reformer. CO_2 emr, the emission ratio of CO_2 to atmosphere, also reduced with higher reformer temperature due to endothermic of reverse boudouard reaction. Total heat required for process is calculated by the difference between heat supplied to each unit in the process and enthalpy of syngas. The minus value means that there is net heat generated from the process. The total heat obtained from process increases with reformer temperature as illustrated in Figure 5.5(b).

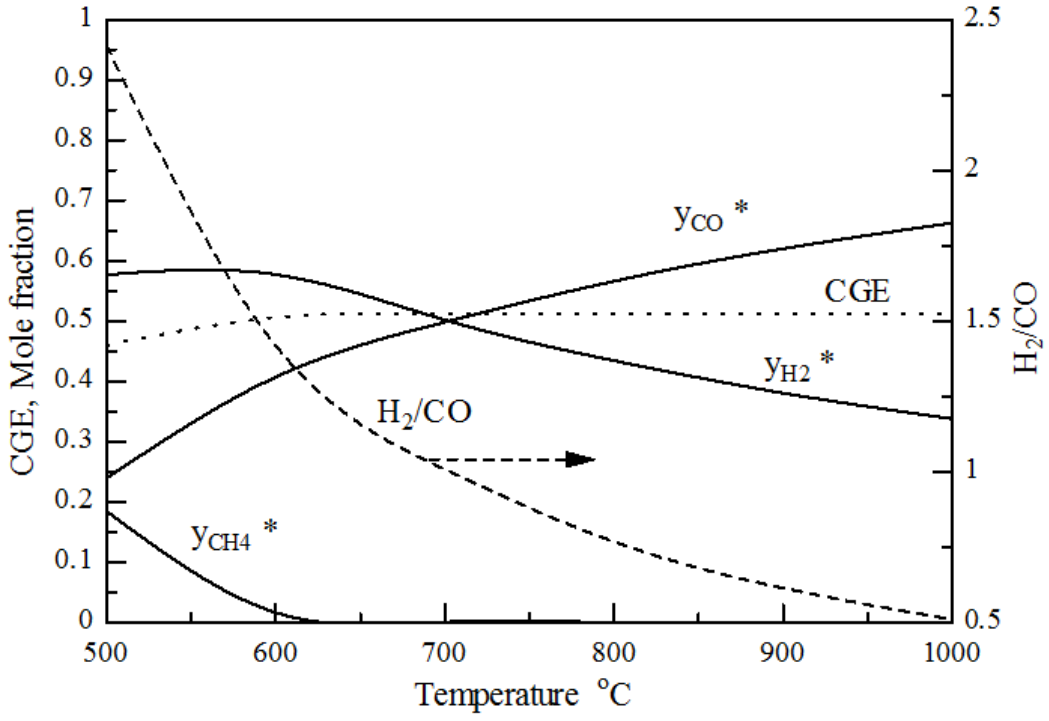

(a) Product gas compositions, CGE and H_2/CO ratio

Note *excluding H_2O and CO_2

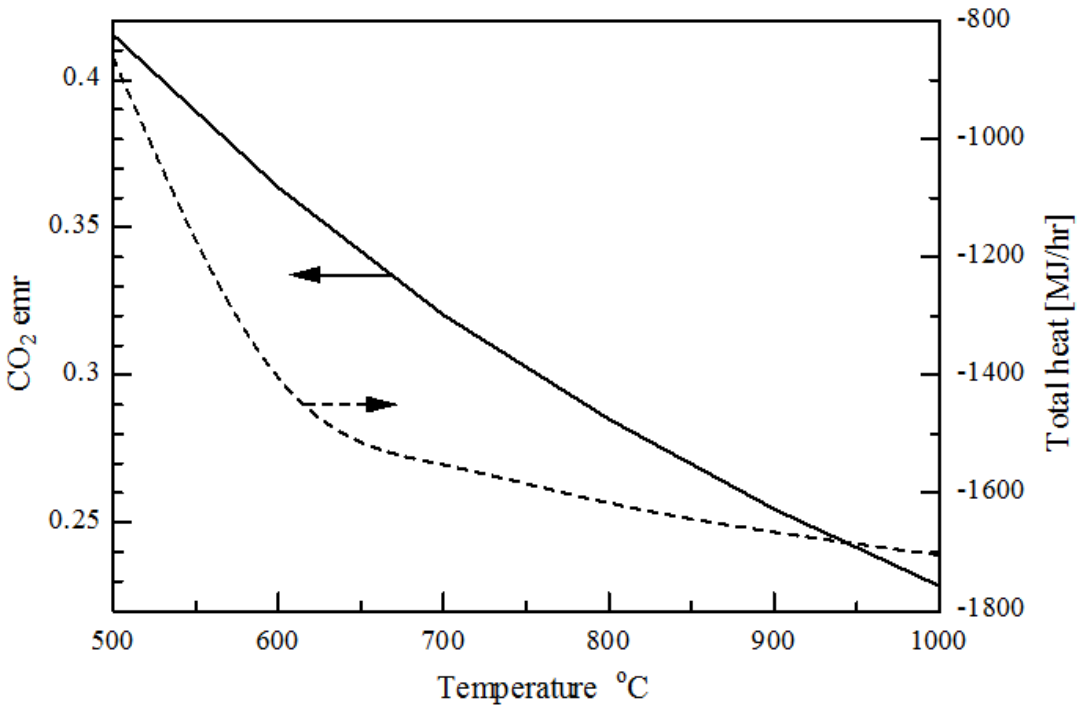

(b) CO_2 emr and total heat

Figure 5.5 Effect of reformer temperature on (a) product gases and (b) CO_2 emr and total heat (T_g = 600 °C, O_2/B = 0.5, CO_2/B and S/B = 1)

5.3.3 Effect of O_2/B feed ratio

Gasifier temperature (T_g) of 600 °C and reformer temperature (T_r) of 700 °C were used as standard condition for the next simulation part. S/B and CO_2/B feed ratio were both fixed as 1 for studying the effect of oxygen feed ratio. O_2/B feed ratio was used at maximum of 0.5 to make the partial oxidation reaction possible. CGE reached the maximum for the O_2/B ratio of 0.2 then dropped with higher feed ratio because at higher O_2, combustion reaction is more favorable than partial oxidation reaction. The product gases composition is reported in Figure 5.6(a). The CO_2 emr value becomes higher with increasing O_2/B ratio, and the total heat increased with presence of O_2 due to exothermic reaction and optimum at O_2/B ratio of 0.2 as displayed in Figure 5.6(b).

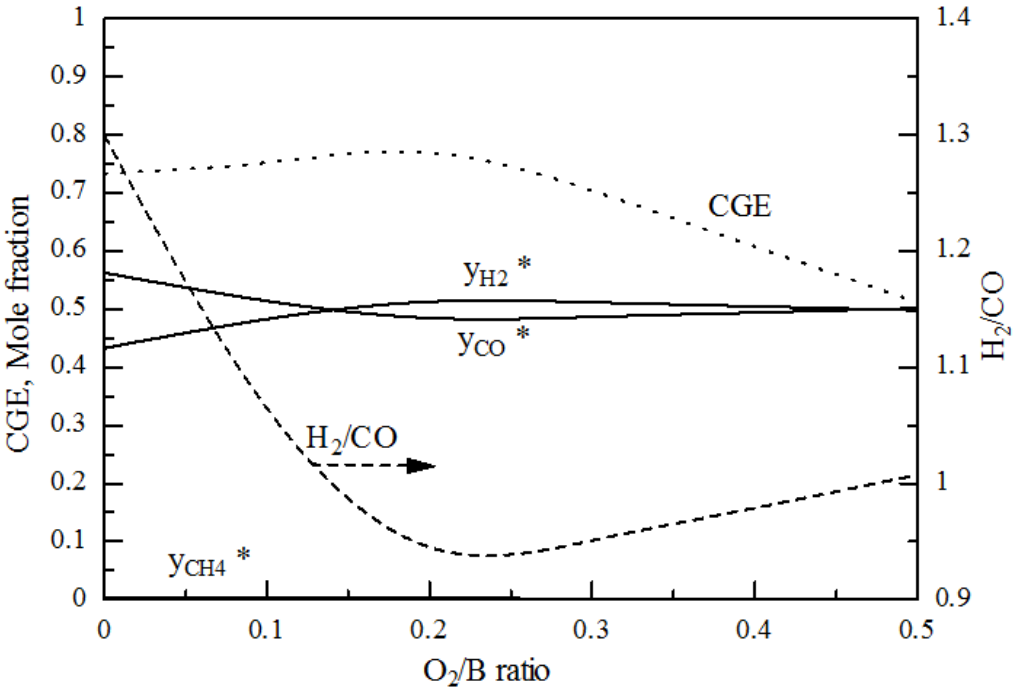

(a) Product gas compositions, CGE and H_2/CO ratio

Note *excluding H_2O and CO_2

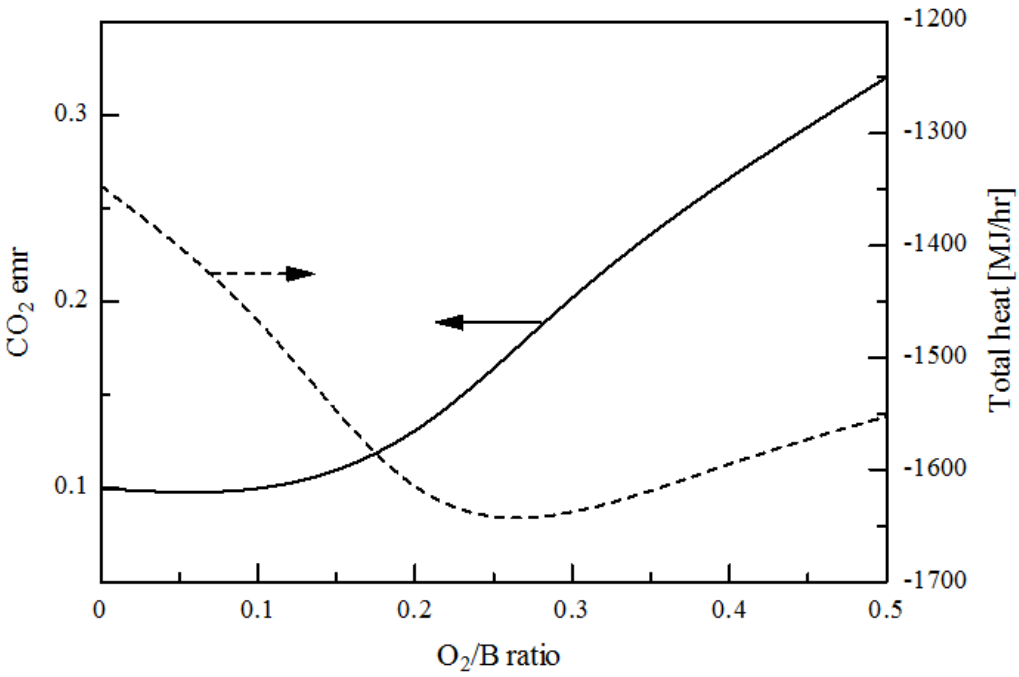

(b) CO_2 emr and total heat

Figure 5.6 Effect of *O_2/B* feed ratio on (a) product gases and (b) CO_2 emr and total heat (T_g = 600 °C, T_r = 700 °C, *CO_2/B* and *S/B* = 1)

5.3.4 Effect of *S/B* feed ratio

Figure 5.7(a) indicates the higher H_2/CO ratio in the product with increasing molar *S/B* feed ratio from 0 to 1, agreeing with Wei *et al*. [10], because of steam reforming and water gas shift reaction. For *S/B* ratio approximately 0.4, CGE achieved the highest at 0.511 and stayed stable. CH_4 was found to be insignificantly small amount. It can also indicate that water gas shift reaction plays an important role in increasing of CO_2 composition, causing CO_2 emr rising up from 0.21 to 0.32, this was also reported by Wei *et al*. [10]. Total heat obtained from process increased with introduced steam by feed ratio from 0 to 0.4, nevertheless, *S/B* feed ratio beyond 0.4 pulled down the heat obtained due to the increased demand for the steam generating unit as shown in Figure 5.7(b).

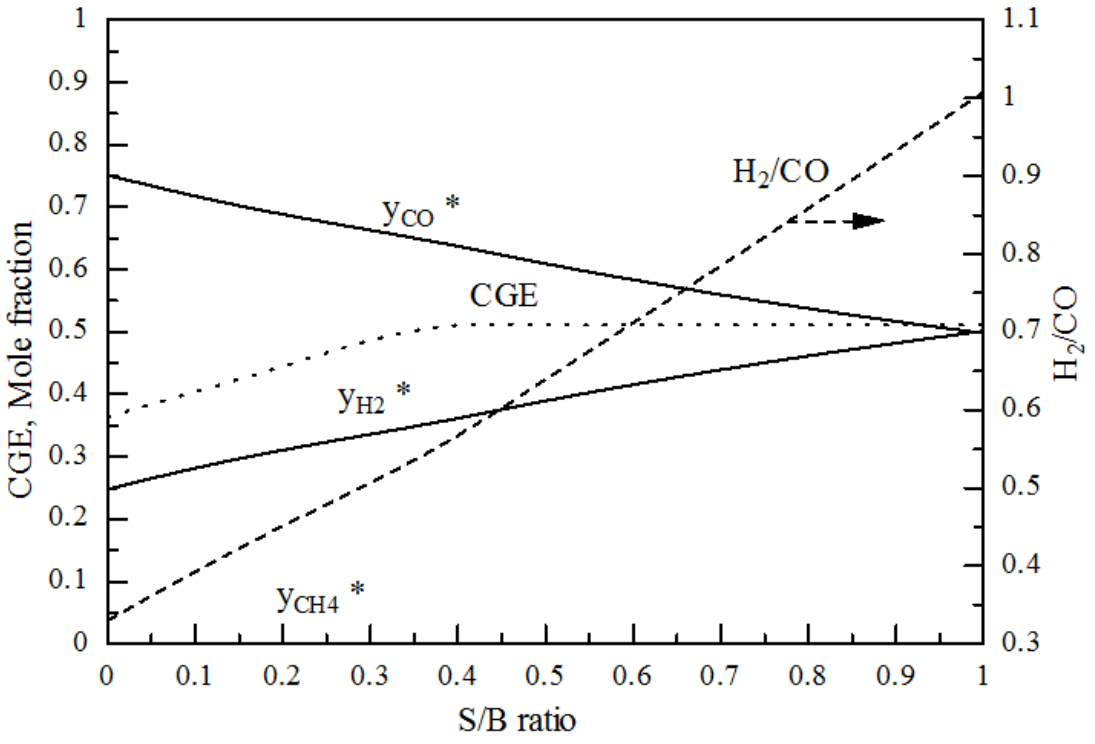

(a) Product gas compositions, CGE and H_2/CO ratio

Note *excluding H_2O and CO_2

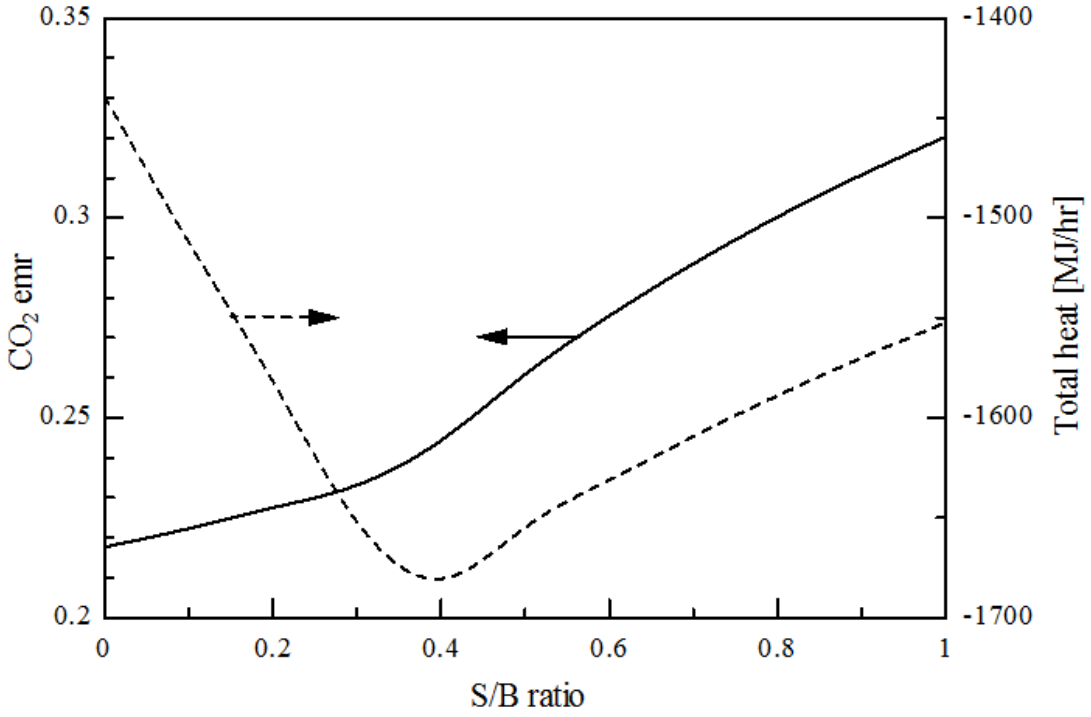

(b) CO_2 emr and total heat

Figure 5.7 Effect of *S/B* feed ratio on (a) product gases and (b) CO_2 emr and total heat (T_g = 600 °C, T_r = 700 °C, *CO_2/B* = 1 and *O_2/B* = 0.5)

5.3.5 Effect of *CO_2/B* feed ratio

This simulation part is investigated the effect of *CO_2/B* ratio. This step is divided into sub-parts for studying the best condition of both *O_2/B* and *S/B* affecting to *CO_2/B* ratio.

Before investigating the effect of *O_2/B* and *S/B* feed ratio on *CO_2/B*, standard conditions of both *O_2/B* and *S/B* were set as 0.5 and 1, respectively. The results are illustrated in Figure 5.8 as follows. For Figure 5.8(a), increasing in *CO_2/B* ration offers lower of H_2 with greater CO because higher CO_2 in feed shifts the reverse boudouard reaction to produce more CO, similar to the reverse water gas shift reaction, resulting in higher and lower in constant rate of CO and H_2, respectively. This results in a relatively constant CGE value at about 0.51 but the H_2/CO ratio could be varied in a range of 1 - 1.9. The results are in good agreement of trend with Chaiwatanodom [11].

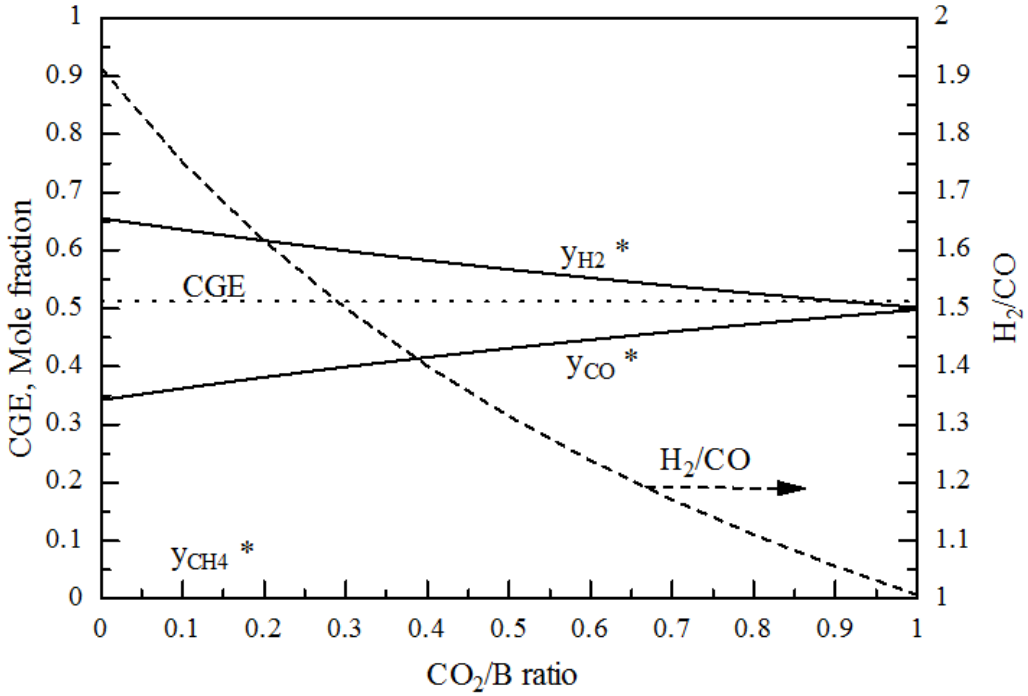

(a) Product gas compositions, CGE and H_2/CO ratio

Note *excluding H_2O and CO_2

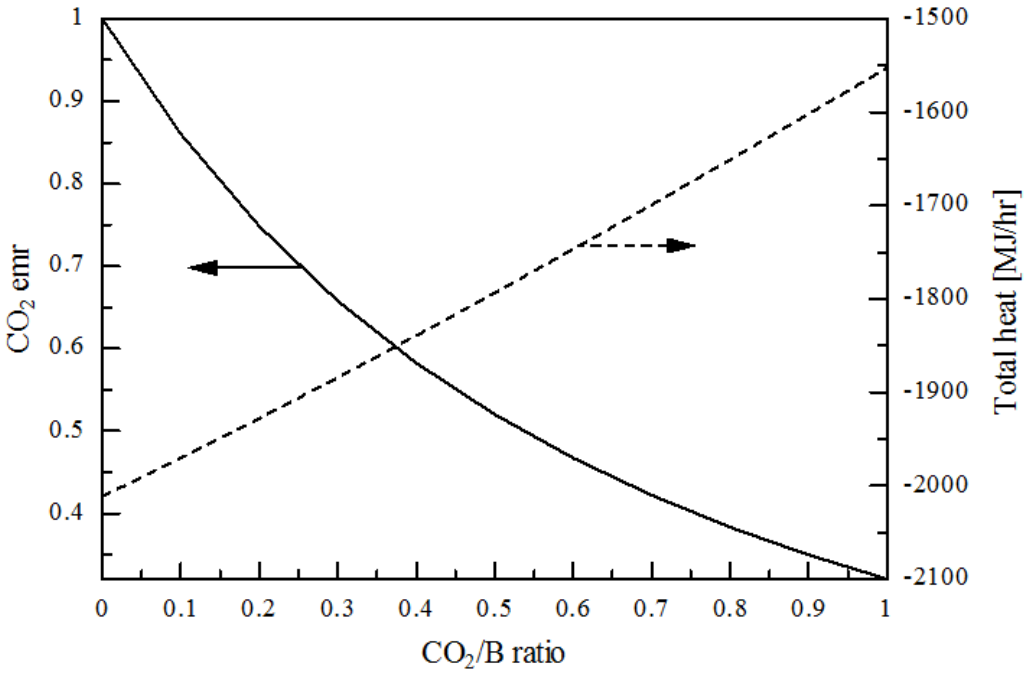

(b) CO_2 emr and total heat

Figure 5.8 Effect of *CO_2/B* feed ratio on (a) product gases and (b) CO_2 emr and total heat (T_g = 600 °C, T_r = 700 °C, *S/B* = 1 and *O_2/B* = 0.5)

The CO_2 emr decreased from 1 to 0.42 when increasing *CO_2/B* feed ratio from 0 to 1, indicating that more recycle of CO_2 back to process can reduce the CO_2 emission. However, heat obtained from the process also reduced from 2,011 MJ/hr to 1,552 MJ/hr by supplying to the CO_2 capture and recycle processes as displayed in Figure 5.8(b).

The next sub-part focued on the effect of *CO_2/B* ratio at the best condition of *O_2/B* feed ratio of 0.2 with *S/B* = 1. The results are shown in Figure 5.9. Trends are almost similar to *O_2/B* of 0.5. Except to CGE, the higher of CGE (indicated more efficiency of syngas product) obtained from *O_2/B* ratio of 0.2 higher than *O_2/B* ratio 0.5 by 0.51 to 0.77. Product gas compositions and syngas ratio are less difference from the previous condition as below in Figure 5.9(a).

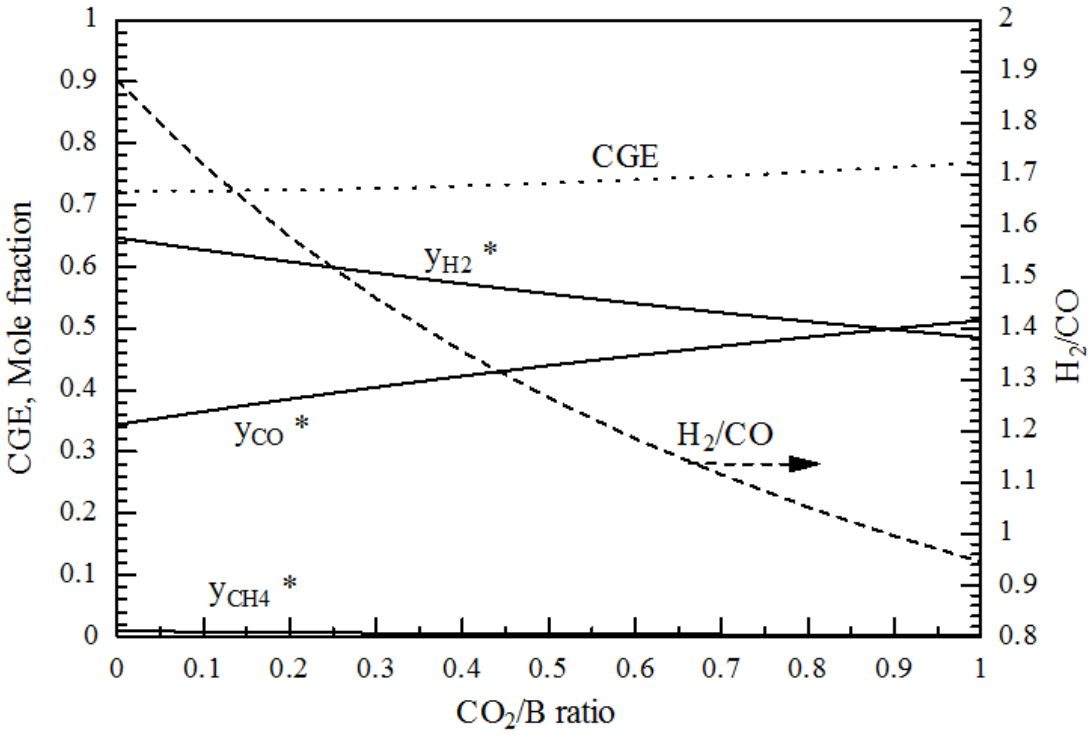

(a) Product gas compositions, CGE and H_2/CO ratio

Note *excluding H_2O and CO_2

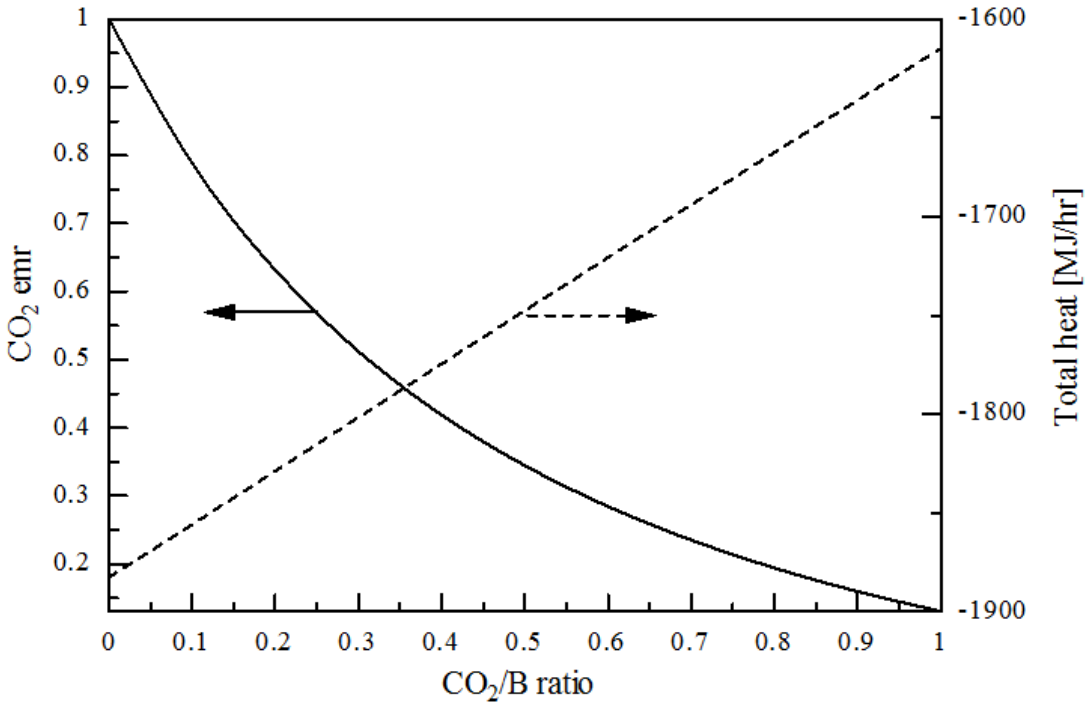

(b) CO_2 emr and total heat

Figure 5.9 Effect of *CO_2/B* feed ratio on (a) product gases and (b) CO_2 emr and total heat (T_g = 600 ºC, T_r = 700 ºC, *S/B* = 1 and *O_2/B* = 0.2)

For *CO_2/B* nearly 1, the CO_2 emr value of 0.13 is less than condition of *O_2/B* = 0.5 because more O_2 in feed stream produced more CO_2 causing to more emission of CO_2 from the process. However, net heat which obtained in this case was lower than the previous condition for *CO_2/B* ratio less than 0.8. This indicated that for *O_2/B* ratio of 0.2 condition, the *CO_2/B* ratio greater than 0.8 did not only offer high value of CGE and net heat obtained from process but also reduced in cost of O_2 feed and also CO_2 emission as shown in Figure 5.9(b).

Next sub-part is focused on the condition at the ratios of *S/B* = 0.4 and *O_2/B* = 0.5. The product gas compositions, syngas ratio, CGE, CO_2 emr and net heat which obtained from process were shown in Figure 5.10 as follows.

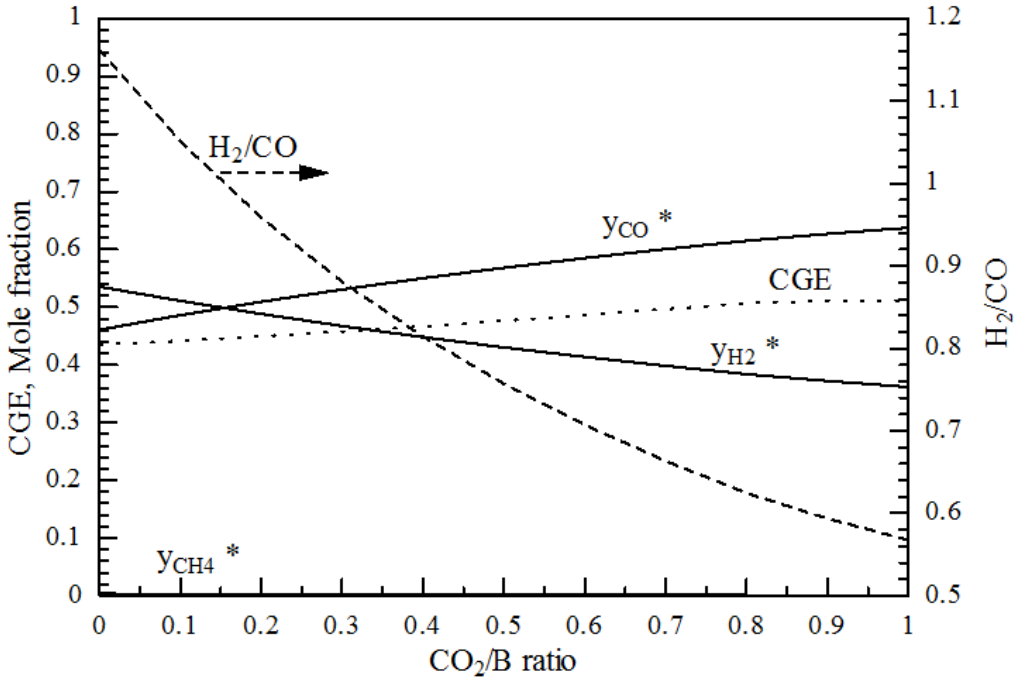

(a) Product gas compositions, CGE and H_2/CO ratio

Note *excluding H_2O and CO_2

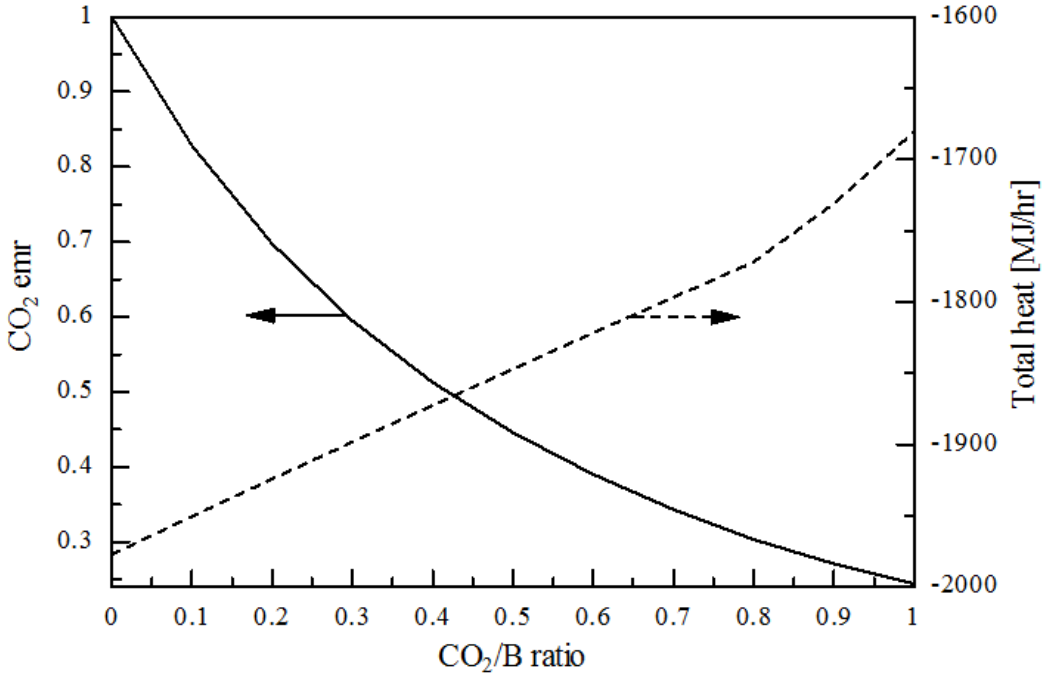

(b) CO_2 emr and total heat

Figure 5.10 Effect of *CO_2/B* feed ratio on (a) product gases and (b) CO_2 emr and total heat (T_g = 600 °C, T_r = 700 °C, *S/B* = 0.4 and *O_2/B* = 0.5)

Figure 5.10(a) shows the product gas compositions. H_2 decreased with increasing *CO_2/B* ratio but CO increased due to the same reason of the previous condition. However in this case, the composition of H_2 was lower than the previous because the lower of steam for reforming with charcoal in the feed and the CO composition was higher because lower of steam caused the reverse boudouard reaction more preferred. CGE reached the maximum at *CO_2/B* of 0.8. For CO_2 emr and net heat shown in Figure 5.10(b), the lowest CO_2 emr achieved was of 0.24 and the net heat obtained was 1,680 MJ/hr for *CO_2/B* = 1. This indicates that lowering the *O_2/B* suitable for reducing the CO_2 emr while the lowering the *S/B* ratio is suitable for reducing the energy supplied to process.

For the best condition of each *O_2/B* and *S/B* feed ratio, the next sub-part study focused on the condition at *O_2/B* and *S/B* of 0.2 and 0.4, respectively. The effect of *CO_2/B* ratio was shown in Figure 5.11.

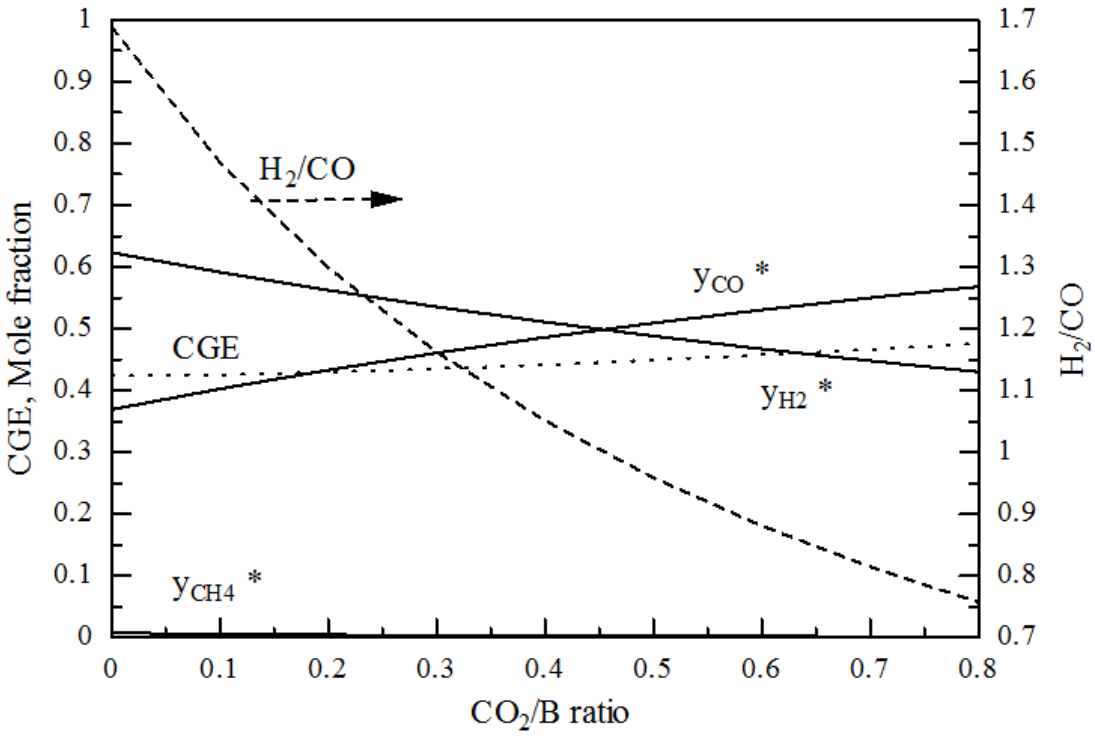

(a) Product gas compositions, CGE and H_2/CO ratio

Note *excluding H_2O and CO_2

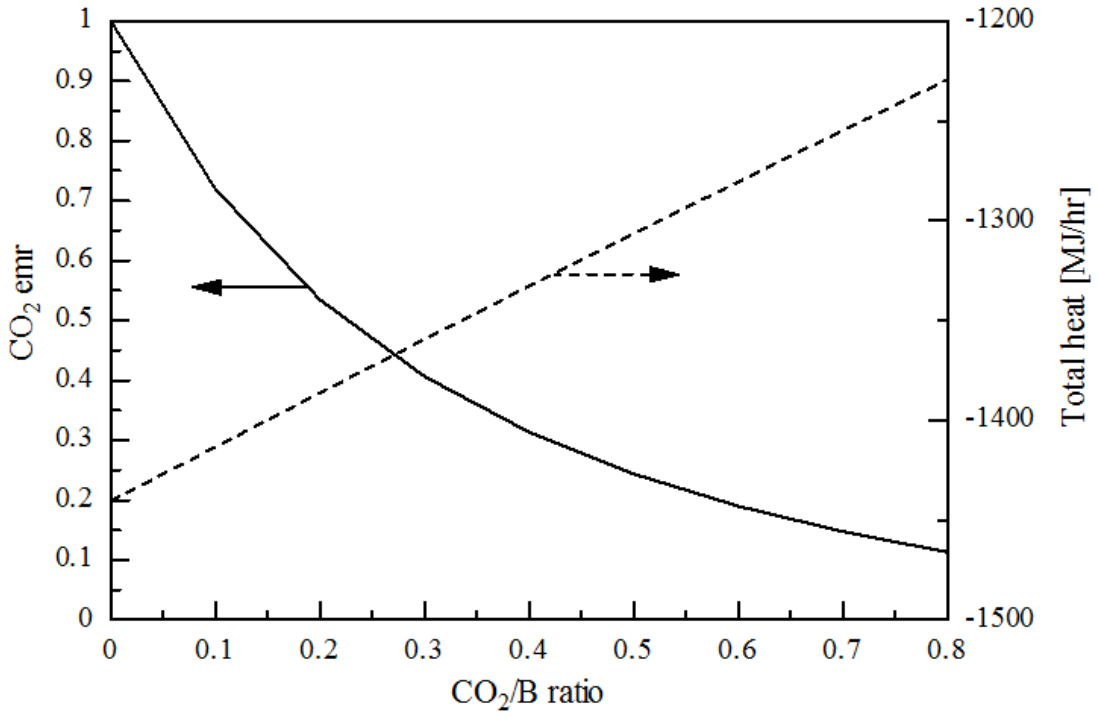

(b) CO_2 emr and total heat

Figure 5.11 Effect of *CO_2/B* feed ratio on (a) product gases and (b) CO_2 emr and total heat (T_g = 600 ºC, T_r = 700 ºC, *S/B* = 0.4 and *O_2/B* = 0.2)

In contrast, the ratio of *CO_2/B* in this case reached the maximum value of 0.8 because the lack of steam and O_2 from feed stream. *S/B* ratio of 0.4 and *O_2/B* ratio of 0.2 are not able to produce enough CO_2 for supplying to the process for the condition of *CO_2/B* ratio higher than 0.8. Figure 5.11(a) shows the similar trend of product gas compositions as the previous condition, however, the CGE is lower than the previous condition because lower syngas was produced. The lack of reaction agents caused the lower yield of produced syngas. The CO_2 emr shows the lowest value of 0.11 when *CO_2/B* ratio is 1. Considering the net heat obtained, this condition also provides the lowest net heat of 1,229 MJ/hr because of low syngas yield.

From all of the previous conditions, the optimum condition in terms of CO_2 emr, CGE and net heat obtained is proposed as *O_2/B* of 0.2 and *S/B* of 0.8. The results were shown in Figure 5.12.

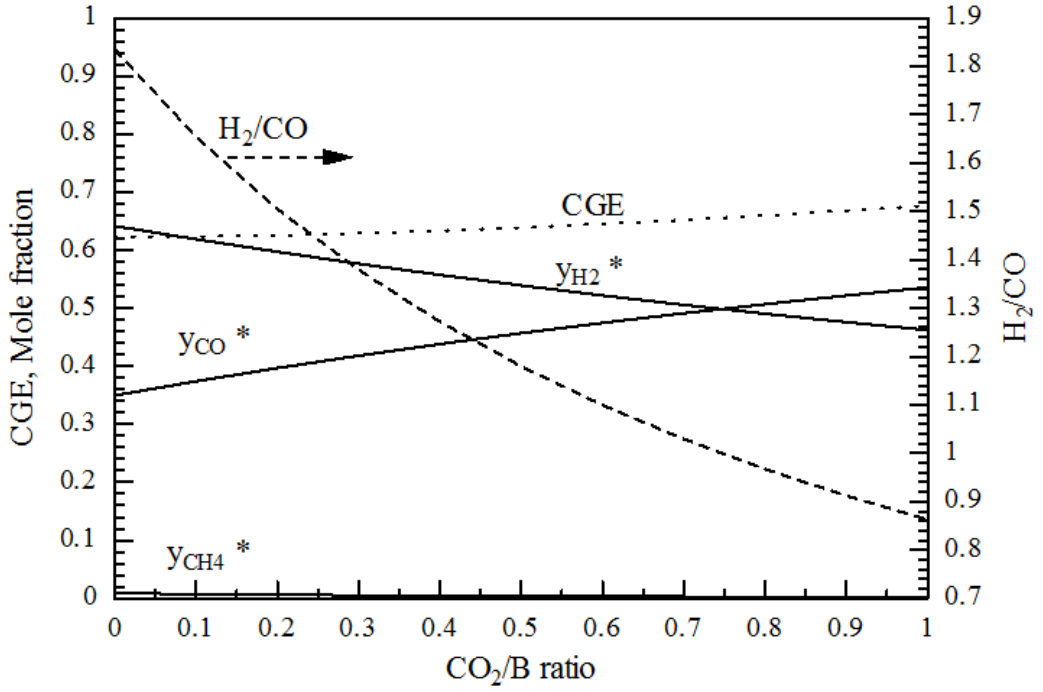

(a) Product gas compositions, CGE and H_2/CO ratio

Note *excluding H_2O and CO_2

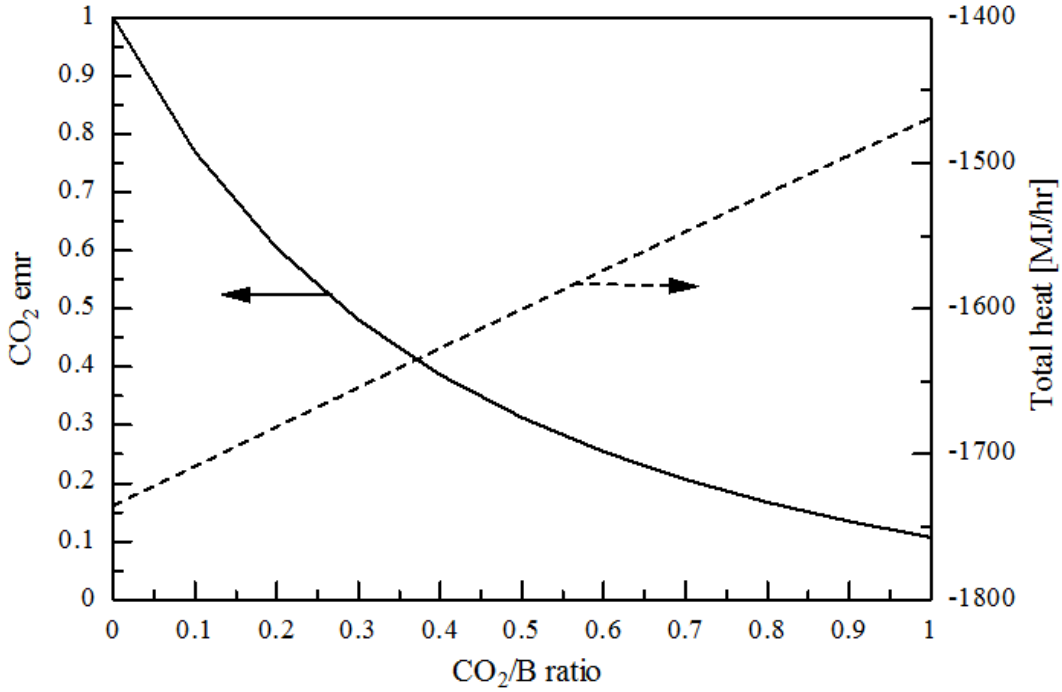

(b) CO_2 emr and total heat

Figure 5.12 Effect of *CO_2/B* feed ratio on (a) product gases and (b) CO_2 emr and total heat (T_g = 600 °C, T_r = 700 °C, *S/B* = 0.8 and *O_2/B* = 0.2)

Figure 5.12(a) shows the similar trend of gas products, but the optimum of this case acquired from the high CGE was almost equal to the case of CO_2/B = 1, O_2/B = 0.2 and S/B = 1. However, the lower S/B of 0.8 in this case offers lower cost in steam generation. Considering CO_2 emr, this case offers the value of 0.10 (Figure 5.12(b)), which was lower than the case of CO_2/B = 1, O_2/B = 0.2 and S/B = 1. Although, the highest net heat obtained from the process, acquired from the case of CO_2/B = 1, O_2/B = 0.5 and S/B = 0.4, is 1,680 MJ/hr but CGE is 0.51 which is lower than that of the present case (CO_2/B 1, O_2/B 0.2 and S/B 0.8) of 0.67 (net heat obtained is 1,468 MJ/hr). Summary of all condition is provided in Table 5.5 as below.

Table 5.5 Summary of simulation with various conditions

Condition	H_2/CO	CGE	CO_2 emr	Net heat obtained (MJ/hr)
Combined gasifier and reformer				
$O_2/S/CO_2/B$ = 0.5/1/0/1	1.91	0.512	1.00	2,011
$O_2/S/CO_2/B$ = 0.5/1/1/1	1.00	0.512	0.32	1,552
$O_2/S/CO_2/B$ = 0.2/1/1/1	0.95	0.769	0.13	1,614
$O_2/S/CO_2/B$ = 0.5/0.4/1/1	0.57	0.511	0.24	1,680
$O_2/S/CO_2/B$ = 0.2/0.4/0.8/1	0.75	0.476	0.11	1,229
$O_2/S/CO_2/B$ = 0.2/0.8/0.8/1	0.97	0.659	0.16	1,520
$O_2/S/CO_2/B$ = 0.2/0.8/1/1	0.86	0.676	0.11	1,468

* $O_2/S/CO_2/B$ means molar feed ratio of O_2, Steam and CO_2 on biomass

Table 5.5 Summary of simulation with various conditions (cont'd)

Condition	H_2/CO	CGE	CO_2 emr	Net heat obtained (MJ/hr)
Without reformer				
$O_2/S/CO_2/B$ = 0.5/1/1/1	1.41	0.505	0.36	1,405
$O_2/S/CO_2/B$ = 0.2/1/1/1	1.21	0.742	0.23	1,234
$O_2/S/CO_2/B$ = 0.5/0.4/1/1	0.73	0.502	0.29	1,507
$O_2/S/CO_2/B$ = 0.2/0.8/1/1	1.10	0.655	0.20	1,158
Gasifier without CO_2 recycle				
$O_2/S/CO_2/B$ = 0.5/1/0/1	2.66	0.498	1.00	2,266

* $O_2/S/CO_2/B$ means molar feed ratio of O_2, Steam and CO_2 on biomass

5.5 Reaction study of combined gasifier and reformer

This part studied the effects of temperature, %Ni loading and feed ratios on product gas compositions, carbon conversion and product gas yield.

5.5.1 Effect of temperature

In order to find out the suitable reaction temperature, tests at various reaction temperatures were conducted. Reaction temperatures of 400 °C, 600 °C and 800 °C were investigated, using only 1 g of charcoal in the quartz tube reactor with feeds of O_2, CO_2 and steam at a ratio of $O_2/CO_2/S/B$ = 0.5/1/1/1. Product gas compositions (excluding H_2O and CO_2) are listed in Table 5.6 as follow.

Table 5.6 Effect of reaction temperature on product gas composition

Biomass	Reaction temperature (°C)	Time (min)	Gas composition (%mol) (excluding H_2O and CO_2)		
			H_2	CO	CH_4
Charcoal	400	30	24.64	33.26	42.09
		60	24.81	34.15	41.03
		120	43.25	56.74	-
		180	42.05	57.94	-
	600	30	43.83	56.16	n/a
		60	47.18	52.72	n/a
		120	59.20	40.80	n/a
		180	100.00	-	n/a
	800	30	12.83	87.17	n/a
		60	24.52	75.47	n/a
		120	100.00	-	n/a
		180	-	-	n/a

The results showed at reaction temperatures of 400 ºC and 600 ºC, 1 g of charcoal was not completely used after 180 minutes of reactions. However, all charcoal was reacted at reaction temperatures of 800 ºC after 120 minutes as observed by no product gas produced anymore (the actual feed ratio is $O_2/CO_2/S/B$ = 0.33/0.66/0.66/1). The mole fractions of product gases at those operating temperatures (excluding H_2O and CO_2) were displayed in Figure 5.13.

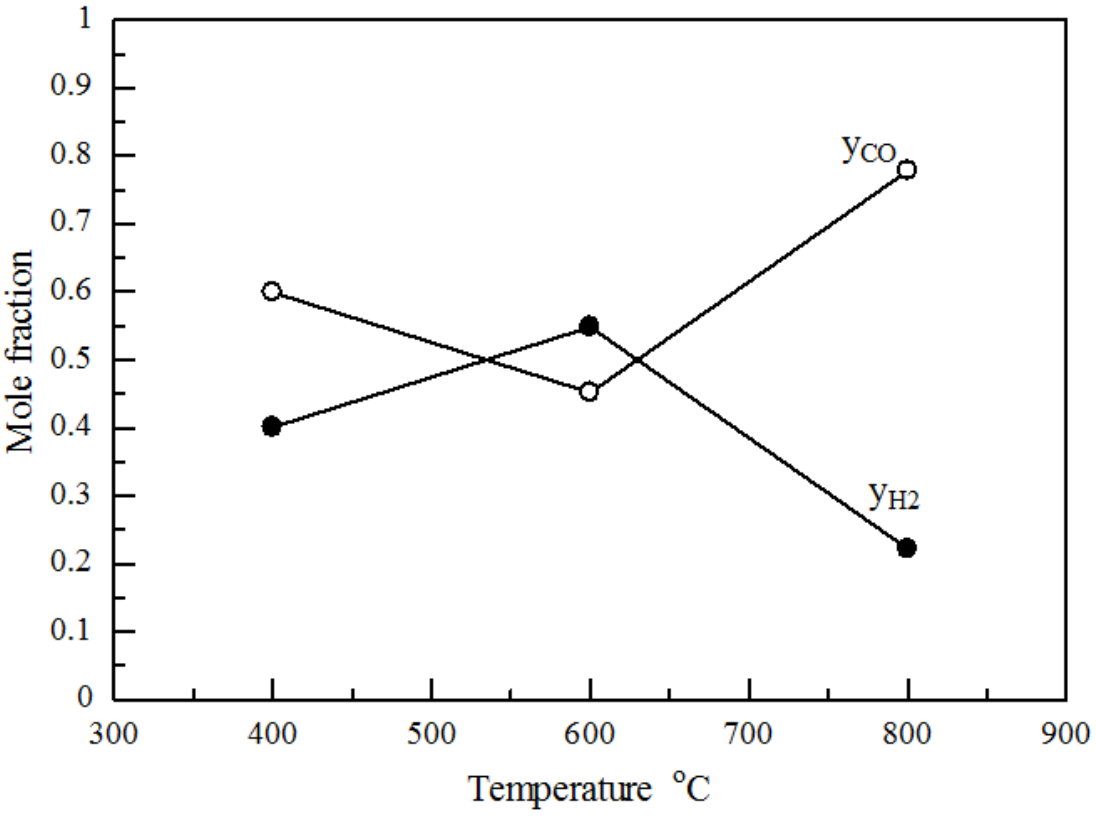

Figure 5.13 Effect of operating temperature on moles fraction of product gases, $O_2/CO_2/S/B$ = 0.5/1/1/1 and Non-catalyst (excluding H_2O and CO_2)

Mole fraction of product gases at 800 ºC contained higher CO than H_2, this is because reverse water gas shift and boudouard reaction are preferred at higher temperature, leading to more CO produced [53]. Carbon conversion and product gas yield were also reported in Figure 5.14.

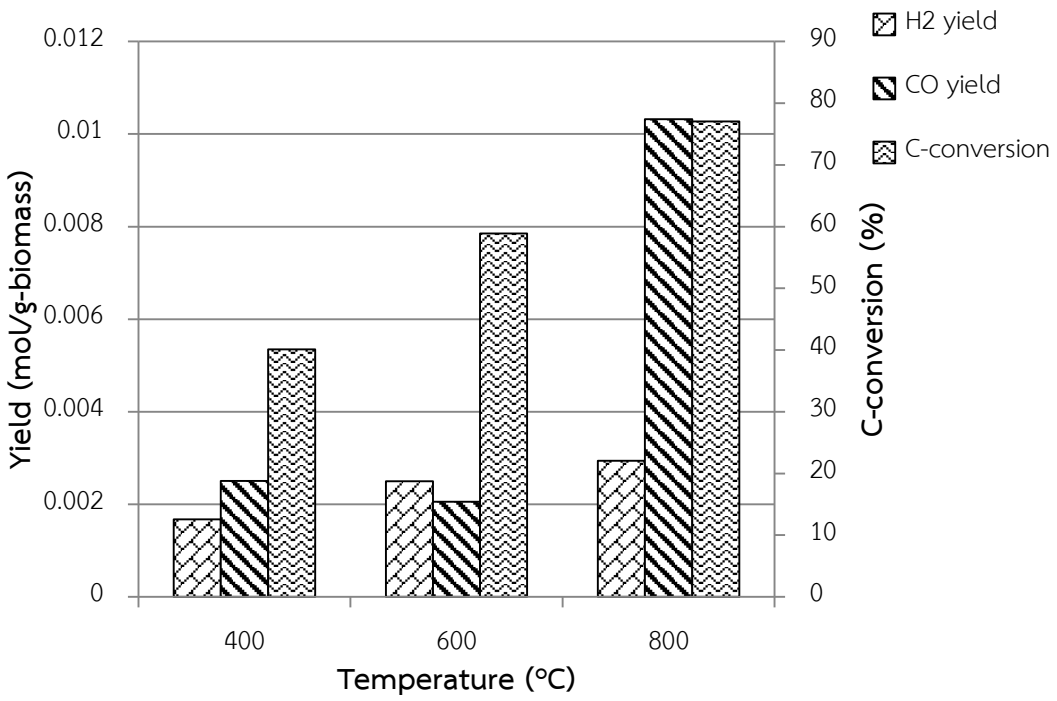

Figure 5.14 Effect of reaction temperature on carbon conversion and product gas yield, $O_2/CO_2/S/B$ = 0.5/1/1/1 and Non-catalyst

Carbon conversion increased with operating temperature from 40% at 400 °C to 77% at 800 °C. Gas yield was calculated by moles of product gas from experiment divided by gram of used biomass. Increasing reaction temperature offers more carbon conversion and product gas yield. For 800 °C, carbon conversion reaches the maximum of 77%, moreover, H_2 and CO yield also reaches the maximum.

5.5.2 Effect of Ni% loading on catalysts

From the result of the highest carbon conversion, the operating temperature of 800 °C and $O_2/CO_2/S/B$ feed ratio of 0.5/1/1/1 were fixed to study the effect of Ni% loading on catalysts. There values of Ni% loading of 5%Ni/SiO_2, 10%Ni/SiO_2 and 15%Ni/SiO_2 were used for evaluating the performance of combined gasifier and reformer process. Product gas compositions are presented in Table 5.7 as follows.

Table 5.7 Effect of Ni% loading on product gas compositions

Biomass	Catalysts	Time (min)	Gas composition (%mol) (excluding H_2O and CO_2)		
			H_2	CO	CH_4
Charcoal	5%Ni/SiO_2	30	12.08	87.92	n/a
		60	22.72	77.28	n/a
		120	n/a	n/a	n/a
		180	n/a	n/a	n/a
	10%Ni/SiO_2	30	12.87	87.13	n/a
		60	23.77	76.23	n/a
		120	32.90	67.10	n/a
		180	46.38	53.62	n/a
	15%Ni/SiO_2	30	11.61	88.39	n/a
		60	16.53	83.47	n/a
		120	32.69	67.31	n/a
		180	n/a	n/a	n/a

For the cases of 10%Ni/SiO_2 and 15%Ni/SiO_2, 1g of charcoal was completely used. However, 5%Ni/SiO_2 reached complete reaction at 100 minutes (the actual feed ratio is $O_2/CO_2/S/B$ = 0.27/0.55/0.55/1).

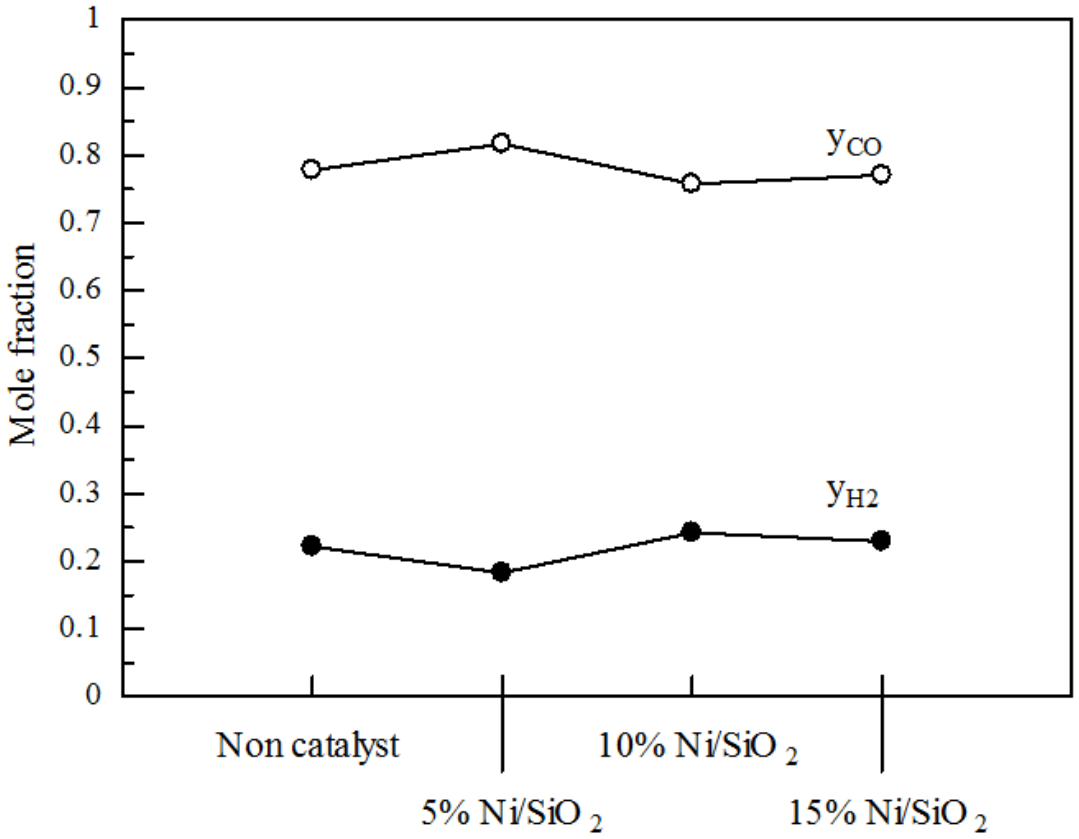

Figure 5.15 Mole fractions of product gases for catalysts with different loading, T = 800 °C and $O_2/CO_2/S/B$ = 0.5/1/1/1 (excluding H_2O and CO_2)

Adding the catalysts was able to improve the performance of the process by increasing H_2 and CO contents. The effects of different Ni% loading were conducted for 3 hours. However, only slight changes in mole fraction of the product gases were observed (Figure 5.15) because the amount of H_2 and CO increased in almost proportional ratio.

Therefore, adding reforming catalysts in the reactor could improve the performance by upgrading syngas product as observed in increasing of product gas yield with higher Ni% loading (Figure 5.16). Then, carbon conversion was also investigated and the results were displayed in Figure 5.16.

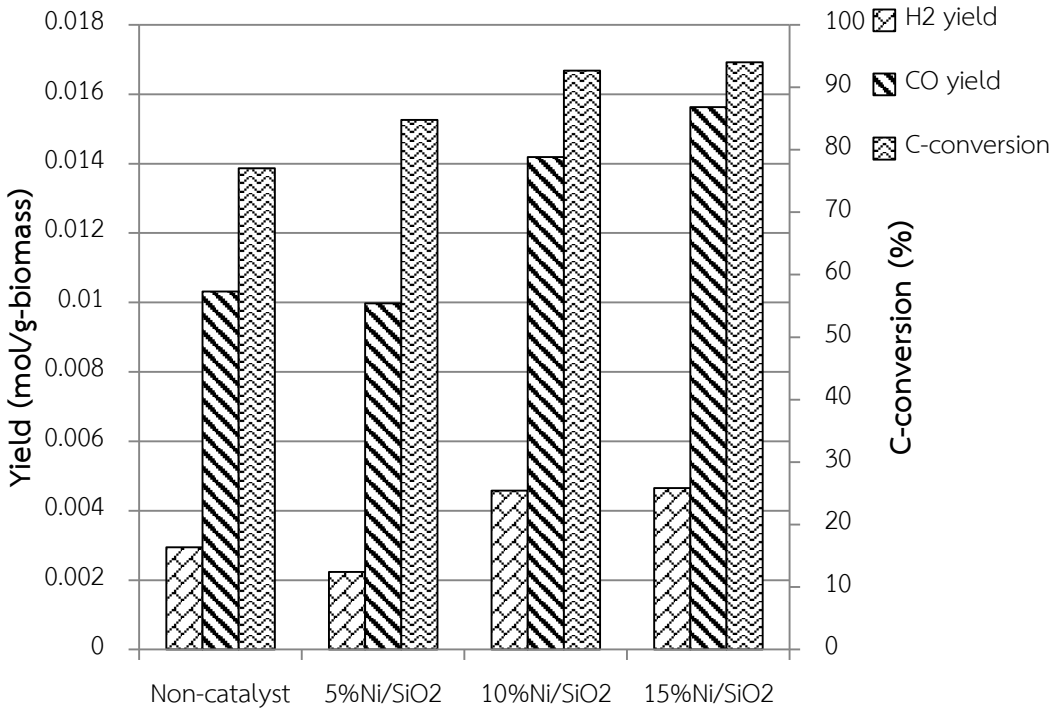

Figure 5.16 Carbon conversions of various catalysts, T = 800 ºC and $O_2/CO_2/S/B$ = 0.5/1/1/1

Carbon to gas conversion was calculated by total moles of carbon atom in gas product divided by moles of 1 g charcoal. So, increasing in carbon conversion is due to increase of CO in syngas product as presented in Figure 5.16. By the reason in quantity of syngas product compared to percentage of Ni loading and carbon conversion, so the optimum catalyst is 10%Ni/SiO_2.

Then, the further studied using 10%Ni/SiO_2 catalyst and operating temperature of 800 ºC were conducted. The results of the effects of O_2/B, S/B and CO_2/B were described as follows.

5.5.3 Effect of O_2/B feed ratio

The presence of O_2 in feed stream offers both advantage and disadvantage. On one hand, higher O_2 causes the reaction preferably to combustion from partial oxidation reaction which means that more CO_2 was produced than CO. On the other hand, introducing O_2 can be reduced heat supplying to the reactor due to the exothermic of combustion reaction [35]. Figure 5.17 shows the total moles of product gas, represented product gas yield, after 3 hours of reaction time, introducing O_2 from ratio 0 to 0.5 could slightly improve the CO via partial oxidation reaction. Product gas composition with time on stream is shown in Table 5.8.

Table 5.8 Effect of O2/B feed ratio on product gas composition

Biomass	O_2/B ratio	Time (min)	Gas composition (%mol) (excluding H_2O and CO_2)		
			H_2	CO	CH_4
Charcoal	0	30	14.50	85.50	n/a
		60	24.33	75.67	n/a
		120	31.07	68.93	n/a
		180	33.05	66.95	n/a
	0.5	30	12.87	87.13	n/a
		60	23.77	76.23	n/a
		120	32.90	67.10	n/a
		180	46.38	53.62	n/a

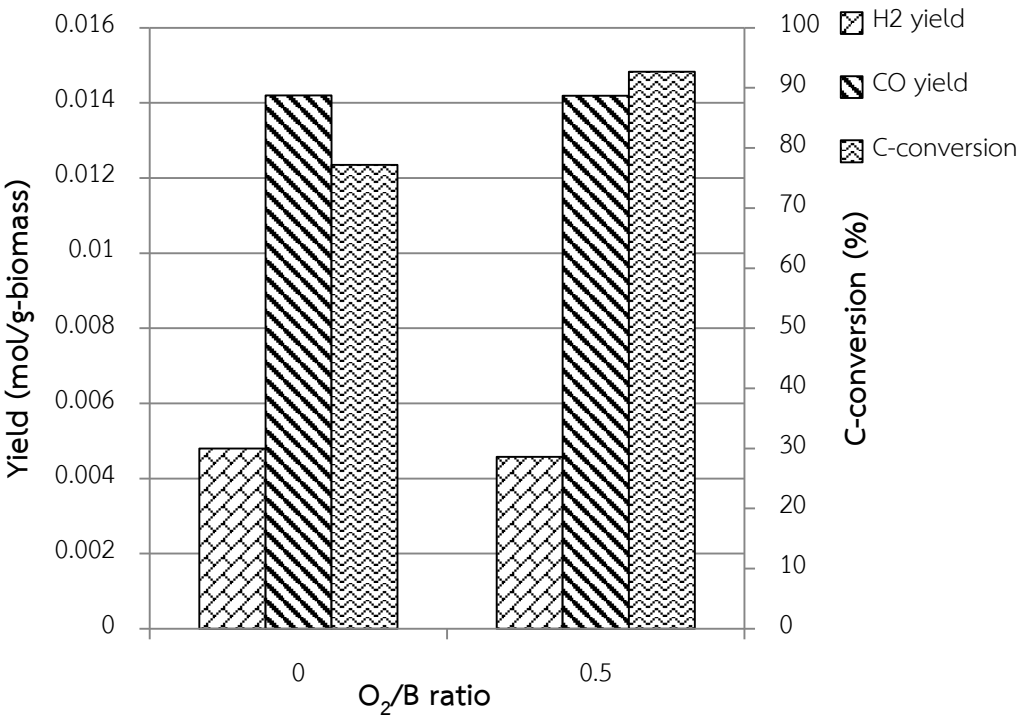

Figure 5.17 Effect of *O_2/B* ratio on carbon conversions and product gas yield, T = 800 °C, *CO_2/S/B* = 1/1/1 and used 10%Ni/SiO_2

Introducing the O_2 can improve the process performance as observed in Figure 5.17, by increasing *O_2/B* ratio from 0 to 0.5 increased the carbon conversion by 17%.

5.5.4 Effect of *S/B* ratio

The effect of *S/B* feed ratio was also investigated in the experimental studies. *S/B* feed ratios were varied by 0, 1 and 2. All the results indicated that 1 g of charcoal was completely used in 3 hours reaction time. The product gas composition is listed in Table 5.9 as below.

Table 5.9 Effect of *S/B* feed ratio on product gas composition

Biomass	S/B	Time (min)	Gas composition (%mol) (excluding H_2O and CO_2)		
			H_2	CO	CH_4
Charcoal	0	30	13.20	86.80	n/a
		60	15.42	84.58	n/a
		120	20.28	79.72	n/a
		180	100.00	-	n/a
	1	30	12.87	87.13	n/a
		60	23.77	76.23	n/a
		120	32.90	67.10	n/a
		180	46.38	53.62	n/a
	2	30	14.67	85.33	n/a
		60	39.22	60.78	n/a
		120	50.91	49.09	n/a
		180	-	-	n/a

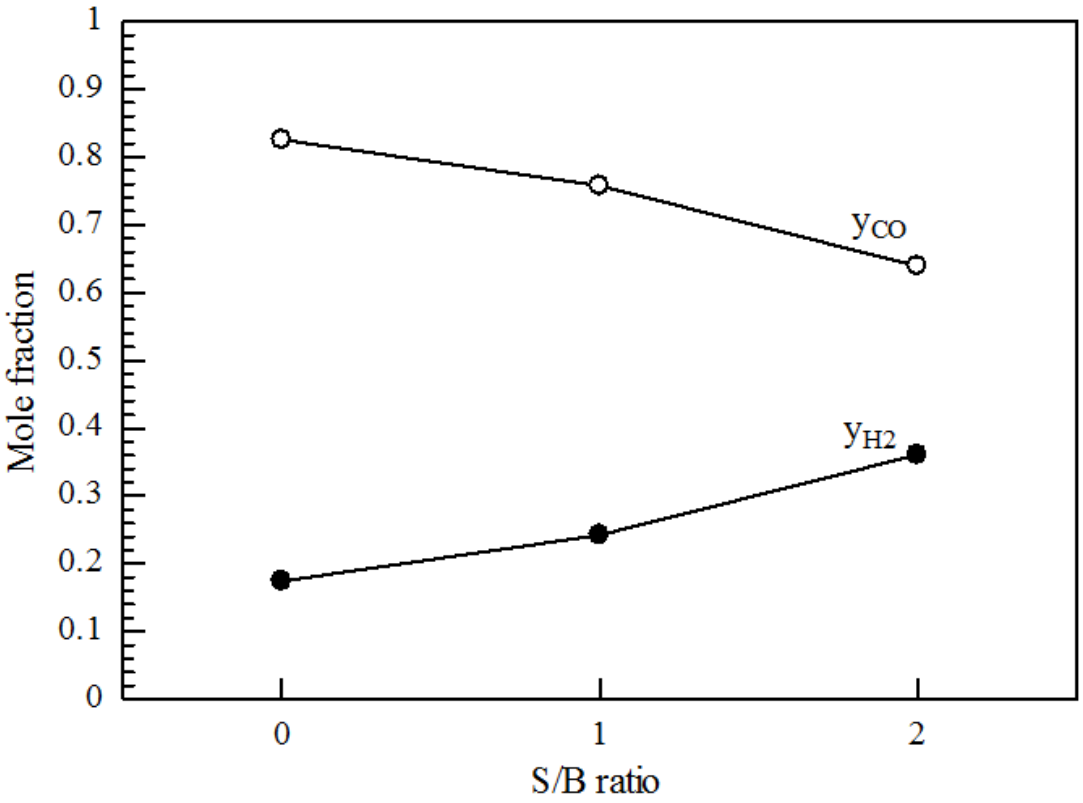

Figure 5.18 Effect of *S/B* feed ratio on mole fraction of product gases, T = 800 °C, $O_2/CO_2/B$ = 0.5/1/1 and used 10%Ni/SiO_2 (excluding H_2O and CO_2)

Figure 5.18 shows the effect of *S/B* ratio on product gas mole fractions. This can be observed that higher *S/B* ratio offers higher mole fraction of H_2 because more steam shifts the steam reforming [15] and water gas shift reaction also plays an important role in decreasing of CO [10], according to the product gas yield (Figure 5.19).

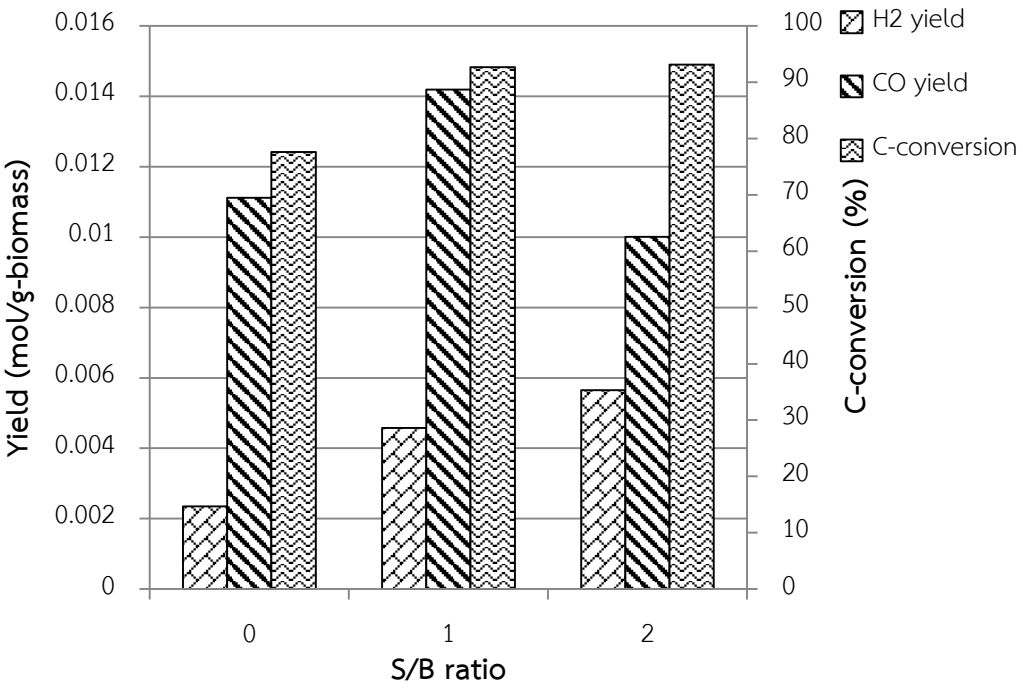

Figure 5.19 Effect of *S/B* feed ratio on carbon conversion and product gas yield, T = 800 °C, $O_2/CO_2/B$ = 0.5/1/1 and used 10%Ni/SiO_2

Figure 5.19 shows that the carbon conversion increased from 77% to 94% by increasing *S/B* ratio from 0 to 2. However, the product gas yield of H_2 increased from *S/B* ratio 0 to 2 due to water gas shift reaction [10]. But, CO yield was observed for the maximum at *S/B* ratio of 1. In overview, in this case of the experimental studies shows poor performance in syngas production due to presence of CO_2 in the feed stream compared to other research with no CO_2 in feed stream [10].

5.5.5 Effect of CO_2/B feed ratio

The effect of CO_2/B ratio is another interesting parameter. The higher CO_2/B ratio indicated the case with more CO_2 recycled back to the process. This offers an advantage in utilizing CO_2 instead of emitting it to atmosphere. Results of product gas composition are shown in Table 5.10 as below.

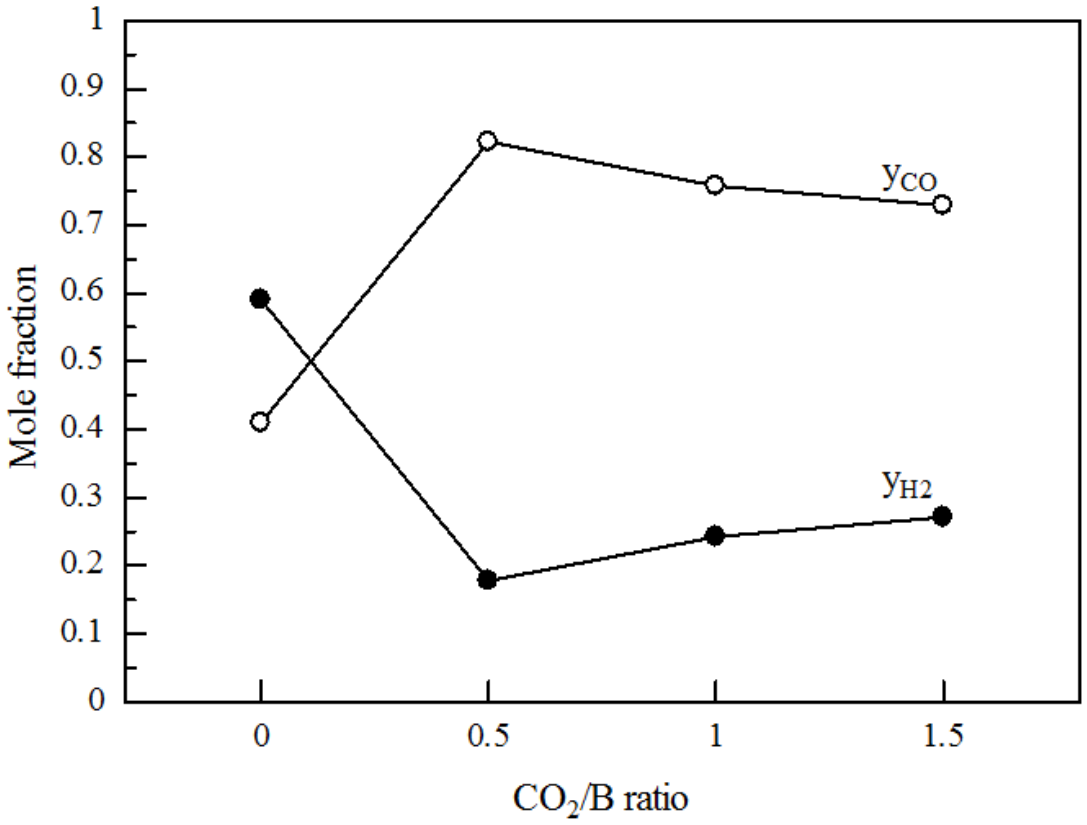

Figure 5.20 Effect of *CO_2/B* feed ratio on mole fraction of product gases on, T = 800 °C, *O_2/S/B* = 0.5/1/1 and used 10%Ni/SiO_2 (excluding H_2O and CO_2)

Table 5.10 Effect of CO_2/B feed ratio on product gas composition

Biomass	CO_2/B ratio	Time (min)	Gas composition (%mol) (excluding H_2O and CO_2)		
			H_2	CO	CH_4
Charcoal	0	30	38.01	61.99	n/a
		60	59.84	40.16	n/a
		120	59.22	40.78	n/a
		180	66.28	33.72	n/a
	0.5	30	14.67	85.33	n/a
		60	16.74	83.26	n/a
		120	20.96	79.04	n/a
		180	29.17	70.83	n/a

Table 5.10 Effect of *CO_2/B* feed ratio on product gas composition (cont'd)

Biomass	*CO_2/B* ratio	Time (min)	Gas composition (%mol) (excluding H_2O and CO_2)		
			H_2	CO	CH_4
Charcoal	1	30	12.87	87.13	n/a
		60	23.77	76.23	n/a
		120	32.90	67.10	n/a
		180	46.38	53.62	n/a
	1.5	30	18.28	81.72	n/a
		60	25.56	74.44	n/a
		120	33.08	66.92	n/a
		180	34.78	65.22	n/a

According to the previous work of Wang *et al*. [15] on the effect of CO_2 to propane molar feed ratio, the results indicated that moles of H_2 in product gas were close in both cases of CO_2 to propane molar ratio 1 and 3. The results from this study, as shown in Figure 5.20, show the similar trend.

For *CO_2/B* ratio of 0, this can represented the main reaction consisting of steam and partial oxidation. This offered the highest H_2 in syngas product and also high CO. But in term of CO_2 emission, this offers the low performance. The suitable ratio was *CO_2/B* = 1 due to the highest moles of H_2 and CO in product gas. Carbon conversion and product gas yield were also investigated as presented in Figure 5.21.

And Figure 5.21 also reported that product gas yield for the case of *CO_2/B* ratio of 0 shows the highest but dropped with the addition of CO_2 in the feed stream. The highest carbon conversion was observed in the case of *CO_2/B* ratio 1; this can be inferred that charcoal was converted into syngas product.

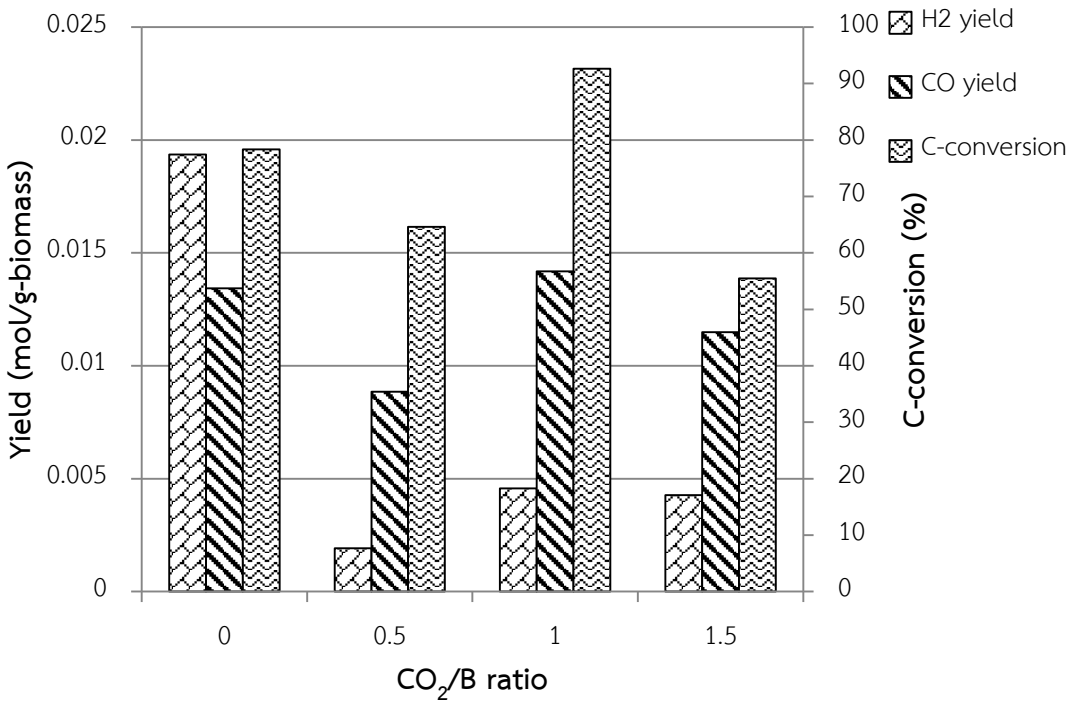

Figure 5.21 Effect of *CO_2/B* feed ratio on carbon conversion and product gas yield, T = 800 °C, *O_2/S/B* = 0.5/1/1 and used 10%Ni/SiO_2

Table 5.11 Syngas ratio on various feed ratio

Conditions	H_2/CO
$O_2/S/CO_2/B$ = 0.5/1/1/1	0.32
$O_2/S/CO_2/B$ = 0/1/1/1	0.34
$O_2/S/CO_2/B$ = 0.5/0/1/1	0.21
$O_2/S/CO_2/B$ = 0.5/2/1/1	0.56
$O_2/S/CO_2/B$ = 0.5/1/0/1	1.44
$O_2/S/CO_2/B$ = 0.5/1/0.5/1	0.22
$O_2/S/CO_2/B$ = 0.5/1/1.5/1	0.37

Finally, Syngas ratio was also observed in all of studied cases. Table 5.11 shows that syngas ratio from various O_2/B was not much different. By increasing S/B ratio, syngas ratio becomes higher. When increasing CO_2/B ratio, syngas ratio can be adjusted in wider range than being adjusted by steam and O_2 (0.2-1.4).

5.6 Comparison of model and experimental

For case of reaction temperature 800 °C, the mole fraction of product gas from experimental was calculation using raw data as shown in Figure 5.22. Comparison of product gas mole fraction on different percentage from modeling and experimental was conducted to investigate the different of modeling and experimental.

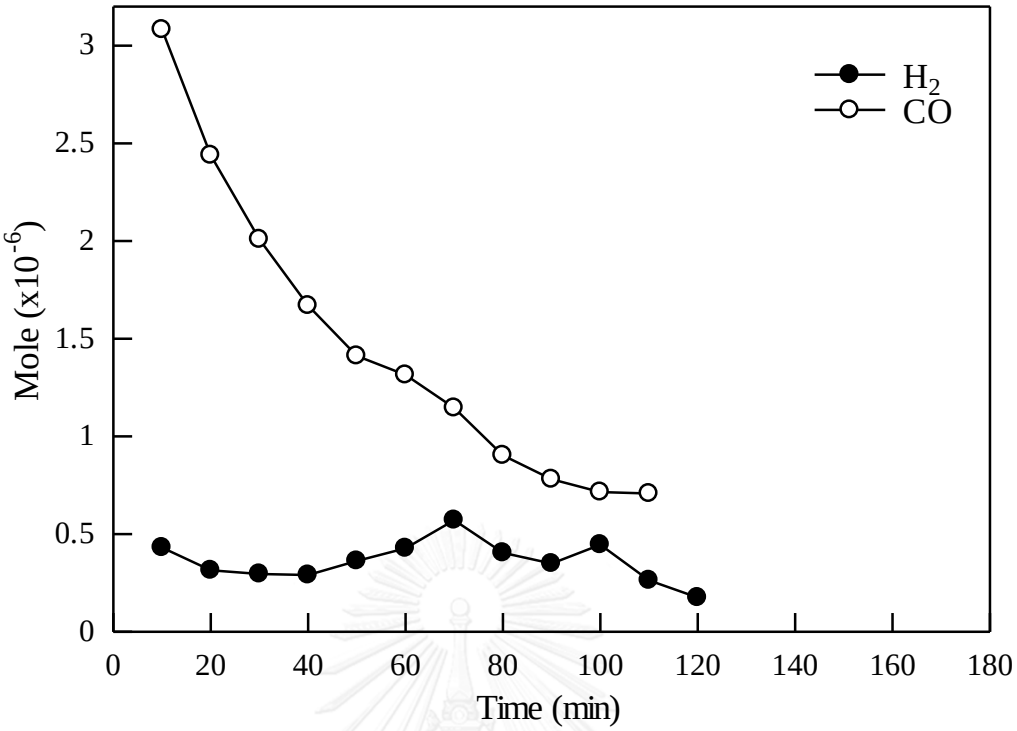

Figure 5.22 Raw result of product gas from experiment
(T = 800 °C, non-catalyst and $O_2/S/CO_2/B$ = 0.5/1/1/1)

For experimental, the product gas mole fraction was calculated as y_{H2} = 0.222 and y_{CO} = 0.778, for modeling, y_{H2} = 0.434 and y_{CO} = 0.566. Then calculate the different percentage between modeling and experimental of H_2 was 48.85% and CO was 37.45%.

CHAPTER 6
CONCLUSIONS AND RECOMMENDATIONS

In this work, the performance of combined gasifier and reformer using charcoal was evaluated on product gas composition, CO_2 emr, CGE, carbon conversion, product gas yield and H_2/CO ratio. The effects of temperature, feed ratio and Ni% loading on catalyst were considered. The conclusions and recommendations for future work were listed below.

6.1 Conclusions

1. The thermodynamic analysis results indicated that the suitable operating temperature was 700 ºC because this temperature offered the highest CGE and optimum net heat obtained from process. The suitable *O_2/B* and *S/B* feed ratios were at 0.2 and 0.4, respectively, which are considered in terms of CGE and net heat obtained. Increasing *CO_2/B* ratio decreased the CO_2 emr, but lower net heat and H_2 content in syngas product were also obtained. H_2/CO ratio was easier adjusted by altering the *CO_2/B* in the feed stream.

2. The results of the experimental study showed the good agreement with thermodynamic analysis simulation. This can be observed from the trend of the results. Higher operating temperature leaded to more carbon conversion and syngas product. Results of *O_2/B* feed ratio deviated slightly from simulation results. The H_2 content in syngas product increased with increasing *S/B* ratio. The higher *CO_2/B* feed ratio offered increasing of CO and decreased H_2. Moreover, the H_2/CO ratio can be adjusted from 0.2 to 1.4 by varying the *CO_2/B* feed ratio.

3. Catalyst characterization revealed that higher Ni% loading on SiO_2 caused reduction in surface area of catalyst as observed by BET method. From the results of H_2-TPR peaks, the suitable reducing temperature was in range of 350 ºC – 400 ºC. 10%Ni/SiO_2 was the optimum catalyst according to the suitable syngas product.

6.2 Recommendation

1. From the reaction studied, using the mass flow controller offered the higher accurate in adjusting flow rate than using the needle valve.

2. Gas chromatography should examine the light hydrocarbons, this offers higher accurate in calculating carbon conversion.

3. The size of quartz tube reactor affects the height of charcoal pack bed, bigger quartz tube reactor offers the shorter pack bed, leading to reduce error in temperature profile of furnace.

4. The effect of catalyst support should be considered.

5. Split furnace to two units can be improved in controlling temperature profile of reactor.

REFERENCES

[1] McKendry, P. Energy production from biomass (part 1) overview of biomass. Bioresource Technology 83 (2002): 37-46.

[2] Cocco, D., Serra, F., and Tola, V. Assessment of energy and economic benefits arising from syngas storage in IGCC power plants. Energy 58 (2013): 635-643.

[3] Sorgenfrei, M. and Tsatsaronis, G. Design and evaluation of an IGCC power plant using iron-based syngas chemical-looping (SCL) combustion. Applied Energy 113 (2014): 1958-1964.

[4] Khine, M.S.S., Chen, L., Zhang, S., Lin, J., and Jiang, S.P. Syngas production by catalytic partial oxidation of methane over (La0.7A0.3)BO3 (A = Ba, Ca, Mg, Sr, and B = Cr or Fe) perovskite oxides for portable fuel cell applications. International Journal of Hydrogen Energy 38(30) (2013): 13300-13308.

[5] Hackett, G.A., et al. Performance of solid oxide fuel cells operated with coal syngas provided directly from a gasification process. Journal of Power Sources 214 (2012): 142-152.

[6] Mondal, P., Dang, G.S., and Garg, M.O. Syngas production through gasification and cleanup for downstream applications — Recent developments. Fuel Processing Technology 92(8) (2011): 1395-1410.

[7] H.C., B. and M.J., C. CO2 as a Carbon Neutral Fuel Source via Enhanced Biomass Gasification. Environment Science Technology 43 (2009): 9030-9037.

[8] Cheng, G., et al. Gasification of biomass micron fuel with oxygen-enriched air: Thermogravimetric analysis and gasification in a cyclone furnace. Energy 43(1) (2012): 329-333.

[9] Moghtaderi, B. Effects of controlling parameters on production of hydrogen by catalytic steam gasification of biomass at low temperatures. Fuel 86(15) (2007): 2422-2430.

[10] Wei, L., Xu, S., Zhang, L., Liu, C., Zhu, H., and Liu, S. Steam gasification of biomass for hydrogen-rich gas in a free-fall reactor. International Journal of Hydrogen Energy 32(1) (2007): 24-31.

[11] Chaiwatanodom, P., Vivanpatarakij, S., and Assabumrungrat, S. Thermodynamic analysis of biomass gasification with CO2 recycle for synthesis gas production. Applied Energy 114 (2014): 10-17.

[12] Renganathan, T., Yadav, M.V., Pushpavanam, S., Voolapalli, R.K., and Cho, Y.S. CO2 utilization for gasification of carbonaceous feedstocks: A thermodynamic analysis. Chemical Engineering Science 83 (2012): 159-170.

[13] Antzara, A., Heracleous, E., Bukur, D.B., and Lemonidou, A.A. Thermodynamic analysis of hydrogen production via chemical looping steam methane reforming coupled with in situ CO2 capture. International Journal of Greenhouse Gas Control 32 (2015): 115-128.

[14] Tomishige, K., Asadullah, M., and Kunimori, K. Syngas production by biomass gasification using Rh/CeO2/SiO2 catalysts and fluidized bed reactor. Catalysis Today 89(4) (2004): 389-403.

[15] Wang, X., Wang, N., Zhao, J., and Wang, L. Thermodynamic analysis of propane dry and steam reforming for synthesis gas or hydrogen production. International Journal of Hydrogen Energy 35(23) (2010): 12800-12807.

[16] Pompeo, F., Nichio, N.N., Souza, M.M.V.M., Cesar, D.V., Ferretti, O.A., and Schmal, M. Study of Ni and Pt catalysts supported on α-Al2O3 and ZrO2 applied in methane reforming with CO2. Applied Catalysis A: General 316(2) (2007): 175-183.

[17] Liu, D., Quek, X.-Y., Wah, H.H.A., Zeng, G., Li, Y., and Yang, Y. Carbon dioxide reforming of methane over nickel-grafted SBA-15 and MCM-41 catalysts. Catalysis Today 148(3-4) (2009): 243-250.

[18] Horváth, A., et al. Sol-derived AuNi/MgAl2O4 catalysts: Formation, structure and activity in dry reforming of methane. Applied Catalysis A: General 468 (2013): 250-259.

[19] Taufiq-Yap, Y.H., Sudarno, Rashid, U., and Zainal, Z. CeO2–SiO2 supported nickel catalysts for dry reforming of methane toward syngas production. Applied Catalysis A: General 468 (2013): 359-369.

[20] Huang, B.-S., Chen, H.-Y., Chuang, K.-H., Yang, R.-X., and Wey, M.-Y. Hydrogen production by biomass gasification in a fluidized-bed reactor promoted by an

Fe/CaO catalyst. International Journal of Hydrogen Energy 37(8) (2012): 6511-6518.

[21] Bermúdez, J.M., Fidalgo, B., Arenillas, A., and Menéndez, J.A. CO2 reforming of coke oven gas over a Ni/γAl2O3 catalyst to produce syngas for methanol synthesis. Fuel 94 (2012): 197-203.

[22] Fakeeha, A.H., Khan, W.U., Al-Fatesh, A.S., and Abasaeed, A.E. Stabilities of zeolite-supported Ni catalysts for dry reforming of methane. Chinese Journal of Catalysis 34(4) (2013): 764-768.

[23] Gao, N., Li, A., Quan, C., and Gao, F. Hydrogen-rich gas production from biomass steam gasification in an updraft fixed-bed gasifier combined with a porous ceramic reformer. International Journal of Hydrogen Energy 33(20) (2008): 5430-5438.

[24] Wu, C. and Williams, P.T. Hydrogen production by steam gasification of polypropylene with various nickel catalysts. Applied Catalysis B: Environmental 87(3-4) (2009): 152-161.

[25] Wu, C., Wang, Z., Huang, J., and Williams, P.T. Pyrolysis/gasification of cellulose, hemicellulose and lignin for hydrogen production in the presence of various nickel-based catalysts. Fuel 106 (2013): 697-706.

[26] Puig-Arnavat, M., Bruno, J.C., and Coronas, A. Review and analysis of biomass gasification models. Renewable and Sustainable Energy Reviews 14(9) (2010): 2841-2851.

[27] Gujar, A.C., Baik, J., Garceau, N., Muradov, N., and T-Raissi, A. Oxygen-blown gasification of pine charcoal in a top-lit downdraft moving-hearth gasifier. Fuel 118 (2014): 27-32.

[28] Rajvanshi, A.K. Biomass Gasification. Alternative Energy in Agriculture. Vol. II. India: CRC Press, 1986.

[29] Schapfer, P. and Tobler, J. Theoretical and Practical Investigations Upon the Driving of Motor Vehicles with Wood Gas. 1937.

[30] Rostrup-Nielsen, J.R. and Hansen, J.B. Steam Reforming for Fuel Cells. (2011): 49-71.

[31] Smith, M.W. and Shekhawat, D. Catalytic Partial Oxidation. (2011): 73-128.

[32] Gao, J., Hou, Z., Lou, H., and Zheng, X. Dry (CO2) Reforming. (2011): 191-221.

[33] Peters, L., Hussain, A., Follmann, M., Melin, T., and Hägg, M.B. CO2 removal from natural gas by employing amine absorption and membrane technology—A technical and economical analysis. Chemical Engineering Journal 172(2-3) (2011): 952-960.

[34] Udomsirichakorn, J. and Salam, P.A. Review of hydrogen-enriched gas production from steam gasification of biomass: The prospect of CaO-based chemical looping gasification. Renewable and Sustainable Energy Reviews 30 (2014): 565-579.

[35] Lv, P.M., Xiong, Z.H., Chang, J., Wu, C.Z., Chen, Y., and Zhu, J.X. An experimental study on biomass air-steam gasification in a fluidized bed. Bioresour Technol 95(1) (2004): 95-101.

[36] Zhang, R., Cummer, K., Suby, A., and Brown, R.C. Biomass-derived hydrogen from an air-blown gasifier. Fuel Processing Technology 86(8) (2005): 861-874.

[37] Song, T., Wu, J., Shen, L., and Xiao, J. Experimental investigation on hydrogen production from biomass gasification in interconnected fluidized beds. Biomass and Bioenergy 36 (2012): 258-267.

[38] Ahmed, I. and Gupta, A.K. Characteristics of cardboard and paper gasification with CO2. Applied Energy 86(12) (2009): 2626-2634.

[39] Garcia, L., Salvador, M.L., Arauzo, J., and Bilbao, R. CO2 as a gasifying agent for gas production from 2 pine sawdust at low temperatures using a Ni-Al coprecipitated catalyst. Fuel Processing Technology 69 (2001): 157-174.

[40] Karim, G.A. and M.M., M. A kinetic investigation of the reforming of natural gas for the production of hydrogen. Hydrogen Energy 5 (1979): 293-304.

[41] Park, H.J., et al. Steam reforming of biomass gasification tar using benzene as a model compound over various Ni supported metal oxide catalysts. Bioresource Technology 101 Suppl 1 (2010): S101-3.

[42] Fierro, V., Klouz, V., Akdim, O., and Mirodatos, C. Oxidative reforming of biomass derived ethanol for hydrogen production in fuel cell applications. Catalysis Today 75 (2002): 141-144.

[43] Vicente, J., Ereña, J., Montero, C., Azkoiti, M.J., Bilbao, J., and Gayubo, A.G. Reaction pathway for ethanol steam reforming on a Ni/SiO2 catalyst including coke formation. International Journal of Hydrogen Energy 39(33) (2014): 18820-18834.

[44] Bermúdez, J.M., Fidalgo, B., Arenillas, A., and Menéndez, J.A. Dry reforming of coke oven gases over activated carbon to produce syngas for methanol synthesis. Fuel 89(10) (2010): 2897-2902.

[45] Zhang, J. and Li, F. Coke-resistant Ni@SiO2 catalyst for dry reforming of methane. Applied Catalysis B: Environmental 176-177 (2015): 513-521.

[46] Li, B., Xu, X., and Zhang, S. Synthesis gas production in the combined CO2 reforming with partial oxidation of methane over Ce-promoted Ni/SiO2 catalysts. International Journal of Hydrogen Energy 38(2) (2013): 890-900.

[47] Rulerk, D., Assabumrungrat, S., and Vivanpatarakij, S. Removal of tar from biomass gasification process by steam reforming over nickel catalysts. Master of Engineering, Chemical Engineering Chulalongkorn University, 2011.

[48] Rodrigues, R., Secchi, A.R., Marcílio, N.R., and Godinho, M. Modeling of biomass gasification applied to a combined gasifier- combustor unit equilibrium and kinetic approaches. 10th International Symposium on Process Systems Engineering (2009).

[49] Channiwala, S.A. and Parikh, P.P. A unified correlation for estimating HHV of solid liqiud and gaseous fuels. Fuel 81 (2002): 1051-1063.

[50] Ghassemi, H. and Shahsavan-Markadeh, R. Effects of various operational parameters on biomass gasification process; a modified equilibrium model. Energy Conversion and Management 79 (2014): 18-24.

[51] Wang, Y., Wu, R., and Zhao, Y. Effect of ZrO2 promoter on structure and catalytic activity of the Ni/SiO2 catalyst for CO methanation in hydrogen-rich gases. Catalysis Today 158(3-4) (2010): 470-474.

[52] Gopaul, S.G. and Dutta, A. Dry reforming of multiple biogas types for syngas production simulated using Aspen Plus: The use of partial oxidation and hydrogen combustion to achieve thermo-neutrality. International Journal of Hydrogen Energy 40(19) (2015): 6307-6318.

[53] Franco, C., Pinto, F., Gulyurtlu, I., and Cabrita, I. The study of reactions influencing the biomass steam gasification process. Fuel 82 (2003): 835-842.

[54] Smith, J.M., Van Ness, H.C., and Abbott, M.M. Introduction to Chemical Engineering Thermodynamics, ed. 7th. McGraw-Hill Science.

APPENDIX

APPENDIX A

Calculation of carbon conversion, CGE, CO2 emr and Total net heat in simulation studied

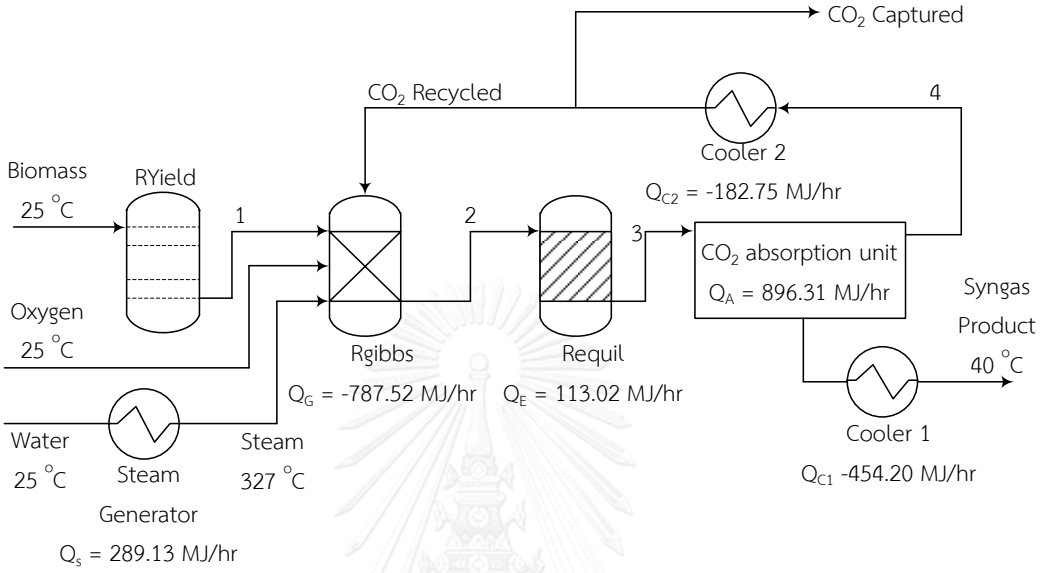

Note: Q_s Net heat of steam generator unit

Q_G Net heat of RGibbs unit

Q_E Net heat of REquil unit

Q_A Net heat of CO_2 absorption unit

Q_{C1}, Q_{C2} Net heat of cooler 1 and cooler 2 units

Figure A.1 Process flow diagram of combined gasifier and reformer (T_g = 600 ºC, T_r = 700 ºC and $O_2/S/CO_2/B$ = 0.5/1/1/1)

For the studied in effect of gasifier temperature, the carbon conversion was calculated using difference of carbon feed rate from stream 1 and stream 2 (Figure A.1) divided by carbon feed rate from stream 1 them multiply by 100 (Eq. 4.2) as showed below.

A.1 Carbon conversion from condition: T_g = 400 °C and $O_2/S/CO_2/B$ = 0.5/1/1/1

Carbon inlet from stream 1 = 5.127 kmol/hr

Carbon outlet from steam 2 = 1.098 kmol/hr

Carbon conversion $= \frac{5.127 - 1.098}{5.127} \times 100$

So, Carbon conversion = 78.58 %

A.2 CGE from condition: T_g = 600 °C, T_r = 700 °C and $O_2/S/CO_2/B$ = 0.5/1/1/1

For studied in effect of reformer temperature, before calculating CGE, the parameters HHV, LHV of biomass and LHV of syngas needed to know. The HHV of biomass was calculated using data from table 5.1 and Eq. 4.1 as showed below.

$HHV_{biomass}$ calculation

X_C = 0.6646

X_H = 0.0437

X_O = 0.2914

$HHV_{biomass} = (0.6646 \times 0.03491) + (0.0437 \times 1178.3) - (0.2914 \times 0.10\ 34)$

So, $HHV_{biomass}$ = 51.48 MJ/kg

Then, LHV of biomass was calculated using Eq. 4.4

$LHV_{biomass}$ calculation

$M_{biomass}$ from stream Biomass (Figure A.1) = 100 kg/hr

$M_H = X_H \times M_{biomass} = 0.0437 \times 100$ = 4.37 kg-H/hr

L_{298} = 2.44 MJ/kg [54]

$$LHV_{biomass} = \frac{(100 \times 51.48) - (0.5 \times 4.37 \times 2.44)}{100}$$

So, $LHV_{biomass}$ = 51.43 MJ/kg

Then, LHV of syngas was calculated using Eq. 4.5

LHV_{syngas} calculation

n_{CO} from stream syngas (Figure A.1) = 4.95 kmol/hr

n_{H2} from stream syngas (Figure A.1) = 5.08 kmol/hr

n_{CH4} from stream syngas (Figure A.1) = 0 kmol/hr

$H^0_{CO,298}$ = 283 MJ/kmol

$H^0_{H2,298}$ = 242 MJ/kmol

$H^0_{CH4,298}$ = 520 MJ/kmol

($H^0_{i,298}$ is obtained from [54])

$M_{syngas} = (4.95 \times 28.01) + (5.08 \times 2.00) = 148.90$ kg/hr

$$LHV_{syngas} = \frac{(4.95 \times 283) + (5.08 \times 242) + (0 \times 520)}{148.90}$$

So, LHV_{syngas} = 17.66 MJ/kg

CGE was calculated using mass flow rate and lower heating value of biomass and syngas (Eq. 4.3) as showed below.

CGE calculation

$$CGE = \frac{148.90 \times 17.66}{100 \times 51.43}$$

So, CGE = 0.511

A.3 CO_2 emr from condition: T_g = 600 °C, T_r = 700 °C and $O_2/S/CO_2/B$ = 0.5/1/1/1

CO_2 emr was calculated using Eq. 4.6 as following step. CO_2 emission is the amounts of CO_2 in stream CO_2 Capture and Syngas Product (Figure A.1). However, CO_2 total is the amounts of CO_2 from stream 3 (Figure A.1).

CO_2 emr calculation

CO_2 emission = 2.41 kmol/hr

CO_2 total = 7.54 kmol/hr

$$CO_2 \text{ emr} = \frac{2.41}{7.54}$$

So, CO_2 emr = 0.32

A.4 Total net heat from condition: T_g = 600 °C, T_r = 700 °C and $O_2/S/CO_2/B$ = 0.5/1/1/1

Total net heat was calculated by summation of net heat from all units in the process. Energy required from CO_2 capture process is 3 MJ/kg-CO_2 captured [33] and CO_2 captured flow rate from stream 4 (Figure A.1) is 298.77 kg/hr

Q_A = 896.31 MJ/hr

Q_s = 289.13 MJ/hr

Q_G = -787.52 MJ/hr

Q_E = 113.02 MJ/hr

Q_{C1} = -454.20 MJ/hr

Q_{C2} = -182.75 MJ/hr

So, Total net heat = 896.31 + 289.13 + (-787.52) + 113.02 + (-454.20) + (-182.75)

So, Total net heat = -126.00 MJ/hr

APPENDIX B

Calibration curve and calculation of product gas mole

Appendix B shows the calibration curve that used for calculate the mole of product gas. Product gases consist of H_2 and CO; however, by-product gases consist of CO_2 and CH_4. The samplings of pure gases were used for make the calibration curve of TCD gas chromatography.

B.1 Calibration curve

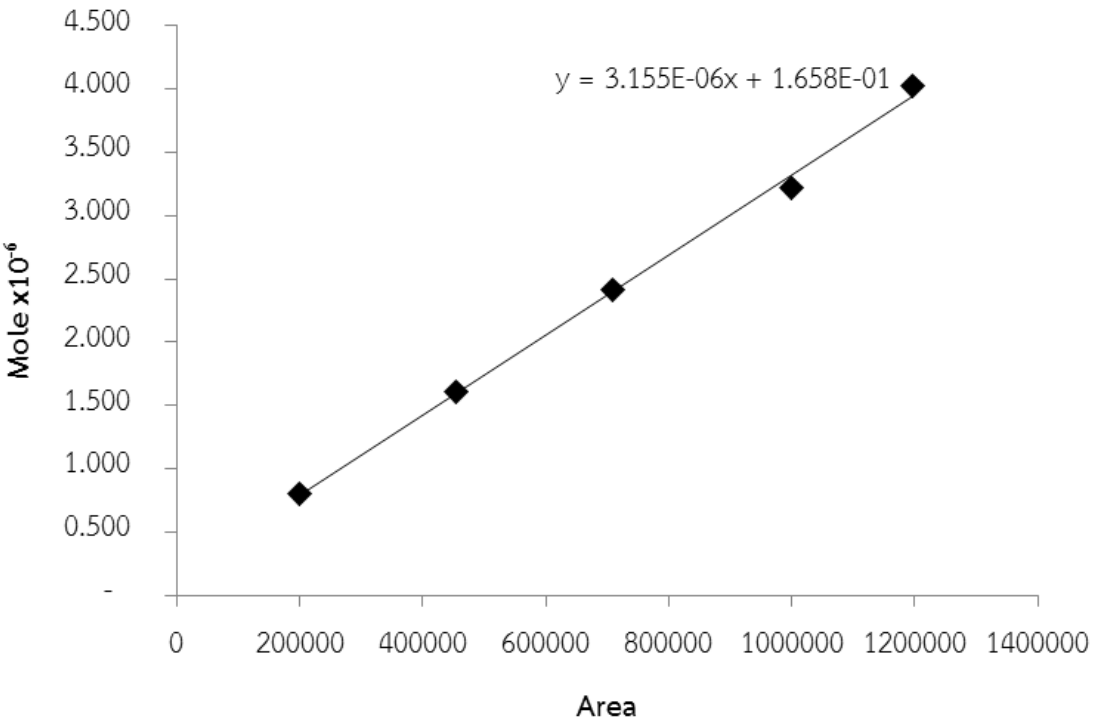

Figure B.1 The calibration curve of H_2

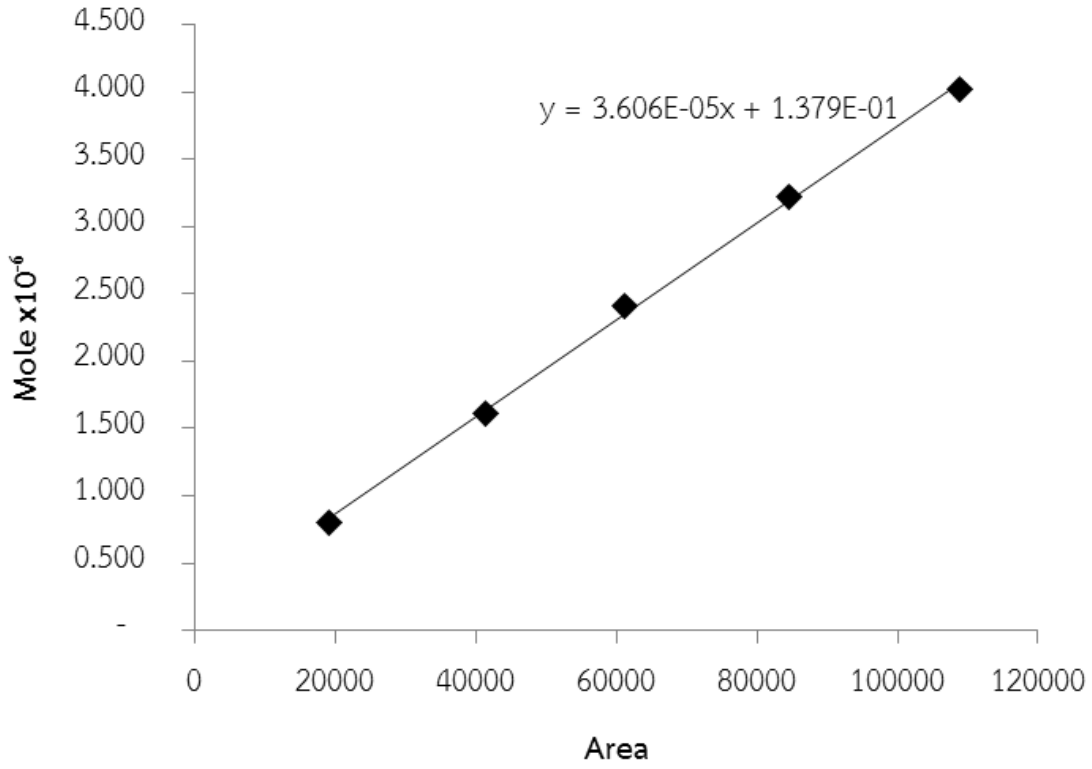

Figure B.2 The calibration curve of CO

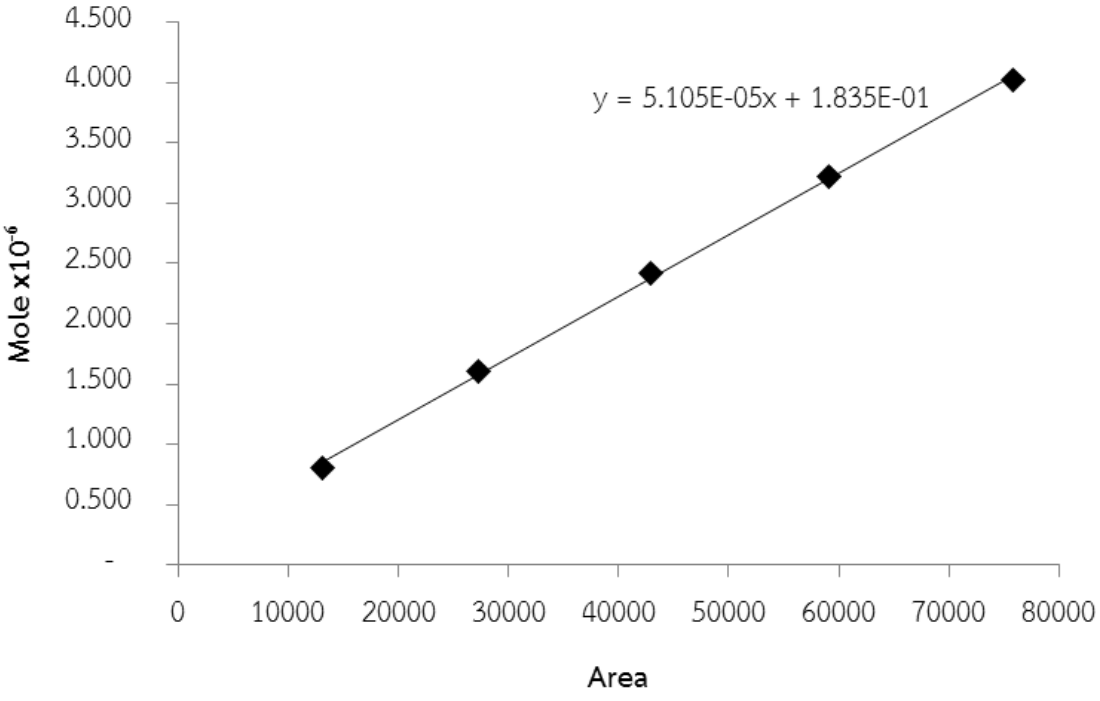

Figure B.3 The calibration curve of CO_2

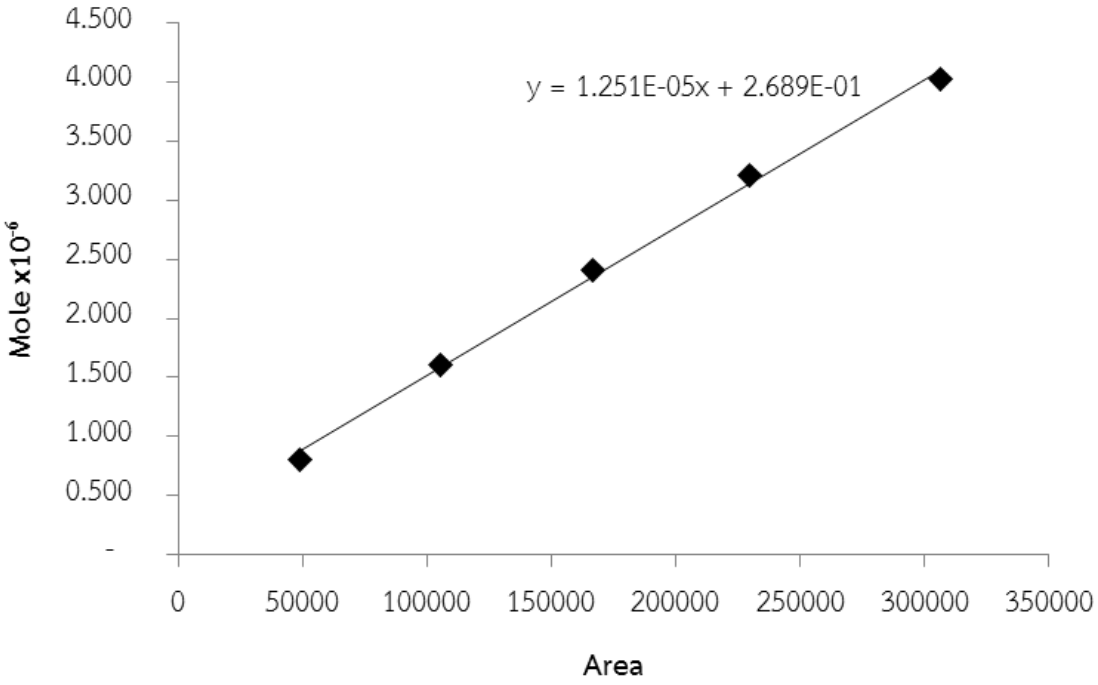

Figure B.4 The calibration curve of CH_4

B.2 Calculation of product gas mole

Case: operating temperature 400 ºC, non-catalyst and $O_2/S/CO_2/B$ = 0.5/1/1/1

Table B.1 H_2 peak area and mole on time

Time (min)	H_2 peak area	H_2 mole ($x10^{-6}$)
10	1522	0.170644
20	1893	0.171814
30	1412	0.170297
40	1762	0.171401
50	929	0.168773
60	807	0.168388
70	995	0.168981
80	1987	0.172111

Table B.1 H_2 peak area and mole on time (cont'd)

Time (min)	H_2 peak area	H_2 mole ($x10^{-6}$)
90	948	0.168833
100	892	0.168656
110	938	0.168801
120	823	0.168438
130	748	0.168201
140	909	0.168709
150	871	0.16859
160	1866	0.171729
170	879	0.168615
180	893	0.168659

For 10 minute,

H_2 peak area = 1522

From figure B.1, H_2 mole = $3.155\times10^{-6}(\text{area})+1.658\times10^{-1}$

So, H_2 mole = $(3.155\times10^{-6}\times1522)+(1.658\times10^{-1}) = 0.170644\times10^{-6}$

Table B.2 CO peak area and mole on time

Time (min)	CO peak area	CO mole ($x10^{-6}$)
10	5803	0.347251
20	3291	0.256661
30	2547	0.22983
40	3725	0.272312

Table B.2 CO peak area and mole on time (cont'd)

Time (min)	CO peak area	CO mole ($x10^{-6}$)
50	2353	0.222834
60	2601	0.231777
70	1802	0.202963
80	3198	0.253307
90	3857	0.277072
100	2386	0.224024
110	2697	0.235239
120	2301	0.220959
130	1496	0.191928
140	2381	0.223844
150	6148	0.359692
160	3496	0.264054
170	6234	0.362794
180	2619	0.232427

For 10 minute,

CO peak area = 5803

From figure B.2, CO mole = $3.606 \times 10^{-5}(\text{area}) + 1.379 \times 10^{-1}$

So, CO mole = $(3.606 \times 10^{-5} \times 5803) + (1.379 \times 10^{-1}) = 0.347251 \times 10^{-6}$

Table B.3 CO_2 peak area and mole on time

Time (min)	CO_2 peak area	CO_2 mole ($x10^{-6}$)
10	175123	9.124952
20	179462	9.346492
30	181619	9.456624
40	186867	9.724575
50	184263	9.59162
60	183539	9.554655
70	182534	9.503341
80	184356	9.596369
90	186979	9.730293
100	188216	9.793452
110	191504	9.96133
120	194500	10.1143
130	193341	10.05512
140	197786	10.28208
150	198269	10.30674
160	199804	10.38511
170	199282	10.35846
180	199085	10.3484

For 10 minute,

CO_2 peak area = 175123

From figure B.3, CO_2 mole = 5.105×10^{-5} (area) $+ 1.835 \times 10^{-1}$

So, CO_2 mole = $(5.105 \times 10^{-5} \times 175123) + (1.835 \times 10^{-1}) = 9.124952 \times 10^{-6}$

Table B.4 CH_4 peak area and mole on time

Time (min)	CH_4 peak area	CH_4 mole ($x10^{-6}$)
10	2578	0.301217
20	3146	0.308327
30	1749	0.29084
40	834	0.279386
50	434	0.274379
60	765	0.278523
70	501	0.275218

For 10 minute,

CH_4 peak area = 2578

From figure B.3, CH_4 mole = 1.251×10^{-5}(area) + 2.689×10^{-1}

So, CH_4 mole = $(1.251\times10^{-5}\times2578)+(2.689\times10^{-1}) = 0.301217\times10^{-6}$

APPENDIX C

Calculation of product gas yield and carbon conversion

The calculation was showed in case of using 10%Ni/SiO_2, operating temperature 800 °C and $O_2/S/CO_2/B$ = 0.5/1/1/1. Details of calculation on product gas yield and carbon conversion were showed below.

C.1 Product gas yield

Table C.1 Mole of product gas from gas chromatography and volumetric flow rate of product gas on sampling times

Sampling times (min)	Flow rate (mL/s)	Mole of H_2	Mole of CO	Mole of CO_2
10	0.38	0.4104	2.4545	9.1465
20	0.38	0.3274	2.4161	10.5767
30	0.37	0.2849	1.9299	10.9656
40	0.40	0.2861	1.6086	11.2152
50	0.40	0.3500	1.4028	11.7206
60	0.41	0.4263	1.3677	11.9389
70	0.42	0.6396	1.3124	11.9536
80	0.43	0.4107	1.3092	11.8164
90	0.43	0.5037	1.1899	11.6898
100	0.41	0.3631	0.9360	11.5575
110	0.41	0.4116	0.9005	11.5326
120	0.39	0.4297	0.8766	11.7515
130	0.39	0.4031	0.8227	11.7724

Table C.1 Peak area of product gas from gas chromatography and volumetric flow rate of product gas on sampling times (cont'd)

Sampling times (min)	Flow rate (mL/s)	Peak area of H_2	Peak area of CO	Peak area of CO_2
140	0.40	0.3601	0.5857	12.1097
150	0.38	0.3139	0.6270	12.2573
160	0.37	0.2767	0.4994	12.3414
170	0.37	0.1999	0.4638	12.5347
180	0.37	0.1689	0.1952	12.9367

For sampling times of 10 min (Table C.1)

$$\text{Mole fraction of } H_2 = \frac{0.4104}{0.4104 + 2.4545 + 9.1465} = 0.0342$$

$$\text{Mole fraction of CO} = \frac{2.4545}{0.4104 + 2.4545 + 9.1465} = 0.2043$$

$$\text{Mole fraction of } CO_2 = \frac{9.1465}{0.4104 + 2.4545 + 9.1465} = 0.7615$$

From ideal gas law, PV=nRT

P = 1 atm

V = 0.38 mL/s (Table B1)

R = 0.08206 L·atm/K·mol

T = 303.15 K

So, $n = \frac{1 \times 0.38 \times 10^{-3}}{0.08206 \times 303.15} = 1.53 \times 10^{-5}$ mol/s

Then, calculate the molar flow rate of each component using mole fraction and molar flow rate of mixture gas

Molar flow rate of H_2 = $0.0342 \times 1.53 \times 10^{-5}$ = 5.22×10^{-7} mol/s

Molar flow rate of CO = $0.2043 \times 1.53 \times 10^{-5}$ = 3.12×10^{-6} mol/s

Molar flow rate of CO_2 = $0.7615 \times 1.53 \times 10^{-5}$ = 1.16×10^{-5} mol/s

The molar flow rate of product gas on each sampling time was presented in Table C.2 as below.

Table C.2 Molar flow rate of product gas on sampling time

Sampling times (min)	Flow rate of H_2 (mol/s)	Flow rate of CO (mol/s)	Flow rate of CO_2 (mol/s)
10	5.22×10^{-7}	3.12×10^{-6}	1.16×10^{-5}
20	3.76×10^{-7}	2.77×10^{-6}	1.21×10^{-5}
30	3.22×10^{-7}	2.18×10^{-6}	1.24×10^{-5}
40	3.51×10^{-7}	1.97×10^{-6}	1.38×10^{-5}
50	4.18×10^{-7}	1.67×10^{-6}	1.40×10^{-5}
60	5.12×10^{-7}	1.64×10^{-6}	1.43×10^{-5}
70	7.77×10^{-7}	1.59×10^{-6}	1.45×10^{-5}
80	5.24×10^{-7}	1.67×10^{-6}	1.51×10^{-5}
90	6.51×10^{-7}	1.54×10^{-6}	1.51×10^{-5}
100	4.66×10^{-7}	1.20×10^{-6}	1.48×10^{-5}
110	5.28×10^{-7}	1.16×10^{-6}	1.48×10^{-5}
120	5.16×10^{-7}	1.05×10^{-6}	1.41×10^{-5}
130	4.86×10^{-7}	9.92×10^{-7}	1.42×10^{-5}
140	4.43×10^{-7}	7.21×10^{-7}	1.49×10^{-5}

Table C.2 Molar flow rate of product gas on sampling time (cont'd)

Sampling times (min)	Flow rate of H_2 (mol/s)	Flow rate of CO (mol/s)	Flow rate of CO_2 (mol/s)
150	3.63×10^{-7}	5.66×10^{-7}	1.42×10^{-5}
160	3.14×10^{-7}	5.23×10^{-7}	1.40×10^{-5}
170	2.25×10^{-7}	2.18×10^{-7}	1.41×10^{-5}
180	1.89×10^{-7}	5.66×10^{-7}	1.45×10^{-5}

Total mole of each product gas was calculated using integral of each molar flow rate (mlo/s) with sampling time (s) by Trapezoidal rule (Eq. C.1) [54]. The example of calculation was showed as follow.

$$\int_a^b f(x)dx = (b-a)\left[\frac{f(a)+f(b)}{2}\right] \qquad (C.1)$$

At sampling time 10 minute (600 sec), H_2 flow rate = 5.22×10^{-7} mol/s

At sampling time 20 minute (1200 sec), H_2 flow rate = 3.76×10^{-7} mol/s

Mole of H_2 from 10 minute to 20 minute was

$$= (1200-600)\left[\frac{(5.22\times10^{-7})+(3.76\times10^{-7})}{2}\right]$$

So, Mole of H_2 from 10 minute to 20 minute = 0.000269 mole-H_2 and other results are showed in Table C.3.

Table C.3 Total mole of product gas on sampling time range

Time range (min)	Total mole of H_2 (mole/g-biomass)	Total mole of CO (mole/g-biomass)	Total mole of CO_2 (mole/g-biomass)
10 – 20	0.000269	0.001768	0.007128
20 - 30	0.000209	0.001485	0.007351

Table C.3 Total mole of product gas on sampling time range (cont'd)

Time range (min)	Total mole of H_2 (mole/g-biomass)	Total mole of CO (mole/g-biomass)	Total mole of CO_2 (mole/g-biomass)
30 – 40	0.000202	0.001245	0.007839
40 – 50	0.000231	0.001094	0.008323
50 – 60	0.000279	0.000995	0.008495
60 – 70	0.000387	0.000970	0.008652
70 – 80	0.000390	0.000980	0.008881
80 – 90	0.000353	0.000963	0.009056
90 – 100	0.000335	0.000821	0.008974
100 – 110	0.000298	0.000707	0.008884
110 – 120	0.000313	0.000662	0.008672
120 – 130	0.000301	0.000613	0.008492
130 – 140	0.000279	0.000514	0.008734
140 – 150	0.000242	0.000434	0.008730
150 – 160	0.000203	0.000388	0.008454
160 – 170	0.000162	0.000327	0.008436
170 - 180	0.000124	0.000222	0.008578
Summation	0.00457	0.01430	0.14513

Finally, summation of total mole of product gas in each sampling time (Table C.3) is product gas yield.

H_2 yield = 0.00457 mole/g-biomass

CO yield = 0.01430 mole/g-biomass

C.2 Carbon conversion

Calculation of carbon conversion was used Eq. 4.5. Formation of CO and CO_2 obtained from table C.3. Details were showed below.

Formation of CO = 0.01430 moles-CO

Formation of CO_2 = 0.14513 moles-CO_2

Feeding of Carbon from biomass (1 gram) = 0.05533 moles-Carbon

Feeding of CO_2 (CO_2/B = 1/1) = 0.05533 moles-CO_2

So, Carbon conversion = $\frac{(0.01430 + 14513 - 0.05533)}{(0.05533 + 0.05533)} \times 100$ = 94.08%

APPENDIX D

Raw data from experimental

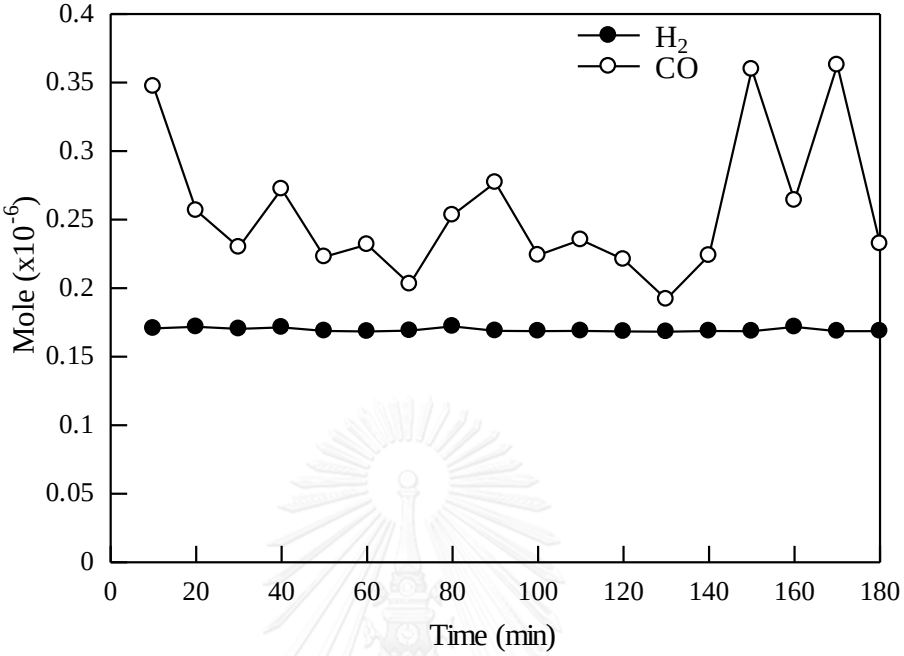

Figure D.1 Raw result of product gas from experiment

(T = 400 °C, non-catalyst and $O_2/S/CO_2/B$ = 0.5/1/1/1)

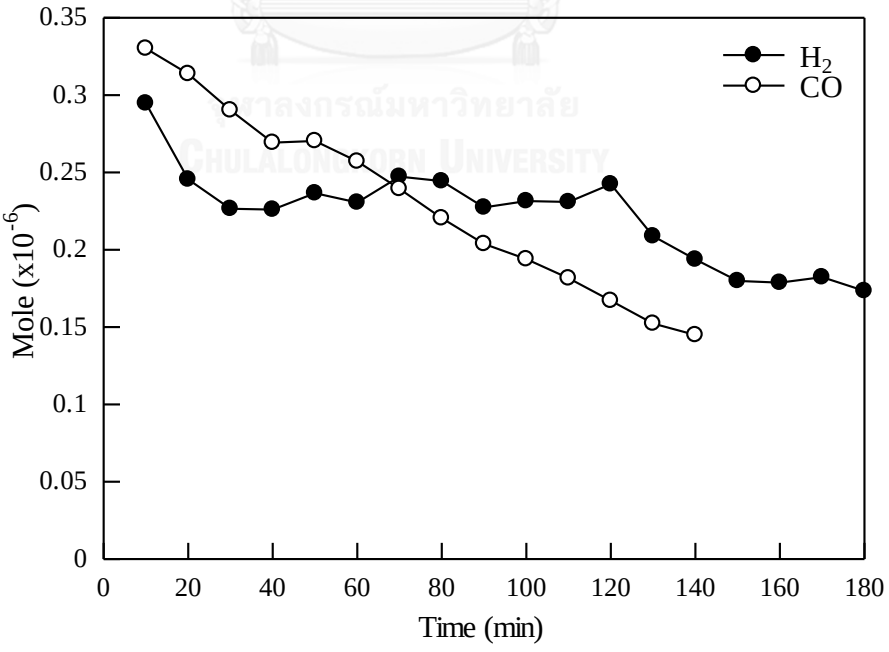

Figure D.2 Raw result of product gas from experiment

(T = 600 °C, non-catalyst and $O_2/S/CO_2/B$ = 0.5/1/1/1)

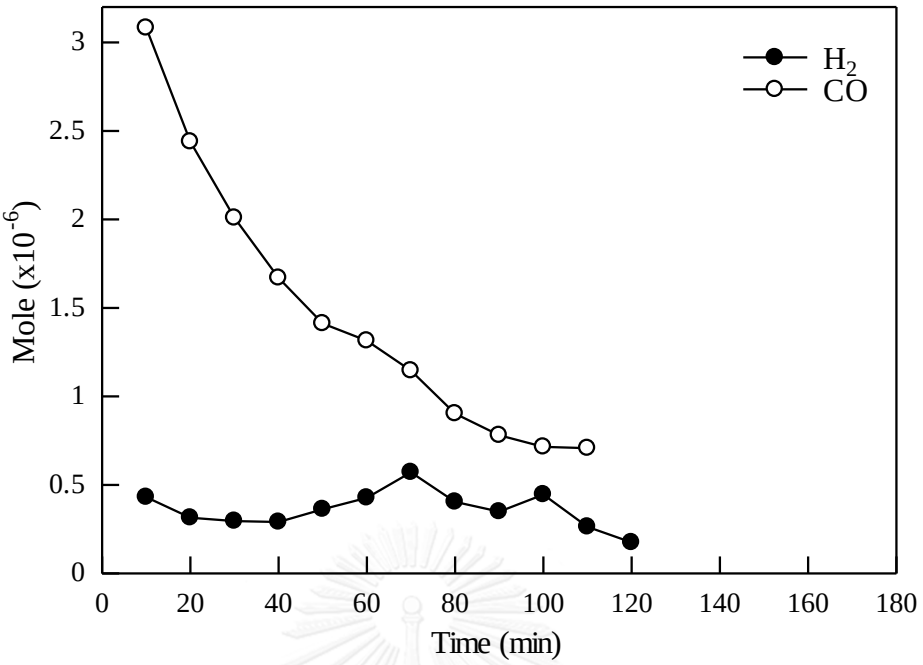

Figure D.3 Raw result of product gas from experiment
(T = 800 °C, non-catalyst and $O_2/S/CO_2/B$ = 0.5/1/1/1)

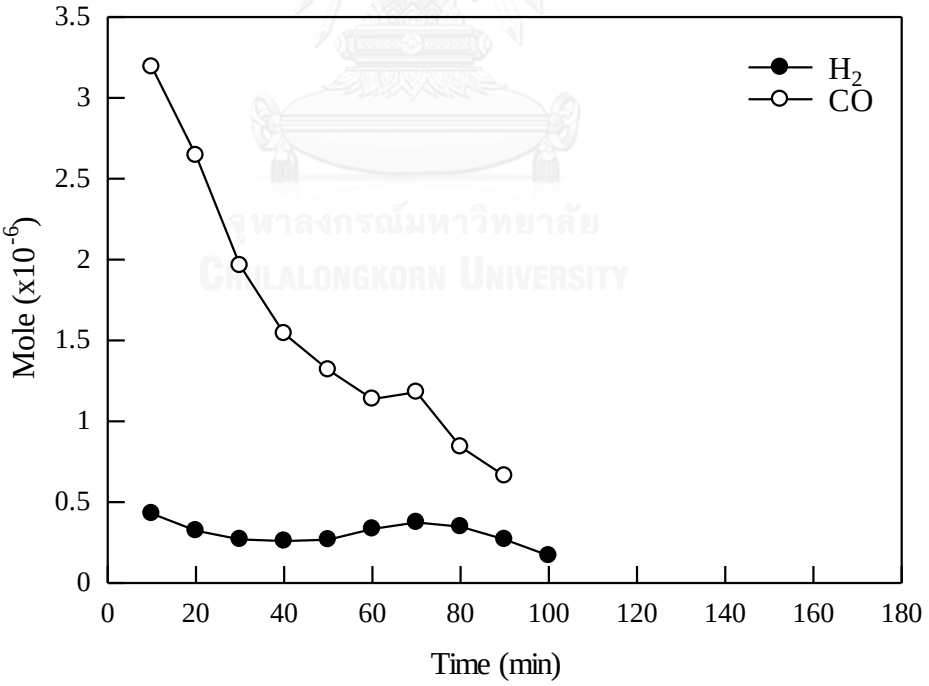

Figure D.4 Raw result of product gas from experiment
(T = 800 °C, 5%Ni/SiO_2 and $O_2/S/CO_2/B$ = 0.5/1/1/1)

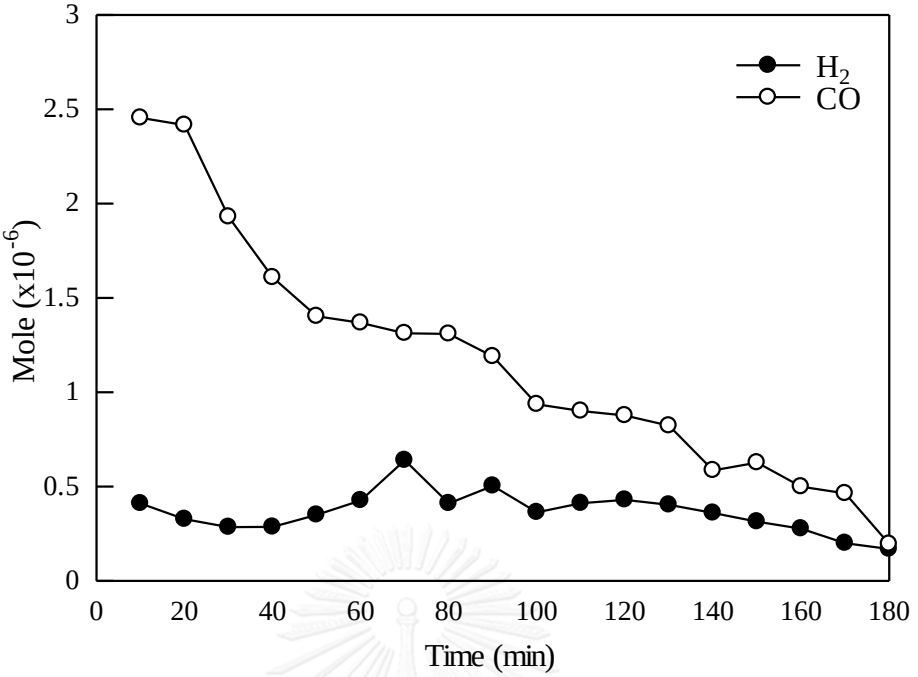

Figure D.5 Raw result of product gas from experiment

(T = 800 °C, 10%Ni/SiO_2 and $O_2/S/CO_2/B$ = 0.5/1/1/1)

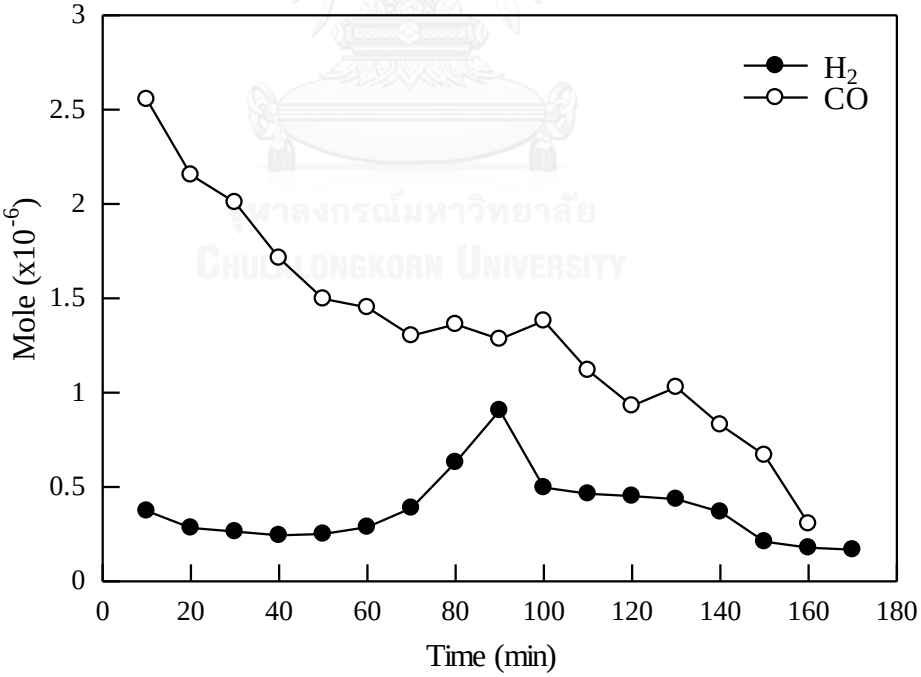

Figure D.6 Raw result of product gas from experiment

(T = 800 °C, 15%Ni/SiO_2 and $O_2/S/CO_2/B$ = 0.5/1/1/1)

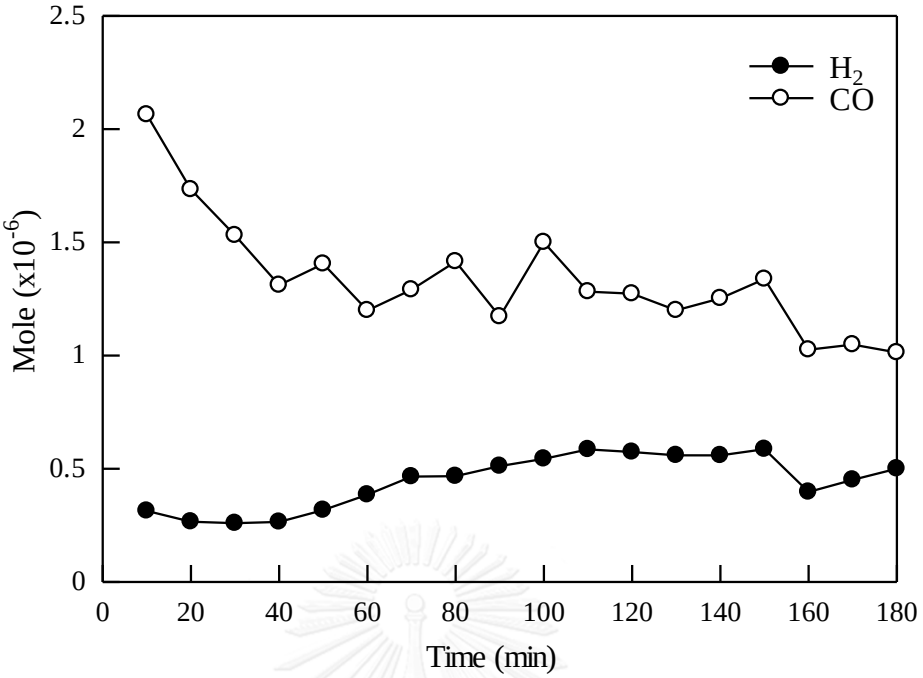

Figure D.7 Raw result of product gas from experiment

(T = 800 °C, 10%Ni/SiO_2 and $O_2/S/CO_2/B$ = 0/1/1/1)

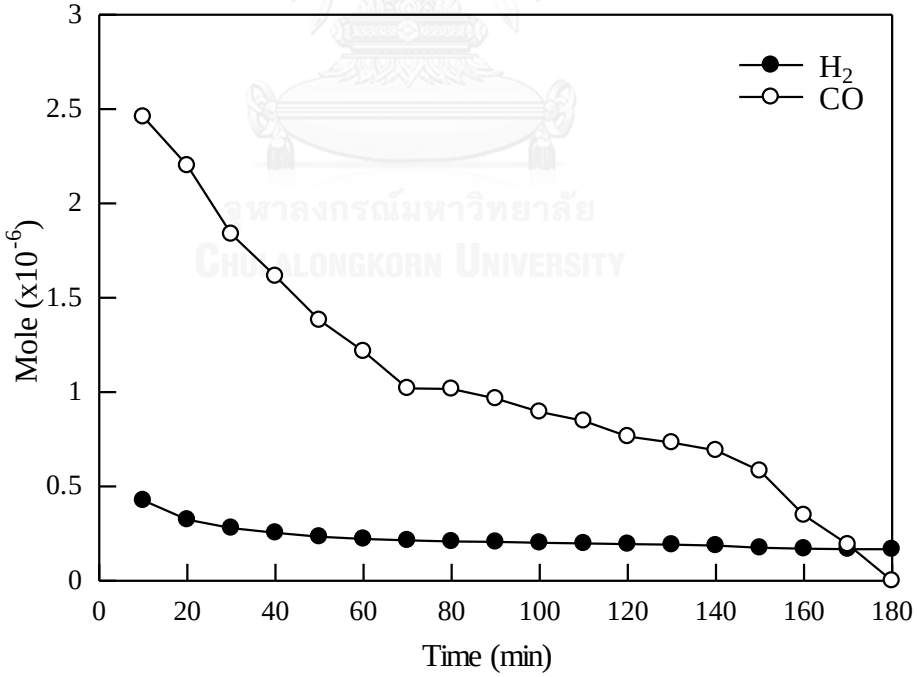

Figure D.8 Raw result of product gas from experiment

(T = 800 °C, 10%Ni/SiO_2 and $O_2/S/CO_2/B$ = 0.5/0/1/1)

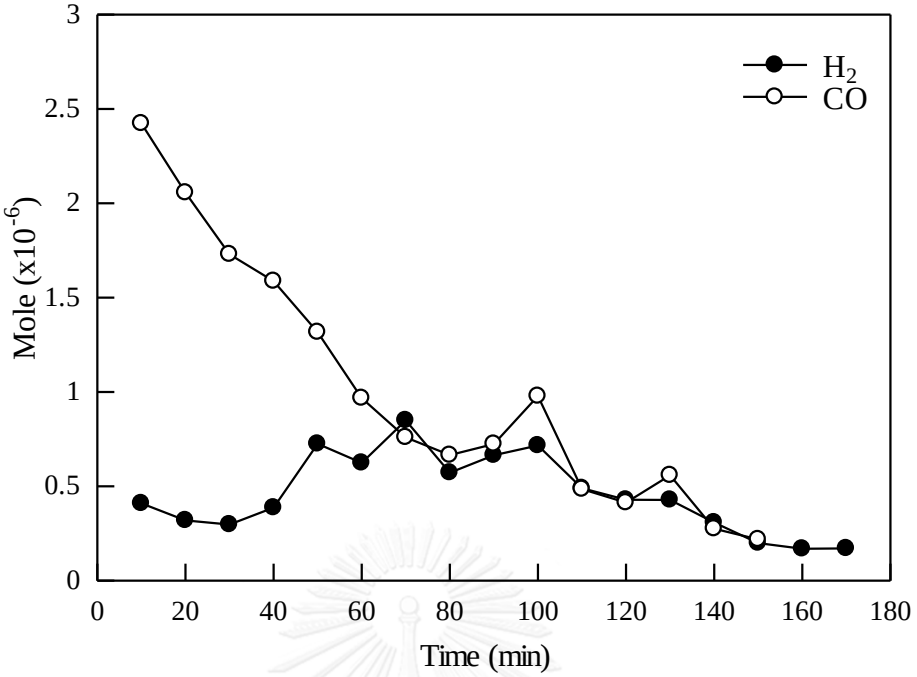

Figure D.9 Raw result of product gas from experiment

(T = 800 °C, 10%Ni/SiO_2 and $O_2/S/CO_2/B$ = 0.5/2/1/1)

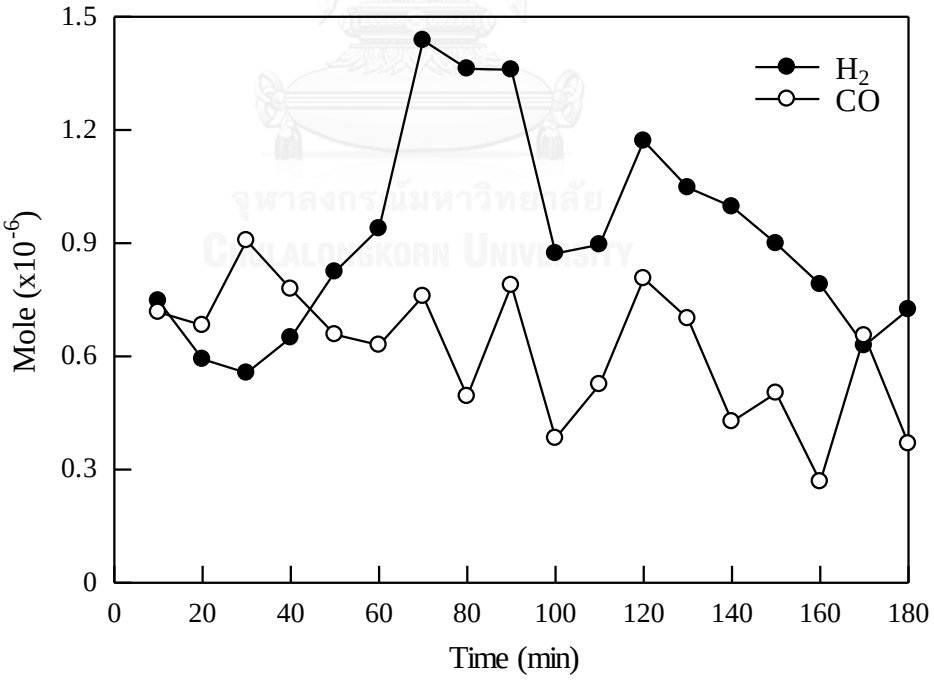

Figure D.10 Raw result of product gas from experiment

(T = 800 °C, 10%Ni/SiO_2 and $O_2/S/CO_2/B$ = 0.5/1/0/1)

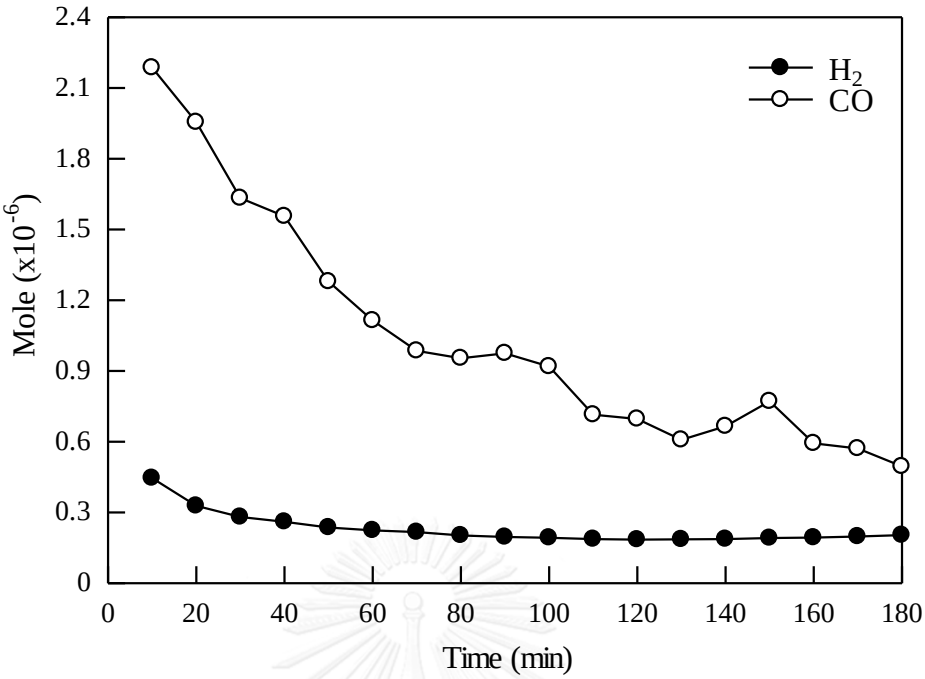

Figure D.11 Raw result of product gas from experiment

(T = 800 °C, 10%Ni/SiO_2 and *O_2/S/CO_2/B* = 0.5/1/0.5/1)

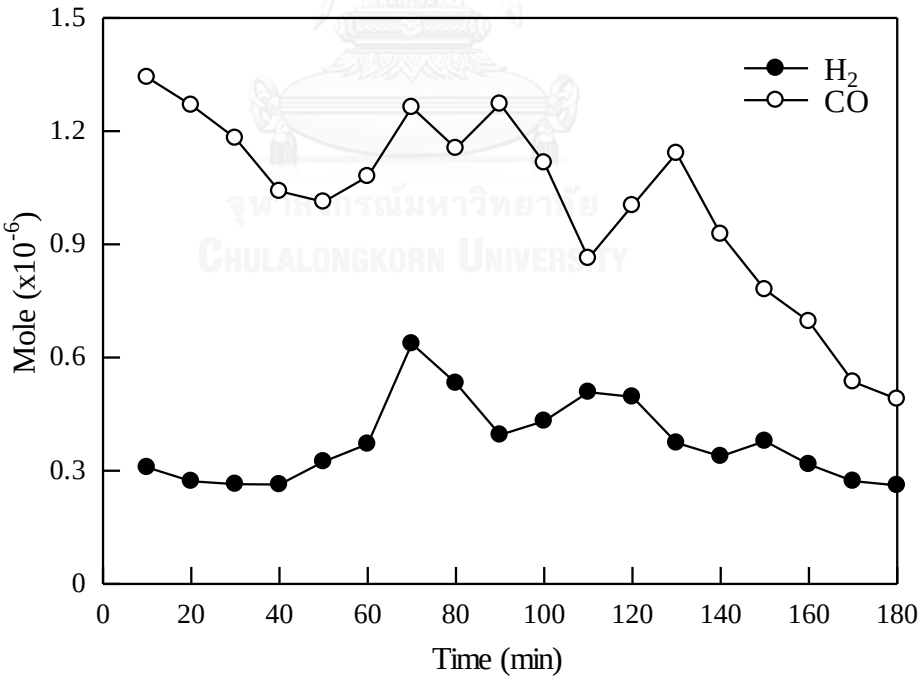

Figure D.12 Raw result of product gas from experiment

(T = 800 °C, 10%Ni/SiO_2 and *O_2/S/CO_2/B* = 0.5/1/1.5/1)

APPENDIX E

Nomenclature

$H^{0}_{i,298}$	Heat of combustion of i component (MJ/kmol)
ΔH_r	Heat of reaction at standard condition 298 K (MJ/kmol)
L_{298}	Latent heat of vaporization of water at standard condition 298 K (MJ/kg)
M	Mass flow rate (kg/hr)
M_H	Mass flow rate of atomic hydrogen in biomass (kg-H/hr)
n_i	Molar flow rate of i component (kmol/hr)
T_g	Gasifier temperature (°C)
T_r	Reformer temperature (°C)
y_{H2}, y_{CO}	Mole fraction of H_2 and CO (-)
CO_2/B	Mole of CO_2 as reaction agent per mole of carbon in biomass (-)
H_2/CO	Molar ratio of H_2 to CO in product syngas (-)
O_2/B	Mole of O_2 as reaction agent per mole of carbon in biomass (-)
S/B	Mole of steam as reaction agent per mole of carbon in biomass (-)

Abbreviations

CGE	Cold gas efficiency (-)
CO_2 emr	CO_2 emission ratio (-)
HHV	Higher heating value (MJ/kg)
LHV	Lower heating value (MJ/kg)

APPENDIX F

List of Publication

Proceeding

Paripat Kraisornkachit, Supawat Vivanpatarakij and Suttichai Assabumrungrat, “SIMULATION OF COMBINED BIOMASS GASIFIER AND REFORMER FOR SYNGAS PRODUCTION ENHANCED BY USING CO_2 RECYCLE” Proceeding of the 9th PACCON 2015, Amari Watergate Hotel Bangkok, Thailand, January 21-23, 2015.

VITA

Mr. Paripat Kraisornkachit was born June 12, 1991 in Bangkok, Thailand. He finished high school from Sri Ayudhya School, Bangkok, Thailand, 2009. He received his Bachelor Degree in Chemical Engineering from Kasetsart University in 2013. He was now studying Master Degree at Department of Chemical Engineering, Chulalongkorn University, Thailand.